Worcester Polytechnic Institute
Digital WPI

Major Qualifying Projects (All Years) | Major Qualifying Projects

December 2013

Low-Power High Frequency Communications

Cecelia R. Franzini
Worcester Polytechnic Institute

Nathan Costa Ferreira
Worcester Polytechnic Institute

Follow this and additional works at: https://digitalcommons.wpi.edu/mqp-all

Repository Citation
Franzini, C. R., & Ferreira, N. C. (2013). *Low-Power High Frequency Communications*. Retrieved from https://digitalcommons.wpi.edu/mqp-all/3859

This Unrestricted is brought to you for free and open access by the Major Qualifying Projects at Digital WPI. It has been accepted for inclusion in Major Qualifying Projects (All Years) by an authorized administrator of Digital WPI. For more information, please contact digitalwpi@wpi.edu.

Low Power HF Communications

A Major Qualifying Project Report

submitted to the Faculty

of the

WORCESTER POLYTECHNIC INSTITUTE

in partial fulfillment of the requirements for the

Degree of Bachelor of Science

by

_____

Nathan Ferreira

_____

Cecelia Franzini

Date: December 19, 2013

_____

Professor Reinhold Ludwig, Major Advisor

Abstract

This research, conducted in the Fall of 2013, investigates the transmission and reception of signals over the High Frequency (HF) band, which includes frequencies between 3 and 30 MHz. HF communications are useful over very long distances, but they often experience performance problems such as channel fading and low data rates of transmission. Our project researches the viability of using left- and right-handed circular polarized signals to increase data rates and link reliability. Two project sites are used for testing and research: a transmit site at The MITRE Corp. in Bedford, Massachusetts, and a receive site 40 miles away at Worcester Polytechnic Institute (WPI) located in Worcester, Massachusetts. Both sites use a cross-dipole antenna setup, as well as the Ettus Universal Software Radio Peripheral (USRP) software defined radio for the transmission and reception systems. With the aid of the collected data, the project aims to evaluate whether the implemented setup allows for the left- and right-hand polarized signals to be separated at the receiver. The separation is important since it results in more reliable communications, less fading, and increased data rate.

Contents

Abstract 1

Background 7

The Ionosphere 7

HF Limitations 8

Objectives 12

Approach 13

VOACAP 13

Hardware Development 14

Overall System Configuration 14

Transmit Chain 14

Receiver Chain 23

Software Development 26

GNU Radio 26

LFM Generation 26

Hybrid Implementation 27

Final Design (MATLAB Implementation) 30

How GNU Radio handles the carrier frequency 32

MATLAB 32

LFM code 32

Post Processing 33

Methodology 34

First Data Collection 34

Second Data Collection 35

Third Data Collection 37

Results 40
Signal Bandwidths 40
Power levels 41
Signal Mode Visibility 41
Measurement Viability 44
Cost Analysis 47
Conclusion 48
Recommendations 49
References 50
Appendix A 52
Matlab Code 52
Generate chirp 52
Generate chirp with 90^o phase shift 52
Generate chirp with -90^o phase shift 53
Tukey Taper 53
Simulate Hybrid 54
Appendix B 55
Dipole Measurements 55
Data Collection II 57
Data Collection III 71

Figures

Figure 1. Example of skywave propagation using the D, E, F1 and F2 layers of the ionosphere [6]. 7
Figure 2. Forestport HF vertical array measurements by MITRE (1990). 9
Figure 3. Left- and right-handed elliptically polarized waves, respectively [10]. 10
Figure 4. Example illustration of refraction angles through different media [11]. 11
Figure 5. VOACAP analysis along with parameters used. 13
Figure 6. Transmit system block diagram showing the transmitting USRPs, pre-amplifiers, high-power amplifiers, filters, and antenna. 14
Figure 7. The ZHL-32A pre-amplifier power gain characteristics are very close to each other, and the zoomed frame shows the characteristic at the desired operating point. 16
Figure 8. High Power Amplifier gain characteristics. 17
Figure 9. Absorptive filter schematic. The antenna is modeled as R1 and connected to a low pass T-network; the high pass T-network is connected to the load resistor R2. 19
Figure 10. Absorptive Filter characteristic where the green is the power across R1 and blue is the power across R2. 20
Figure 11. Characteristic of absorptive filter I with measurements at several frequencies. 20
Figure 12. Characteristic of absorptive filter II with measurements at several frequencies. 21
Figure 13. Interior and exterior of finished filter. 21
Figure 14. Cross-dipole antenna configuration (top view). 22
Figure 15. Receive system block diagram showing the antenna, band pass filters, low-noise amplifiers, and receive USRPs. 23
Figure 16. Network Analyzer photo of WPI cross-dipole VSWR. 24
Figure 17. LNA gain characteristic with the zoomed-in area better showing the differences in gains. These amplifiers do not go into compression for this range of inputs. 25
Figure 18. GRC flowchart to create and simulate LFM. 27
Figure 19. Microstripline form of quadrature hybrid utilizing lambda-quarter transformer [15]. 28
Figure 20. Illustration of how a quadrature hybrid works with multiple inputs. 28
Figure 21. Software implementation of hybrid in GRC. 29
Figure 22. Final receive flowchart for testing. 31
Figure 23. Final transmit flowchart for testing. 31
Figure 24. Time domain plot of a tapered, 20kHz chirp. 33

Figure 25. Received 20kHz LFM in Worcester. 35
Figure 26. Lowest power measurement, F1-jF2 at 6W. 41
Figure 27. 20kHz LFM at 10W with two F layer bounces. 42
Figure 28. 20kHz F1+jF1 signal at 78.5W with two F-layer bounces and a ground wave. 43
Figure 29. 20kHz F1+jF1 signal at 9W with two F-layer bounces and a ground wave. 44
Figure 30. Doppler data versus time for data collections II and III. 45
Figure 31. . Phase versus time for data collections II and III. 46
Figure 32. Small Dipole measurements 55
Figure 33. CWS ByteMark Bal-300 Balun Schematic[19] 56
Figure 34.2:33/F1/3kHz/34W – F layer, one mode 57
Figure 35.2:37/F1/3kHz/10W – F layer? One mode 58
Figure 36.2:50/F1/20kHz/39.82dBm – F layer, one mode, two on second bounce 59
Figure 37.2:59/F1/20kHz/45.46dBm – F layer, one mode 60
Figure 38.3:02/F1/20kHz/34WdBm – F layer, one mode 61
Figure 39.3:16/F1+jF1/3kHz/39.56dBm – one mode 61
Figure 40.3:25/F1+jF1/3kHz/45.44dBm – F layer, one mode 62
Figure 41.3:30/F1+jF1/20kHz/39.56dBm – F layer, two modes 63
Figure 42.3:32/F1+jF1/20kHz/45.44dBm – F layer, two modes? 63
Figure 43.3:37/F1-jF1/20kHz/39.56dBm – one mode 64
Figure 44.3:40/F1-jF1/20kHz/45.44dBm – F layer, one mode, two modes on second bounce 65
Figure 45.3:44/F1-jF1/3kHz/39.56dBm – F layer, two modes(?) 65
Figure 46.3:46/F1-jF1/3kHz/45.44dBm – F layer (3 bounces?), one mode 66
Figure 47.3:49/F1+jF2/3kHz/38.1dBm – one mode 66
Figure 48.4:04/F1+jF2/3kHz/43.94dBm – F layer, two modes 67
Figure 49.4:14/F1+jF2/20kHz/38.1dBm – F layer, two modes 67
Figure 50.4:17/F1+jF2/20kHz/44dBm – F layer, two modes (?) 68
Figure 51.4:20/F1-jF2/3kHz/38dBm – F layer, one mode, two on second bounce 68
Figure 52.4:22/F1-jF2/3kHz/44dBm – F layer, one mode, two(?) on second bounce 69
Figure 53.4:26/F1-jF2/20kHz/38dBm – F layer, two modes 69
Figure 54.4:28/F1-jF2/20kHz/44dBm – F layer (three bounces), two modes 70
Figure 55.11:38/F1/20kHz/39.18dBm – one mode 71

Figure 56.11:43/F1/20kHz/45.24dBm – F layer, one mode (two on second bounce?) 72
Figure 57.11:47/F1/20kHz/48.07dBm – F layer, one mode, ground wave 72
Figure 58.11:53/F1/90kHz/38.84dBm – F layer, one mode 73
Figure 59.11:57/F1/90kHz/44.88dBm – F layer, one mode, ground wave 74
Figure 60.12:06/F1/90kHz/48.13dBm – F layer, one mode 74
Figure 61.12:21/F1+jF1/20kHz/39.44dBm – F layer, one mode, ground wave 75
Figure 62.12:25/F1+jF1/20kHz/45.52dBm – F layer, one mode (two on second bounce), ground wave . 75
Figure 63.12:29/F1+jF1/20kHz/48.95dBm – F layer, two modes, ground wave 76
Figure 64.12:38/F1+jF1/90kHz/39.22dBm – F layer(?), two modes on second bounce 76
Figure 65.12:42/F1+jF1/90kHz/44.85dBm – F layer, two modes, ground wave 77
Figure 66.12:45/F1+jF1/90kHz/48.25dBm – F layer, two modes(?), ground wave 77
Figure 67.12:54/F1-jF1/20kHz/39.48dBm – F layer, one mode, ground wave 78
Figure 68.1:01/F1-jF1/20kHz/45.56dBm – F layer, one mode(?), ground wave 79
Figure 69.1:05/F1-jF1/20kHz/49.93dBm – F layer, one mode, ground wave 80
Figure 70.1:15/F1-jF1/90kHz/39.0822dBm – F layer, one mode(?) 81
Figure 71.1:19/F1-jF1/90kHz/44.95dBm – F layer, one mode (two on second bounce), ground wave 82
Figure 72.1:22/F1-jF1/90kHz/48.20dBm – F layer, two modes, ground wave 82
Figure 73.1:45/-F1+jF2&jF1-F2/20kHz/41.25dBm – F layer, two modes(?), ground wave(?) 83
Figure 74.1:57/F1+jF2&F1+jF2/90kHz/40.43dBm – F layer, two modes(?), ground wave(?) 83
Figure 75.2:08/-F1+jF2&F1-jF2/90kHz/40.43dBm – F layer, two modes(?), ground wave(?) 84

Background

The HF spectrum is used internationally for communications, government time stations, marine weather radar, amateur radio, and many other applications. One major advantage of HF is that the electromagnetic waves can travel long distances by implementing so-called skywave propagation, which occurs when the signal refracts off the ionosphere [1]. An example of this type of propagation is shown in Figure 1. The figure illustrates how signals refract off different layers of the ionosphere, allowing for over the horizon communication without direct line of sight. Unfortunately, the ionosphere changes with the time of day, season, sunspot cycle, solar activity and location, which affects the signal's propagation behavior. As a result, it can restrict the maximum usable frequency for propagation.

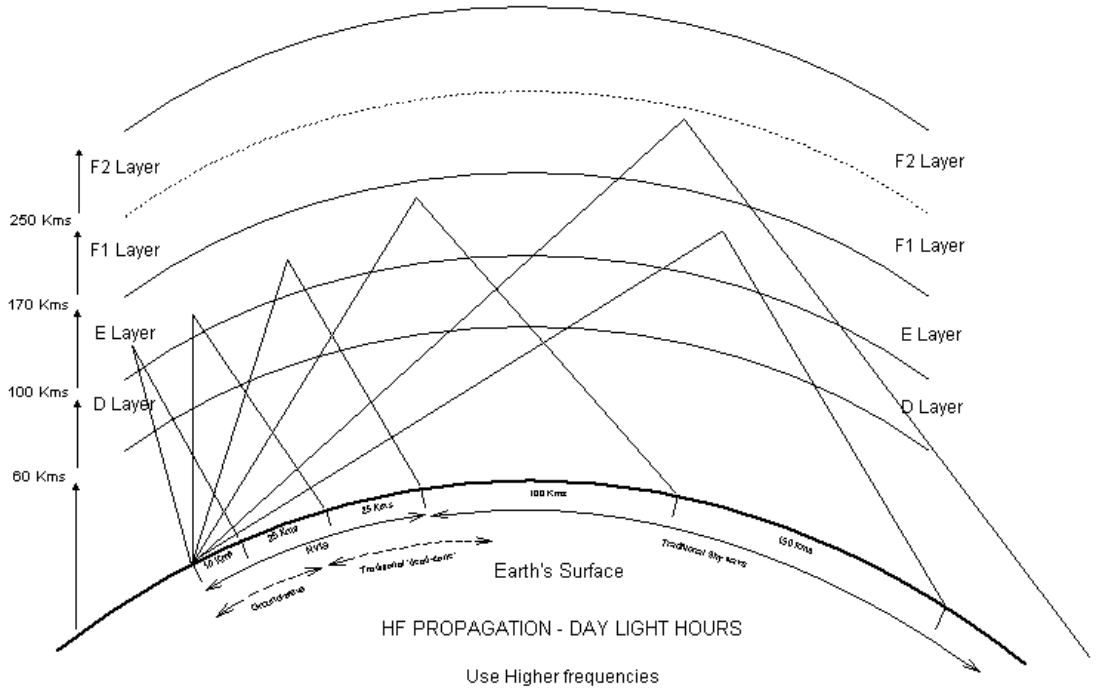

Figure 1. Example of skywave propagation using the D, E, F1 and F2 layers of the ionosphere [6].

The Ionosphere

The ionosphere is a layer of the Earth's atmosphere that is formed when extreme ultraviolet (EUV) light ionizes electrons, creating a layer of plasma [1]. There are different layers of the ionosphere that have different molecular make-ups and ion concentrations; they are illustrated in Figure 1. The lowest layer of the ionosphere is the D layer, which is found around 50 to 90km above the earth's surface. Next is the E layer, which is around 100km above the surface. The E layer has a higher electron

density than the D layer by an order of magnitude. The last layer is the F layer, which occupies altitudes of about 150 to 600km above the earth. In the daytime during summer months, the F layer can split into the F_1 and F_2 layers. During the night, in the absence of sunlight, all of the layers nearly disappear due to the reduced ionization, with the exception of the F_2 layer. As a result of the complex layered composition of the ionosphere, electromagnetic propagation is significantly affected by variables such as time of day or weather. Usable frequencies and elevations change depending on the varying ionosphere, therefore it can be difficult to provide reliable communications.

HF Limitations

There are two major challenges in HF communications: channel fading and relatively low data transmission. Channel fading is the repetitive rise and fall in signal level, and is usually caused by one of four effects:

- changes in the ionosphere
- rotation of the polarization of the electromagnetic fields
- variations in ionospheric signal absorption over time
- drop in the maximum usable frequency below the operating frequency [1].

Figure 2 shows an HF measurement made by MITRE in 1990; it is an example of this phenomenon. A vertical array (1200 ft.) was constructed in Forestport, New York, with a digital receiver on each element. The measurement was conducted over a 60-second acquisition period. The top plot is the signal strength of a broad beam (with no elevation directivity), showing that fading is significant. The vertical axis, named relative energy, is simply a measure of power that has been normalized to an arbitrary reference value. The bottom plot shows beam forms in elevation steps; it makes it clear that the ionosphere is stable for this time period at certain elevation angles and that the fading must be due to destructive interference between layers of the ionosphere. The middle plot shows the power for the three transmission modes at elevation angle of 6, 9 and 17 degrees, which show much less fading than the broader beam (ECRS) response. Each elevation fades differently because the signal may be scattering off different layers of the ionosphere or may be bouncing more than once.

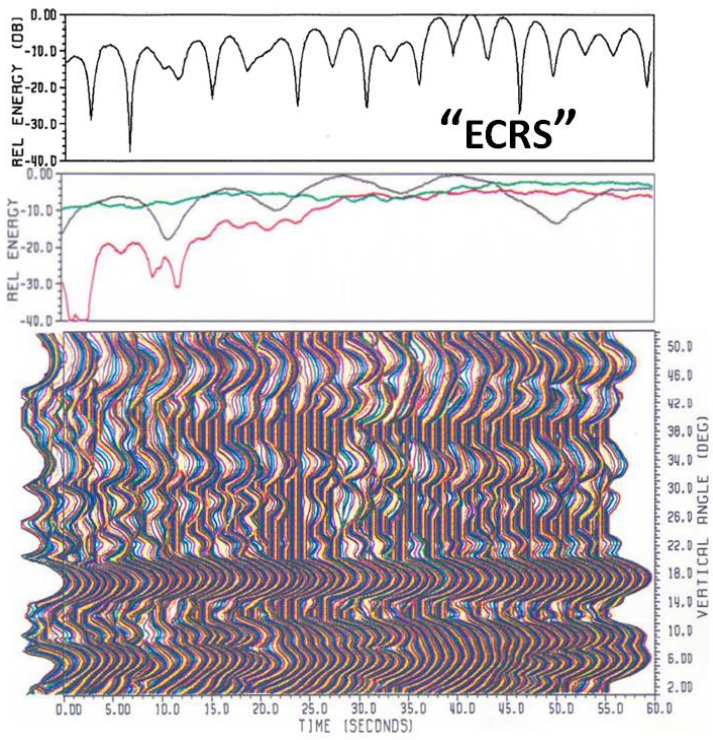

Figure 2. Forestport HF vertical array measurements by MITRE (1990).

In order to attempt to increase the data rate of HF communications, research into multiple input, multiple output (MIMO) communication for this platform is ongoing. It is reasoned that an array of antennas would achieve this goal. However, the wavelength of an HF signal is very large; it can range from 10 - 100m [7]. Antennas in a phased array are typically spaced at distances of half a wavelength or less, depending on the angle of transmission [8]. If they are spaced at more than half a wavelength, there is the possibility of receiving grating lobes. The effect of grating lobes can result in a high gain in an unwanted location of an antenna pattern. However, even less than half an HF wavelength can be on the order of tens of meters. This means that in order for the array elements to be appropriately spaced, they would have to be much too far apart to be practical in actual application [4].

One alternative to an array of antennas would be to transmit waves with two different polarizations. The ionosphere is an anisotropic medium, which implies that its refraction characteristics are directionally dependent [3]. As a result, there exist two propagation modes in the ionosphere: Ordinary (O) and Extraordinary (X). When an electromagnetic wave encounters the ionosphere, it splits into these two modes and becomes elliptically polarized. For a wave to be elliptically polarized, the electric field vector must rotate and change magnitude as it propagates [1]. The case of a constant magnitude is known as circular polarization. X and O modes are oppositely polarized; when a wave splits

into these two modes, one is right-hand circularly polarized and one is left-hand circularly polarized. Combining both polarization states will result in a linearly polarized wave. The difference between these two polarizations states is the direction of rotation, which can be seen schematically in Figure 3. It is clear that the electric field vector performs a helical rotation in the direction of propagation.

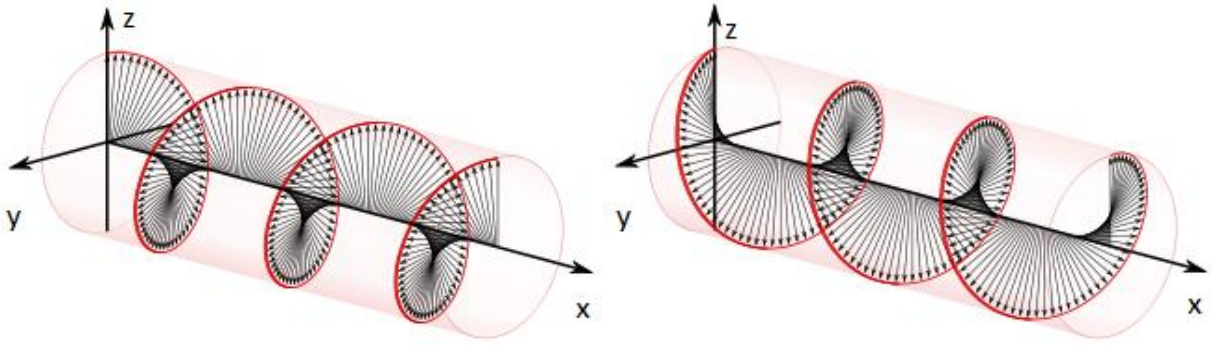

Figure 3. Left- and right-handed elliptically polarized waves, respectively [10].

Because of the different polarization, each one interacts with the ionosphere differently, especially with respect to the refractive index [9]. The refractive index describes how fast a wave travels through a medium according to Snell's Law:

$$\frac{sin\theta_1}{sin\theta_2} = \frac{v_1}{v_2} = \frac{n_2}{n_1} \qquad (1)$$

where θ_1 is the angle of incidence, θ_2 is the angle of refraction, v_1 is the wave velocity in the first medium, v_2 is the wave velocity in the second medium and n_1 and n_2 are the refractive indices of the mediums [3]. These angles are illustrated in Figure 4, and total internal reflection is the case that is of interest for skywave propagation. Also shown in the figure is the critical angle, which is the largest possible angle that still results in a refracted wave. Because the polarization of a wave will affect its angle θ_2, it is clear from equation (1) that waves of different polarizations will have different v_2 velocities.

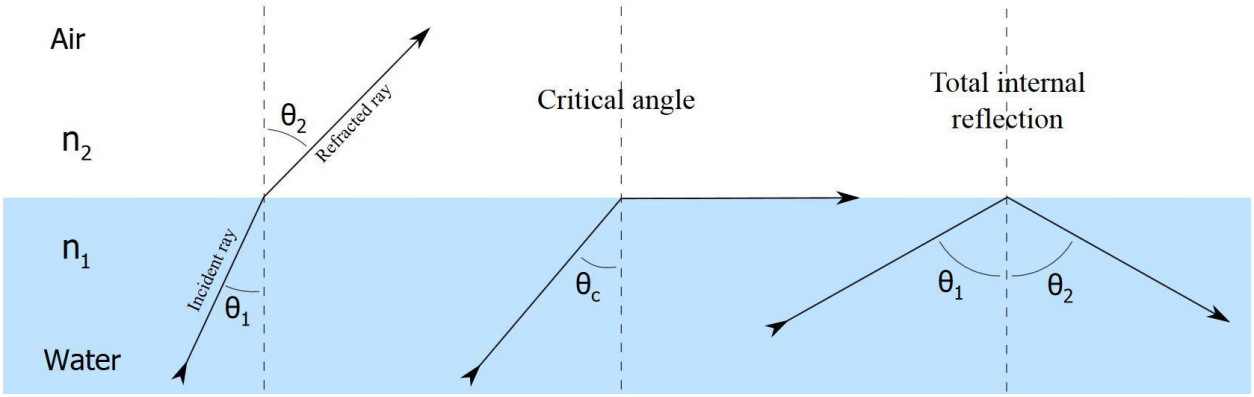

Figure 4. Example illustration of refraction angles through different media [11].

Because X and O have opposite polarizations and therefore different refraction angles, they travel through the ionosphere at different velocities; one wave polarization arrives later than the other. It is important to be able to separate these modes from one another upon reception of a signal so that it can be reconstructed properly. Research has confirmed that a MIMO setup can increase the data rate of HF communication as it allows more than one message to be transmitted and received at once[14]. The goal of this MQP project is to investigate whether sending two simultaneous signals of different polarizations (right- and left-hand circular) will allow the X and O modes to be successfully separated in order to send multiple messages at once without the use of large antenna arrays.

Objectives

The goal of our research involves several well-defined items which can be summarized as follows:

- *Analyze the demonstration channel to confirm the HF channel availability during the period of test*
    - This consists of performing a Voice of America Coverage Analysis Program (VOACAP) analysis. It predicts the Signal-to-Noise ratio (SNR) and other parameters for customized HF circuits and conditions [2]. This will allow the chosen transmission path to be characterized in order to determine operating frequency that should be used for the experiment. We can rely on a cross-dipole antenna and that we will be transmitting from Bedford, MA to Worcester, MA, which is enough information to complete the VOACAP.
- *Develop 3kHz, 20kHz and 90kHz communication waveforms*
    - Two waveforms of different bandwidths will be transmitted and received to investigate the differences in the ability to separate their X and O components. Since a 3 kHz waveform may be much harder to separate, 20 kHz and 90 kHz waveforms will be used as well.
- *Leverage low cost software defined radios and use MITRE antennas for demonstration*
    - The Ettus USRP N210 software defined radio will be used in conjunction with GNU Radio software to handle the transmission and reception of waveforms in the form of reading signals to send and saving received data for post-processing.
- *Perform an over the air test*
    - The transmit location for this test will be MITRE in Bedford, MA, and the receive location will be WPI in Worcester, MA. Cross-dipole antennas will be set up at both locations. The three chosen communication waveforms will be transmitted under different conditions (time of day, etc.) at the frequency determined by the VOACAP analysis. Data will be collected for analysis.
- *Analyze test data*
    - The data from the over the air test will be analyzed to see if the X and O modes can be separated.
- *Develop a set of Recommendations for MITRE*

Approach

VOACAP

The VOACAP analysis served to characterize the signal path between Bedford, MA, and Worcester, MA, at the time of transmission. Figure 5 shows the parameters used for this analysis, as well as the Signal-to-Noise Ratio (SNR), Maximum Usable Frequency (MUF), and Frequency of Optimal Transmission (FOT). This information tells us at what frequencies we can transmit, and at what times of day. From the figure, it is clear that we can transmit below 8MHz during the day (our time zone is four hours behind UT), but at night the MUF drops as low as 4MHz. Our frequency allocation is at 5.005MHz with a 100 kHz bandwidth. Because most of our testing will occur during the day, we decided to transmit at 5.055MHz. This frequency is within our allocation, and is usable throughout the day with reasonable SNR. For the purposes of this experiment, an SNR of at least 20 dB is desired.

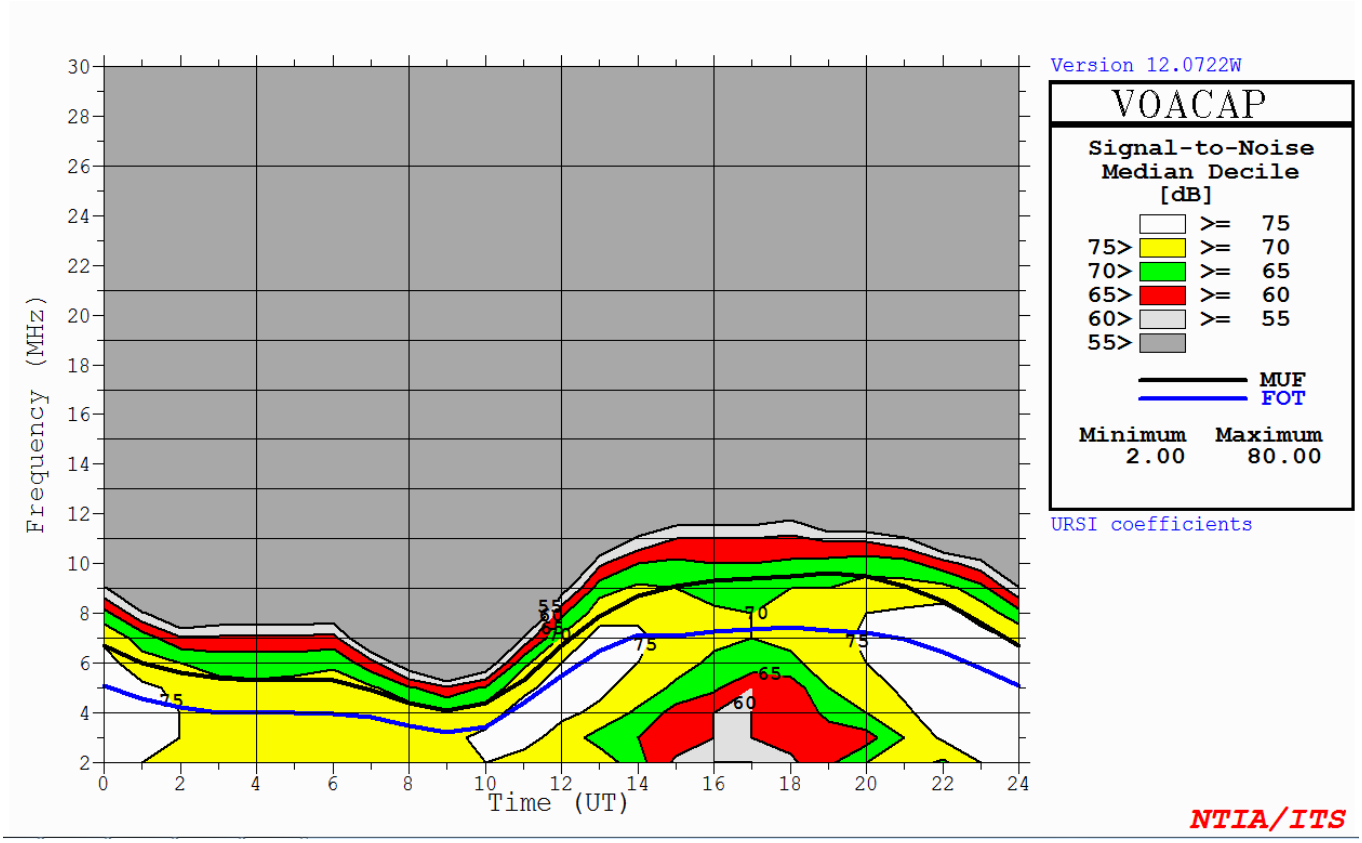

Figure 5. VOACAP analysis along with parameters used.

Hardware Development

Overall System Configuration

In order to properly transmit and receive the desired waveform, it was important to configure the appropriate hardware. We will describe all the hardware systems we employed and for what particular purpose.

Transmit Chain

Figure 6 shows a general block diagram of the hardware needed to transmit our signal. We had to be able to produce an output power of at least 10W to the antenna. The power had to be adjustable in order to study the various transmission protocols, such as the trade-offs between power, time of day, solar activity, etc.

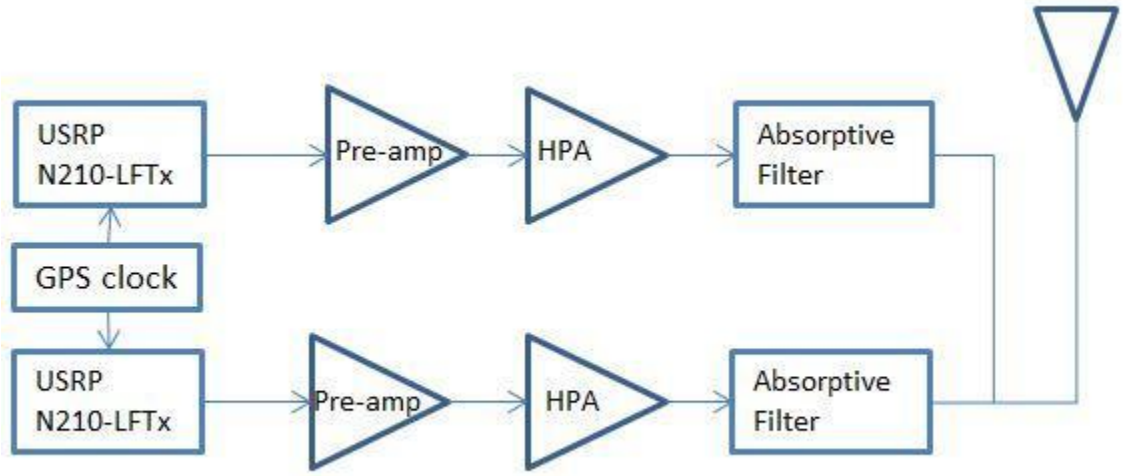

Figure 6. Transmit system block diagram showing the transmitting USRPs, pre-amplifiers, high-power amplifiers, filters, and antenna.

The system block diagrams are as follows:

- Ettus USRP N210
    - The USRP N210 software defined radio is created with a modular design, allowing it to run from DC to 6GHz depending on the daughter boards used with the system [17]. When using the radio, a computer acts as the processor through its Gigabit Ethernet interface.

For this project two USRPs will be creating and sending each polarized signal and its waveform, while two more receive and store the data of each polarized signal at the other end. One computer at each end controls both radios which are connected by a MIMO cable. This allows the radios to start transmitting at the same time. The radios each have LFTX daughter boards that allow for transmission of signals from DC to 30MHz [17].

- GPS clock
    - The transmit site uses the Symmetricom XLi SAASM GB-GRAM rubidium clock to provide a pulse-per-second and 10 MHz reference clocks. This clock has better than picosecond frequency accuracy. It is important for the USRPs to use GPS disciplined clocks so that both the transmit and receive time references are identical, which prevents discrepancies in frequency and time between the two sets of radios. This helps combat issues such as drift or phase offset.
- Pre-amplifiers
    - The output power of the USRPs is about 3.5-4dBm. This needs to be increased to about 40dBm for transmission, with a maximum transmit power of approximately 50dBm for testing. The pre-amplifiers are the first of two necessary amplification stages to reach this power. For this stage, the ZHL-32A amplifier has a gain of about 30dB, as can be seen in the characteristic in Figure 7. Pre-amps I and II differed in gain by only .03dBm, at our operating point of 3.5-4dBm, where pre-amp III has a gain that is at least .07dBm greater than the other two.

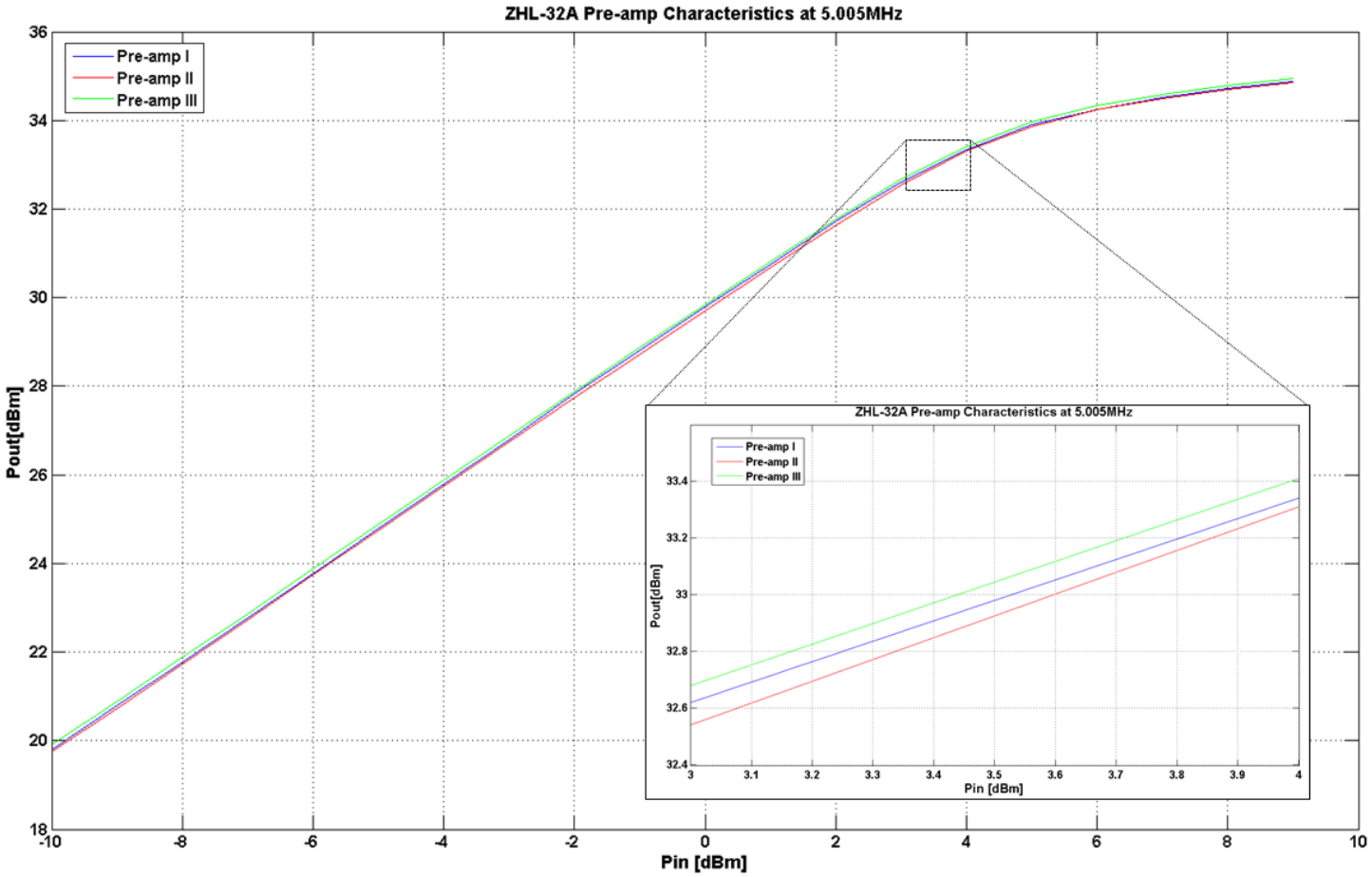

Figure 7. The ZHL-32A pre-amplifier power gain characteristics are very close to each other, and the zoomed frame shows the characteristic at the desired operating point.

- High Power Amplifiers
    - The TC300 amplifiers were used to drive the high power output. The amplifiers require at least 1W input, which is why the pre-amplifier stage was necessary. Even though the systems are capable of producing up to 100W, for the purpose of our experiment we configured our system to generate up to 40W. The characteristic for both amplifiers can be seen in Figure 8. From the measured data, the 1dB compression point is at about 27dBm. As a result, we are operating in the non-linear range to get the desired output power. Because of this and because the gains of the amplifiers are dissimilar, the output power was measured and adjusted before each transmission to make sure the channels were well-matched, ideally within a few tenths of a dB.

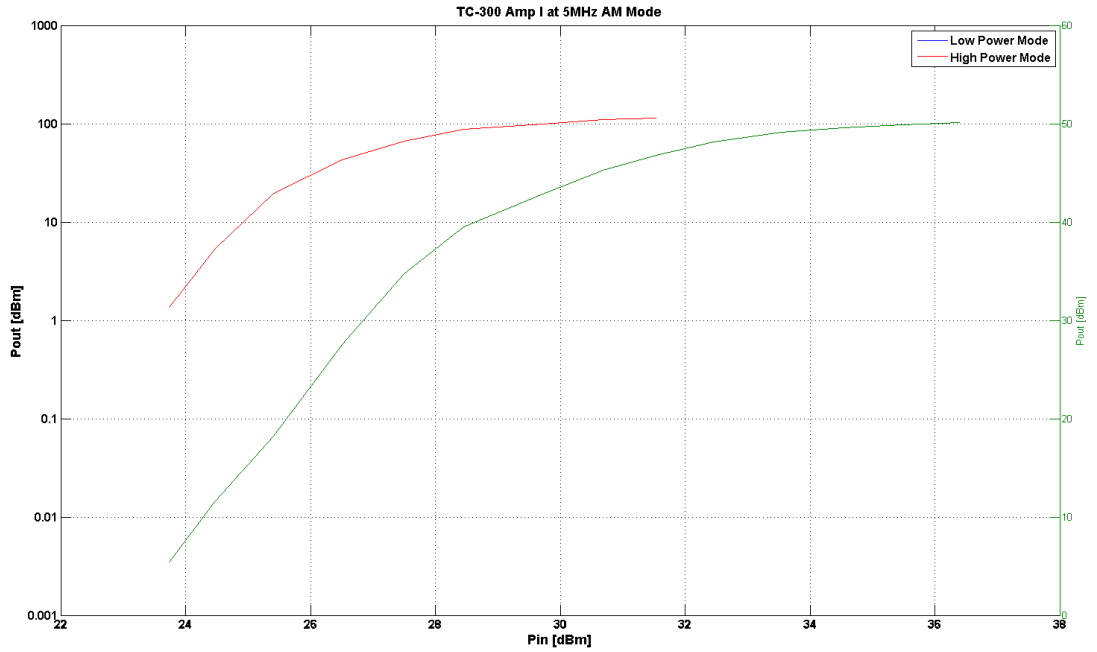

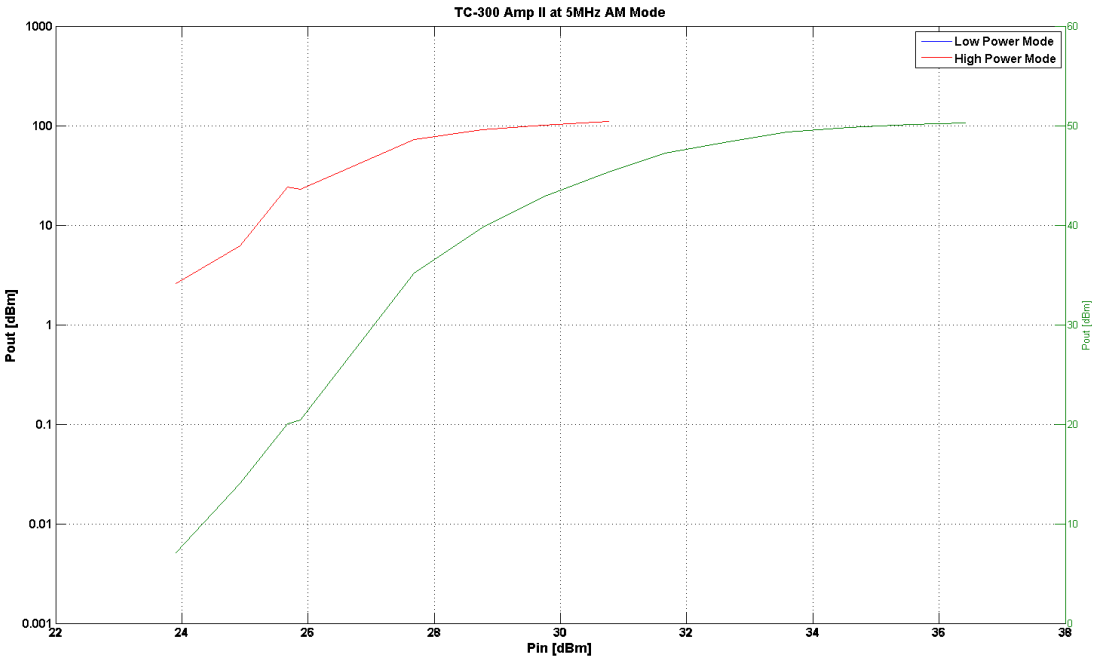

Figure 8. High Power Amplifier gain characteristics.

- Absorptive Filter
    - The TC300 power amplifiers generate unwanted harmonics at relatively high power levels, the highest of which was only 5dB below our desired power level. In order to eliminate these, we built absorptive filters. The schematic can be seen in Figure 9. The filter consists of a high-pass and low-pass filter in parallel, each of which is implemented as a three-pole Chebyshev filter. The load to the low-pass filter, R1, is the antenna. The load to the high-pass filter, R2, is a dummy load that absorbs the unwanted power so that it does not reflect back into the amplifier causing oscillation. This is why an absorptive filter design was used instead of a band pass filter, which would have reflected power into the amplifier.
    - The air core inductors were hand-wound with solid copper 16-gauge wire with a half-inch diameter. The .5μH inductor required seven turns, and the 1.1μH inductor required 11 turns [12]**.** UHF connectors were employed for the input and output ports because, although not quite as reliable as N-connectors, they were more readily available.
    - The ideal behavior of this filter is seen in Figure 10**.** It is clear that there is a high pass and low pass filter, and that the cutoff frequency of the low pass filter is about 9MHz. The harmonics the TC300 amplifiers were putting out were particularly high at 15MHz. According to the characteristic, there is about 20dB of attenuation at this frequency. A filter with more poles would have a steeper slope, but given time and resources, this was the most practical solution. Figures 11 and 12 show the characteristics of the completed filters. They are very similar to each other, and at 15MHz, which is the first large harmonic, the power is reduced by about -14.5dB, which is enough attenuation as we are transmitting at low power levels. This is not quite as much attenuation as the simulation suggested the filters would provide, although it is sufficient for our purposes. This discrepancy is most likely due to the inexact inductor values; we were unable to measure the exact value of the hand-wound inductors.

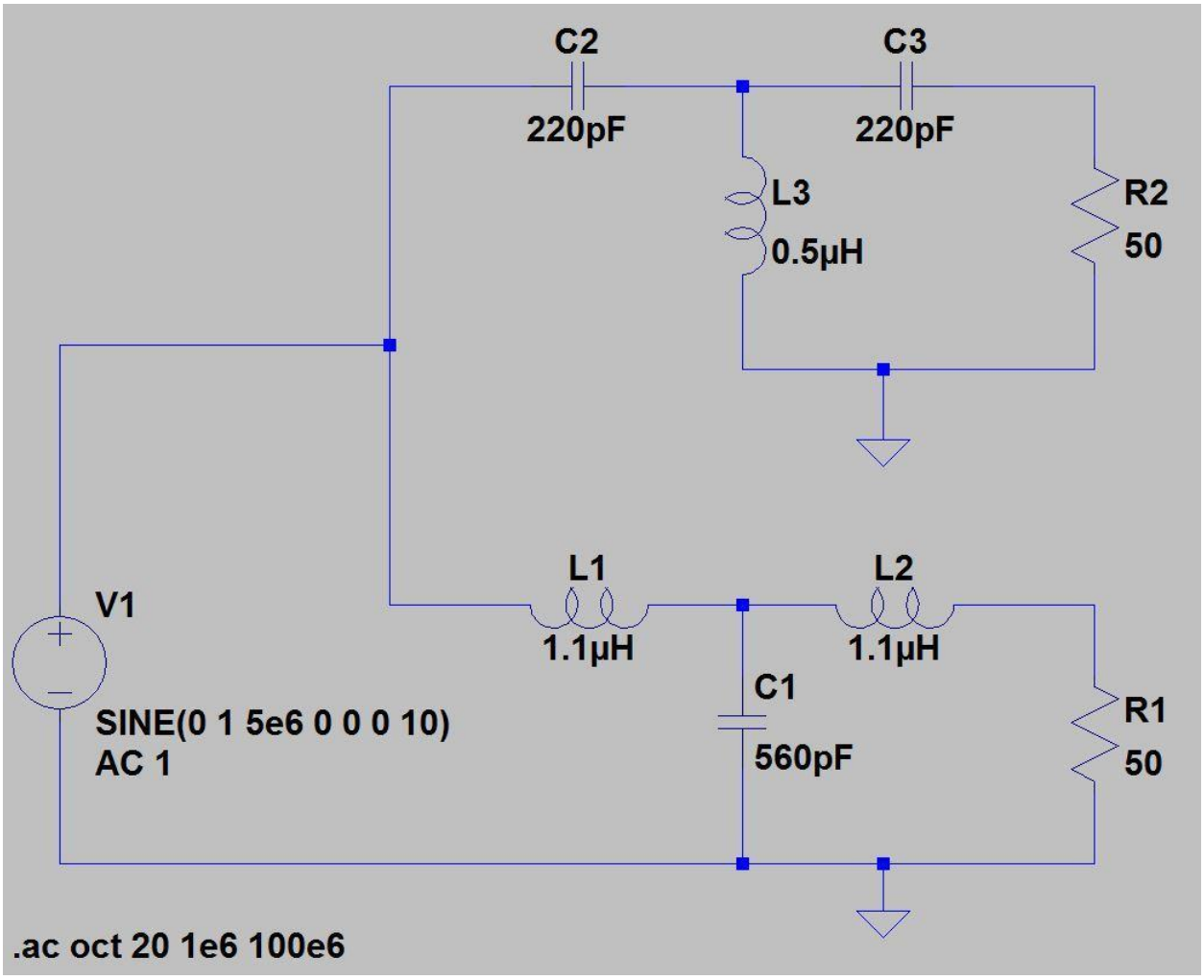

Figure 9. Absorptive filter schematic. The antenna is modeled as R1 and connected to a low pass T-network; the high pass Tnetwork is connected to the load resistor R2.

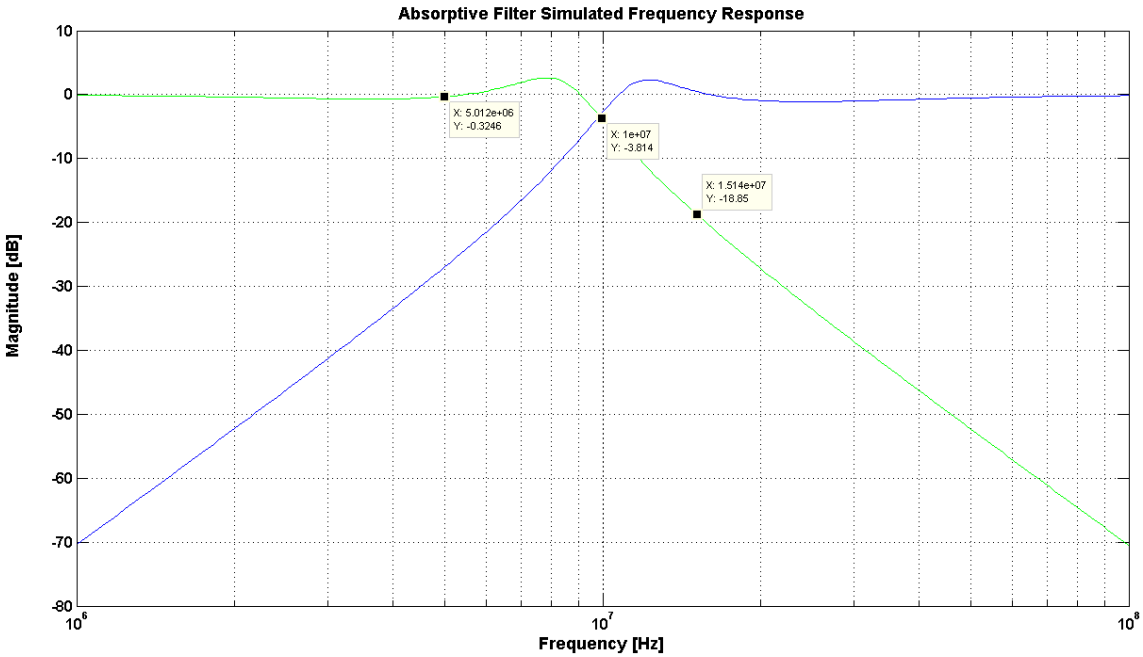

Figure 10. Absorptive Filter characteristic where the green is the power across R1 and blue is the power across R2.

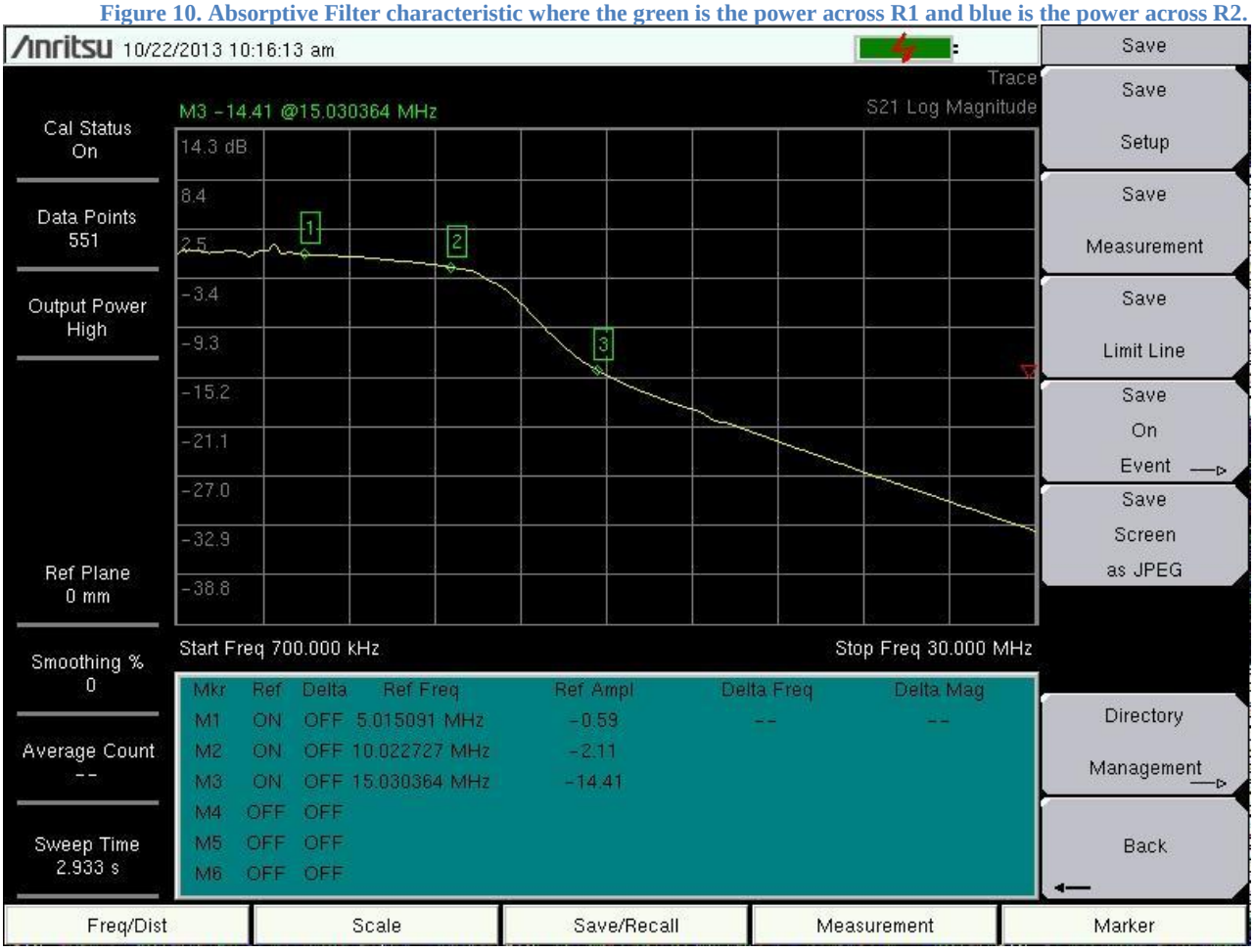

Figure 11. Characteristic of absorptive filter I with measurements at several frequencies.

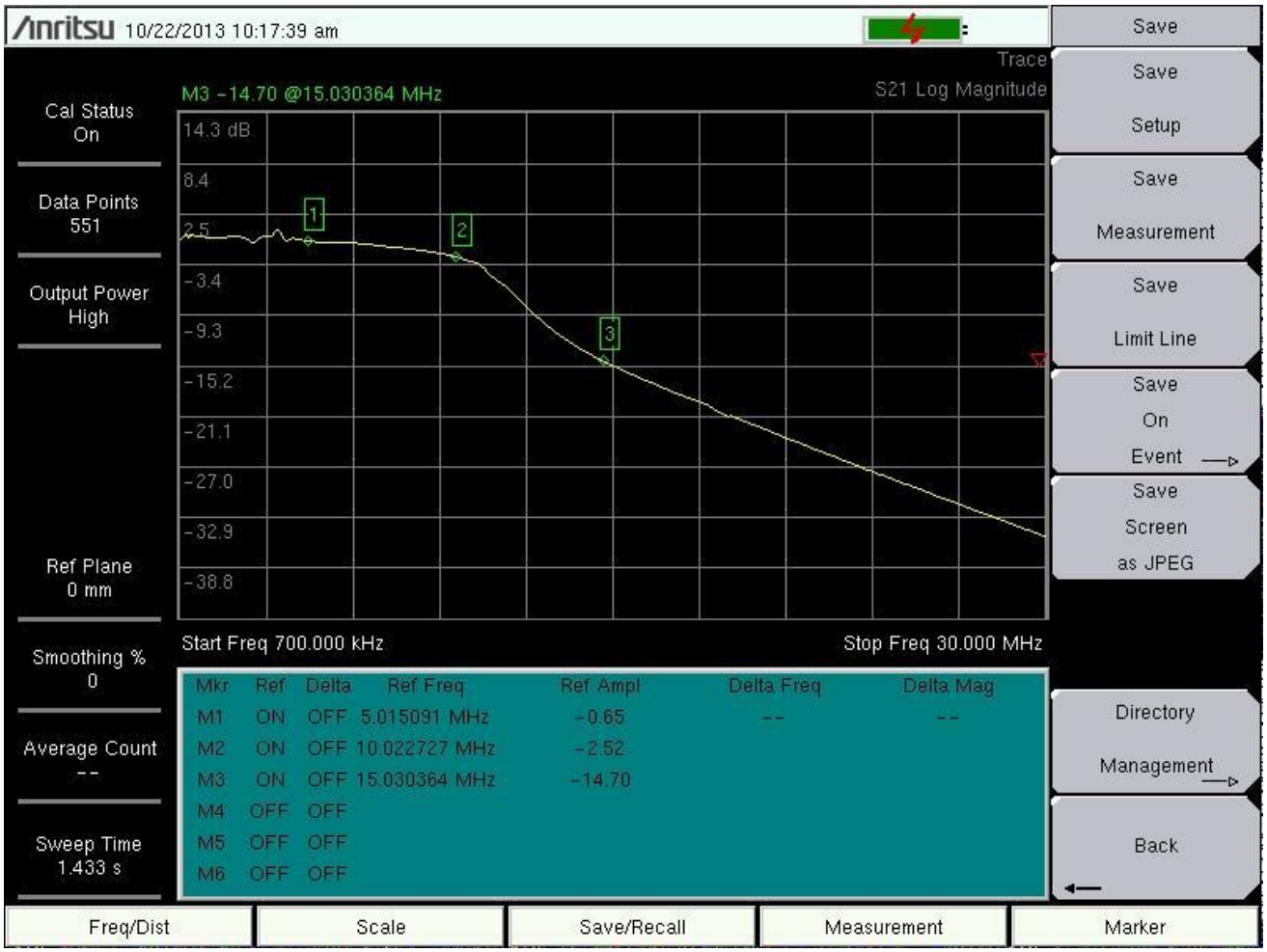

Figure 12. Characteristic of absorptive filter II with measurements at several frequencies.

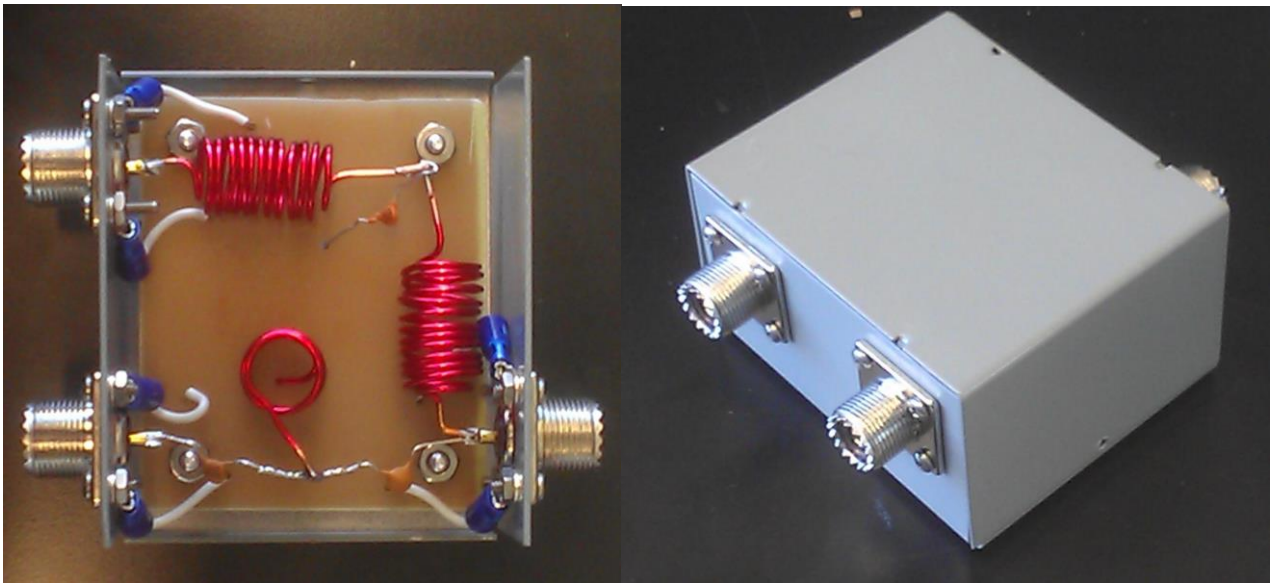

Figure 13. Interior and exterior of finished filter.

- Cross-Dipole Antenna
    - In order to achieve the polarized signals desired for this experiment, a cross dipole antenna 30 feet tall with a 108 foot diameter located at MITRE in Bedford was used. The antenna consists of a 30 foot mast, wires, and resistors, constructed in a design similar to two orthogonal bowties, as shown in Figure 14. Each bowtie forms its own separate dipole and as such acts as its own antenna, which allows for two separate signals to be sent simultaneously. Then as the dipoles are orthogonal, both a right and left handed polarized signal are able to be sent at once. Each dipole with its corresponding wires is attached to its own separate CWS ByteMark Bal-300 balun at the top of the mast. These baluns are then attached to cables leading to the transmit equipment set up at the other end. A schematic for this balun can be found in Appendix II in Figure 33.

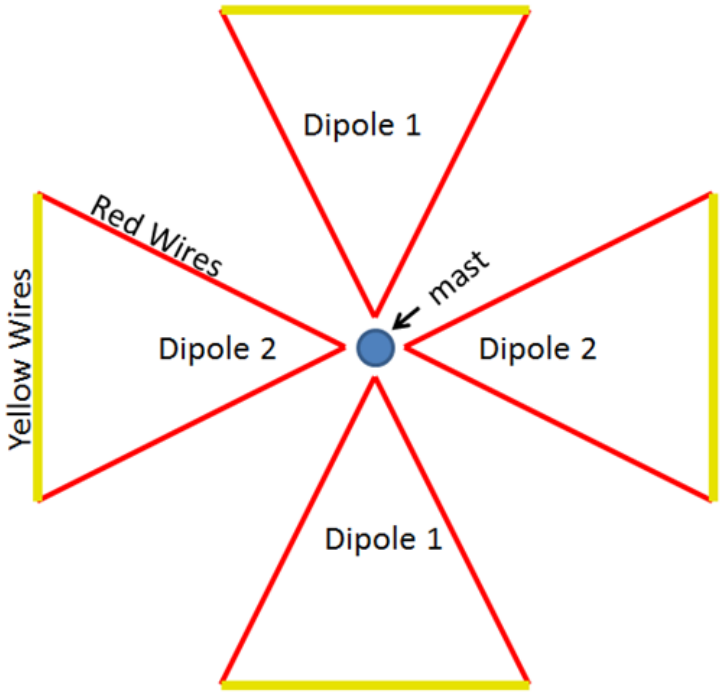

Figure 14. Cross-dipole antenna configuration (top view).

In addition, we needed two DC power supplies; the pre-amplifiers require 24V and the HPAs require 12V. We used an Anritsu MS2034A portable spectrum analyzer to measure our power levels and variable attenuators which were inserted directly after the USRPs in order to allow us to change the high power

output. The dummy loads for the absorptive filters we used were one 30dB 500W Tenuline Coaxial Attenuator, and one 50Ω 250W Termaline Coaxial Resistor.

Receiver Chain

Figure 15 shows the system block diagram for the receive end of the chain which receives the transmitted signal and records it. Filters and low-noise amplifier were implemented to increase the SNR of the received signal and remove out of band noise.

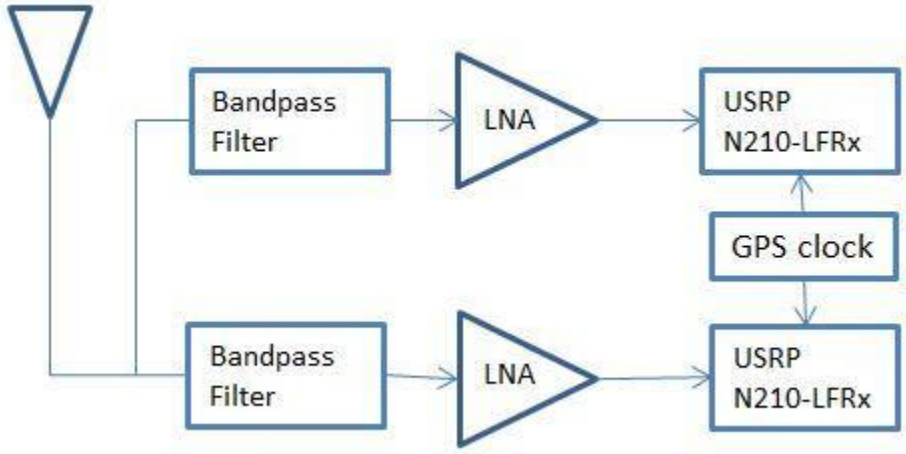

Figure 15. Receive system block diagram showing the antenna, band pass filters, low-noise amplifiers, and receive USRPs.

The system block diagrams are as follows:

- Cross-dipole antenna

  This is the same antenna as the one used for transmit, except that it is a smaller version standing 16 feet tall with a 64 foot diameter. We set it up at WPI, and the Voltage Standing Wave Ratio (VSWR) was measured to make sure the antenna was working properly and can be seen in the following figure. Typically, a VSWR between 1.4 and 2 required, with a ratio of 2:1 being prime. It can be seen in Figure 16 that at 5MHz the antenna is operating as expected. A more detailed illustration of the dipole used can be seen in Figure 32 located in Appendix II.

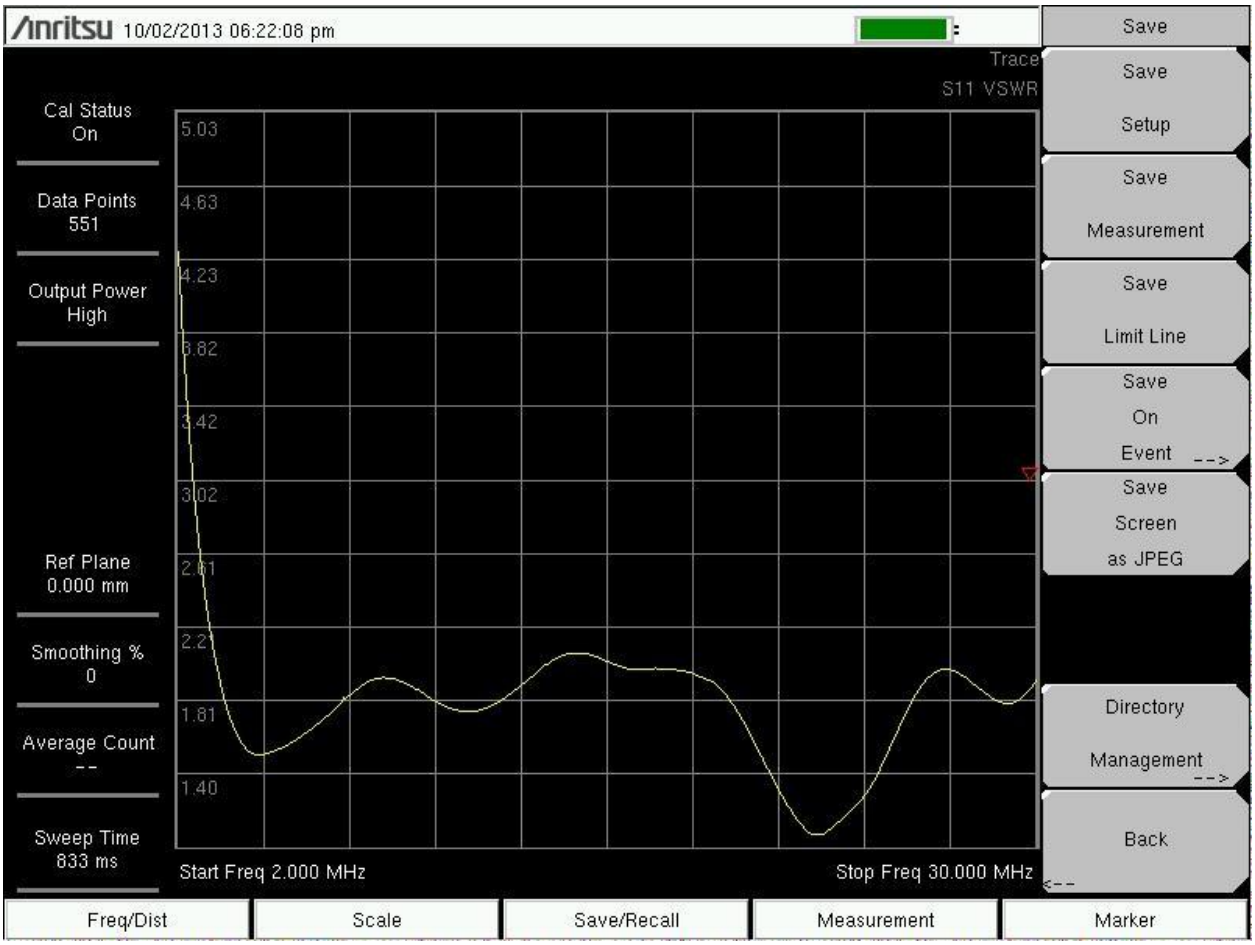

Figure 16. Network Analyzer photo of WPI cross-dipole VSWR.

- Band pass Filters
  - The first thing done with the signal after receiving it is to filter out everything not in our band. The Heros SCR Preselector, which is a tunable band pass filter, accomplished this filtering. On the filters, the 5-9MHz band was selected, and then they were tuned to a center frequency of 5.055MHz.
- Low-noise amplifiers
  - The amplifier we used after the filter was the ZFL-500LN, intended to increase the received signal with minimal amplification of the noise, measured by its noise figure of 2.9dB [16]. It was operated at 12V DC, which resulted in a gain of about 27dB. A higher gain of about 30dB could have been achieved with a 15V DC drive, but we were limited by our available power supplies. The gain characteristic can be seen in Figure 17. LNAs I and III were chosen because they had a

difference in gain of about 0.14dBm, where LNA II had a difference in gain of at least 0.21dBm from either of the others.

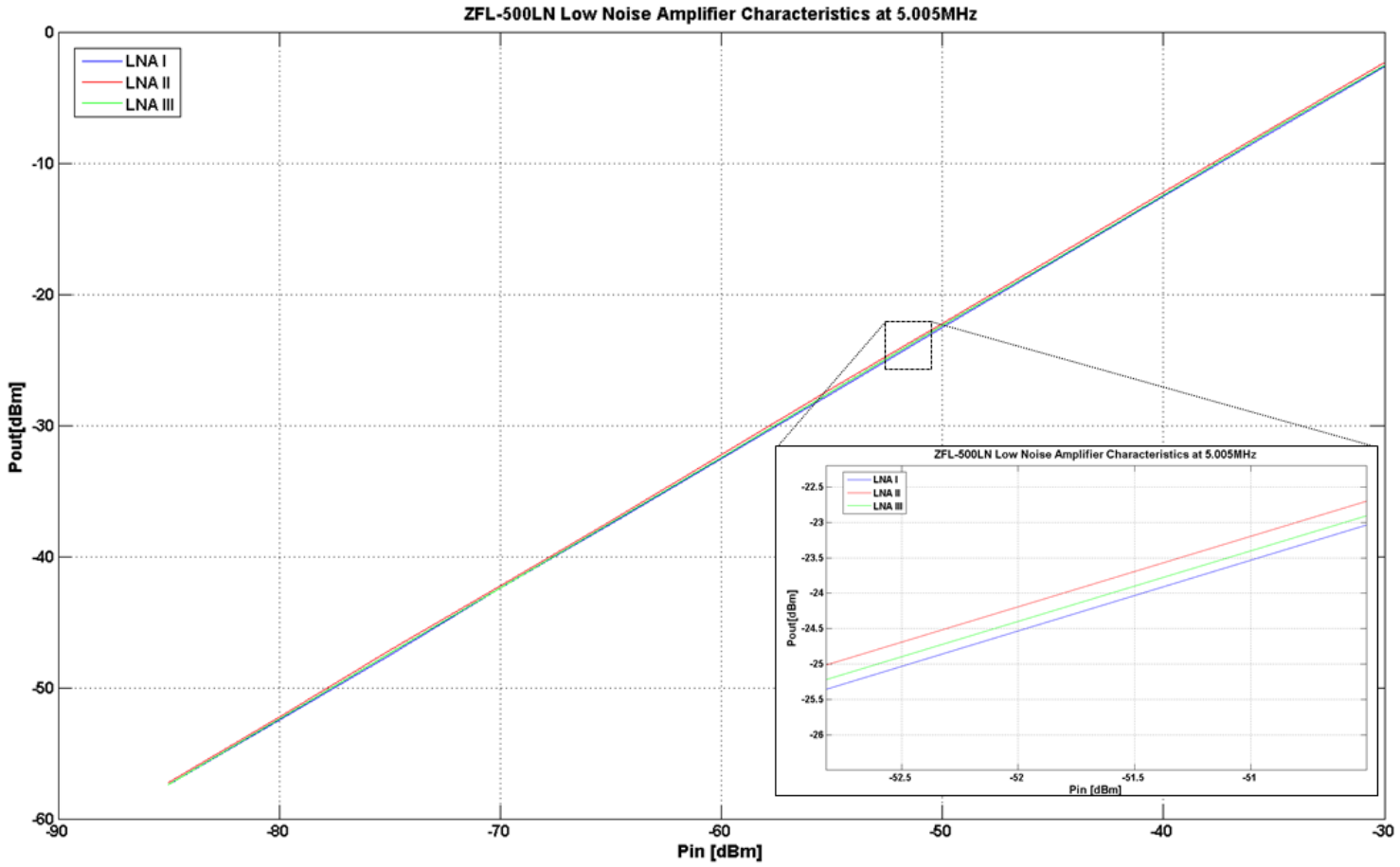

Figure 17. LNA gain characteristic with the zoomed-in area better showing the differences in gains. These amplifiers do not go into compression for this range of inputs.

- Ettus USRP N210
    - These radios also received and recorded the signal. They only differ from the transmit radios in their daughter cards; they use the LFRx cards. The LFRx daughter card allows for reception between DC to 30MHz [17].
- GPS clock
    - The receive site uses a GPS10RBN rubidium clock to provide pulse-per-second and 10 MHz reference clocks. It is accurate to parts in 10^{-15} and also locks on to a GPS signal.

Other hardware included one DC power supply to power the filters and LNAs, a computer to control the radios, and various connectors and cables.

Software Development

GNU Radio

GNU Radio is an open-source software development toolkit that allows for signal processing through the use of blocks, simulation, and interfacing with Software Defined Radios (SDR). With direct support from the Ettus USRP family, it provides the tools necessary to program the SDR. Gnu Radio is also coupled with GNU Radio Companion (GRC). GRC provides a visual way to program and simulate using flowcharts and blocks. Data is passed from one block to the next and handled on a block by block basis, creating a module design [18]. Each flowchart in GRC must begin with a source and end with a sink, and these sources and sinks are defined from the computer's point of view. This means that if one wishes to transmit, they would send the data to a USRP sink, which would send the data from the computer to the USRP.

LFM Generation

The signal chosen for transmission was a linear frequency modulated signal (LFM), also known as a chirp. This is a signal that starts at a chosen frequency and increases or decreases linearly to another specified frequency over a given amount of time. Sending a chirp covers all frequencies in its bandwidth and therefore is a good representation of the various signals that can be present in that range, and also makes post-processing more straightforward.

We created several LFMs with various bandwidths. The three different bandwidths were 3 kHz, 20 kHz, and 90 kHz. For all of these, the length of the chirp was .02 seconds which is equivalent to a waveform repetition frequency of 50Hz. This means there are 50 waveforms in one second. In GRC, this waveform was accomplished using the frequency modulation block. This block works by modelling the frequency modulation of a sine wave after an input signal. For example, a saw tooth signal will result in an LFM that increases in frequency, while a triangle wave would result in one that increases and then decreases linearly. Sending a saw tooth signal with the aforementioned repetition frequency created the desired LFM. An example of the flowchart used is shown in Figure 18. Other important blocks present in the flowchart include the File Sink, which automatically saves the data it receives in a complex binary format, which can later be read by MATLAB. There is also a Throttle block that limits the simulation to whatever rate is specified in the block. This is only needed for flowcharts that are simulations and do not

contain hardware parts. The other blocks are simply variables used elsewhere in the flowchart, or blocks needed to change data types throughout the chain.

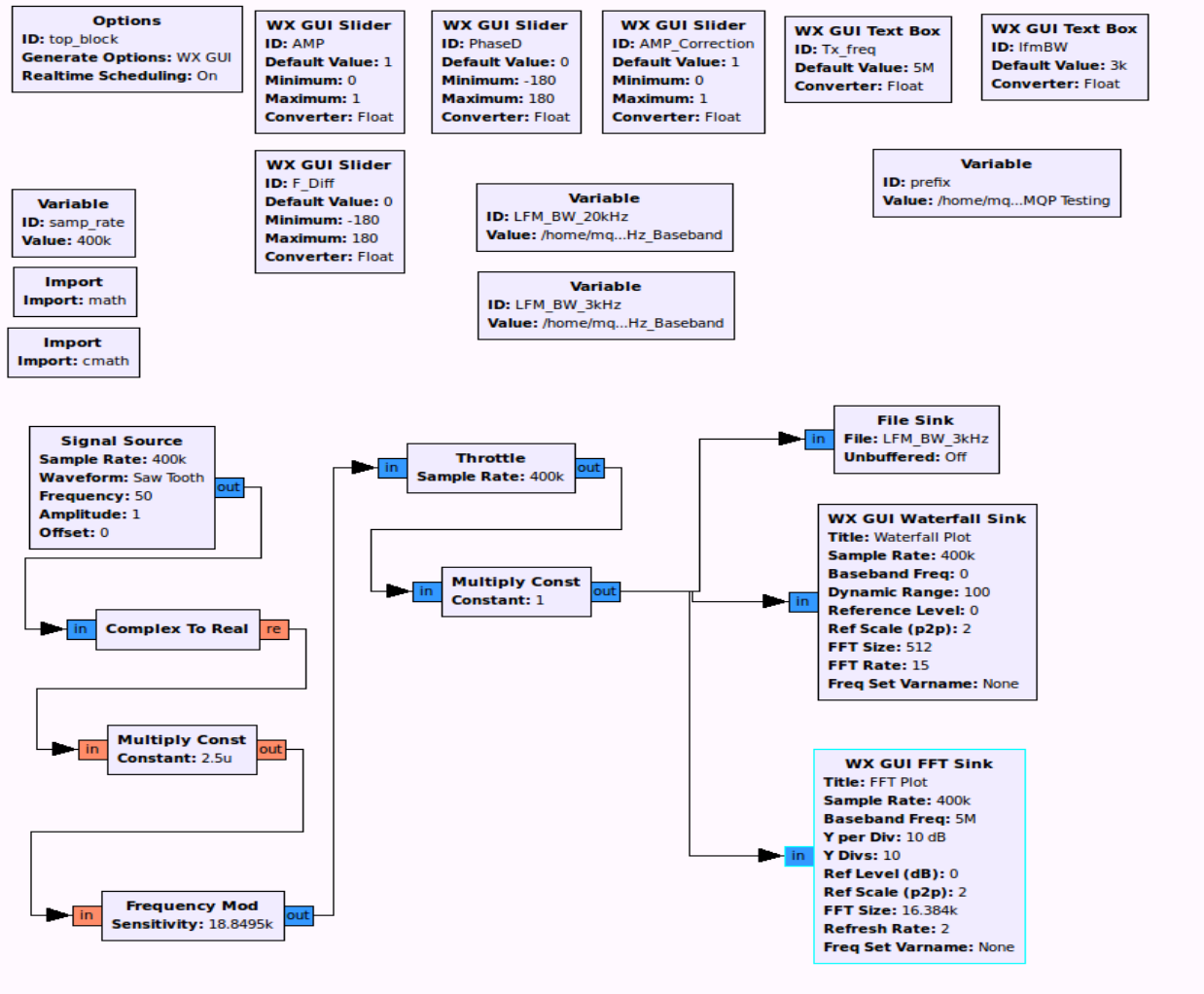

Figure 18. GRC flowchart to create and simulate LFM.

Hybrid Implementation

The purpose of a quadrature hybrid is to have a "90^{o} phase difference between the outputs of the through and coupled arms," [15]. An example of a quadrature hybrid in microstrip line form can be seen in Figure 19. It implements lambda-quarter length strips to achieve the phase shift. The lambda quarter transformer is typically used for impedance matching, in this figure at ports 2 and 3, and has the 90^{o} phase difference, where port 2 is the through arm and port 3 is the coupled arm. Power is divided evenly between the two ports and because this device is symmetric, any port can be used as an input. If a signal were to be input on two of the ports, ports 1 and 4 for example, the signals would be summed on the

output ports. An illustration of this can be seen in Figure 20. If each of these outputs is transmitted on different arms of the cross-dipole at the same time, the signals will be circularly polarized.

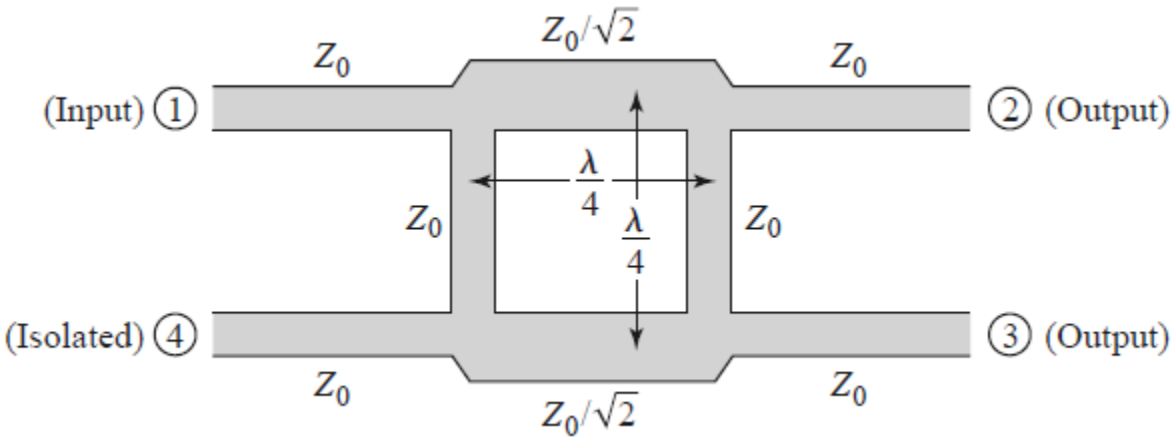

Figure 19. Microstripline form of quadrature hybrid utilizing lambda-quarter transformer [15].

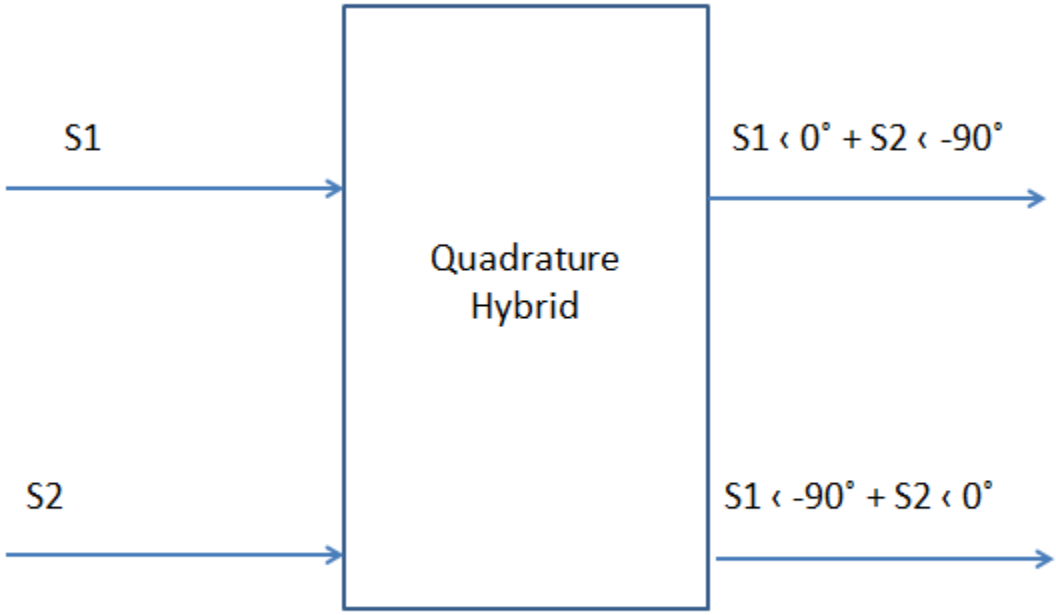

Figure 20. Illustration of how a quadrature hybrid works with two inputs S1 and S2.

However, we were unable to acquire a quadrature hybrid within our time frame because the frequency of operation is very low in the HF spectrum and it is not commonly used. As a result, the lead

time for obtaining the component was too long. It was decided that the quadrature could be implemented in software; it would be straightforward to shift the signals by 90º and then sum them. The hybrid was implemented both in MATLAB as well as GNU Radio, with the final decision being to use the MATLAB version for testing to save on processing power. For reference, the GNU Radio implementation is shown in Figure 21 and the MATLAB code can be found in Appendix A. Figure 21 depicts the flowchart to build the hybrid in GNU Radio. Similarly to the previous GRC flowchart, two LFMs are created at the start of each chain using a signal source block. Each LFM is then split, and a multiply constant block shifts one of the splits by 90 degrees. This is done by multiplying by cos(90*180/pi)+j*sin(90*180/pi). Finally, the four signals are added together to create the outputs of a quadrature hybrid as shown in Figure 20, and each of the two signals are sent to their respective USRP radios. One more multiply constant block right before the input to one of the radios is for aligning the phases of the radios. It was calculated before official testing by observing the phase offset on an oscilloscope when sending a simple sinusoid. This phase offset remains constant as long as the radios are on.

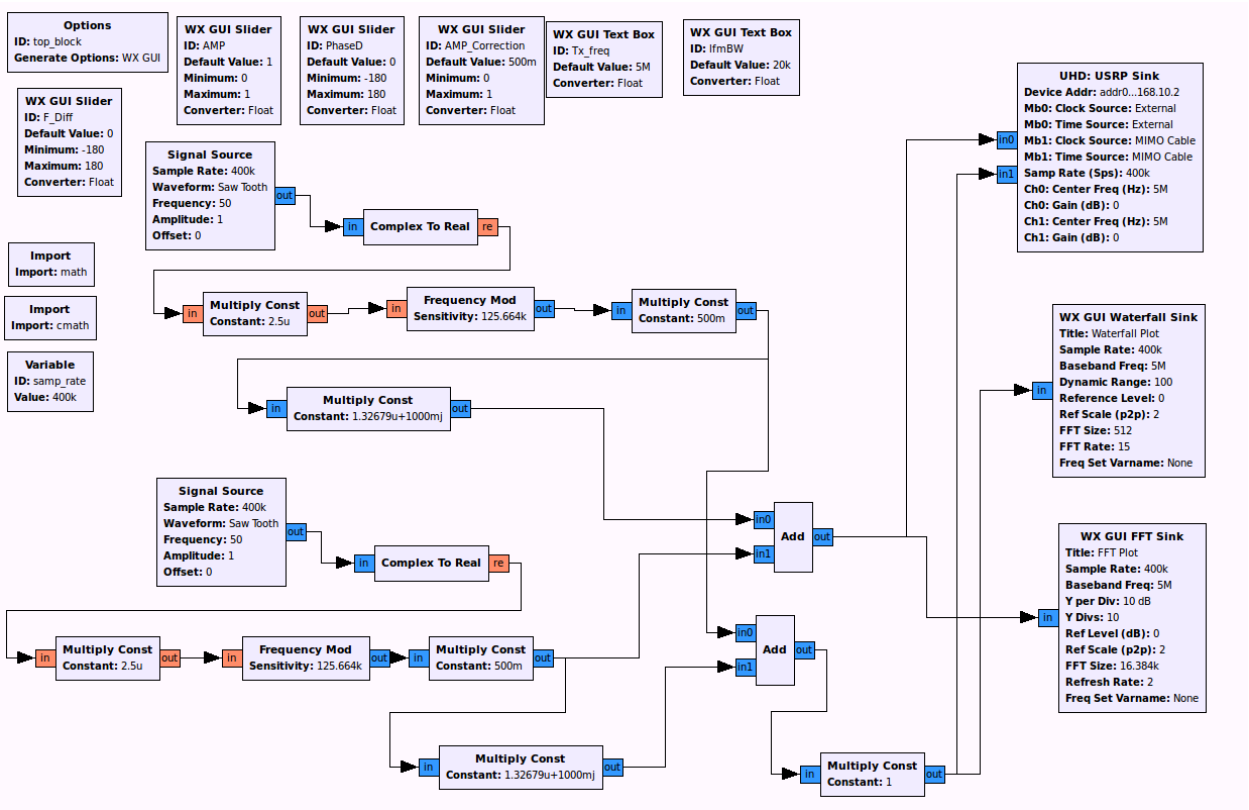

Figure 21. Software implementation of hybrid in GRC.

The two signals that we would send would have the same bandwidth, but would be offset in frequency by 10Hz. This would allow for various post-processing parameters to be calculated and to see if the signals could be separated at the receiver.

Final Design (MATLAB Implementation)

In the end, all of the waveforms were generated in MATLAB instead of in GNU radio. Those waveforms could then be saved as a file and be read by GRC, which would allow the radios to transmit the desired signal. The flowcharts of the protocols to read in the file and transmit it, as well as to receive the signal and save the data in a file are shown in Figures 22 and 23.

Using MATLAB to generate waveform files had several advantages. As GRC no longer had to generate the waveform while transmitting the required processing power was significantly reduced. In addition, using MATLAB allowed the signal to be tapered in amplitude at its ends in the time domain. This taper cleans up the edges of the LFM, as it smooths out the transition of the signal from the end frequency back to the start frequency. This transition, if not smoothed out, may introduce unintended transmissions outside of the LFM's bandwidth.

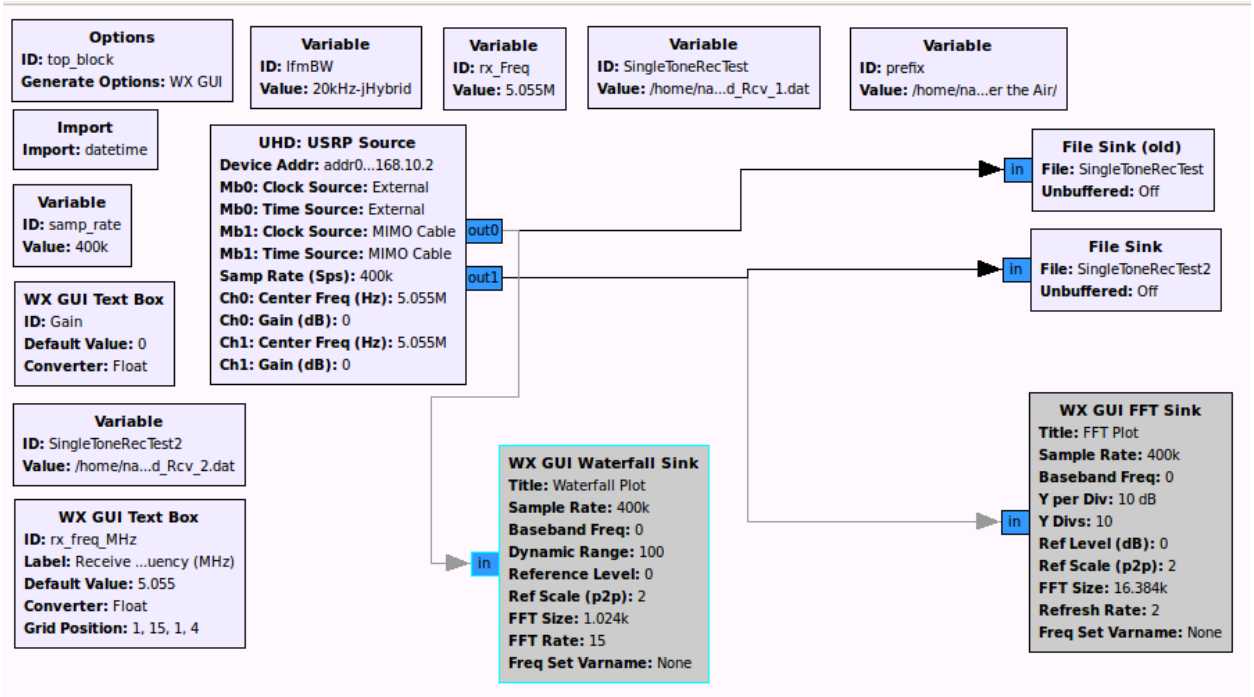

Figure 22. Final receive flowchart for testing.

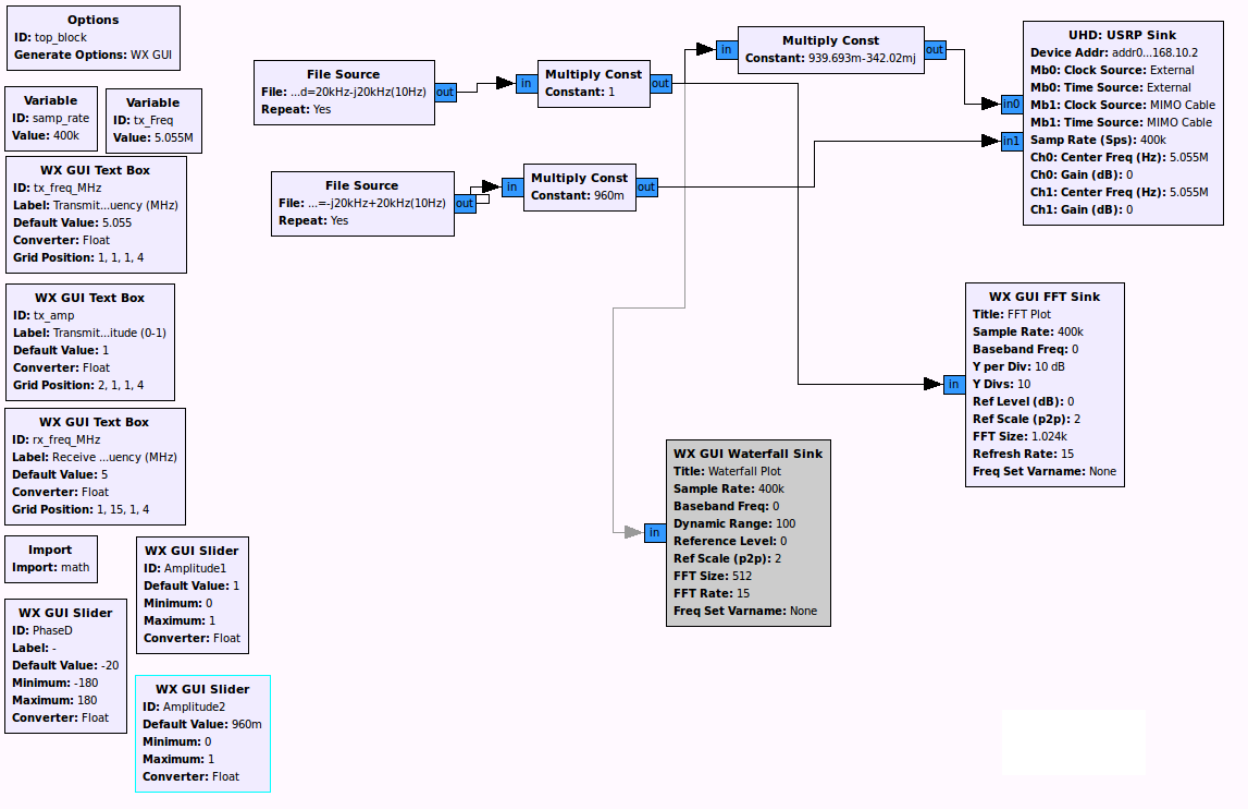

Figure 23. Final transmit flowchart for testing.

In Figure 22 it can be seen that the flowchart starts with a USRP source and goes directly into a file sink. This results in data received from the USRP to go directly into a file with no signal processing in between. There are also two GUI interfaces, a waterfall plot and FFT plot. When receiving, the GUIs would first be used to check if the desired bandwidth was free, and then to check if the received signal could be seen. Then the GUIs were disabled to conserve computer processing power, and the file sinks were enabled. This was repeated for each measurement.

For transmit, Figure 23 shows the flowchart implemented. A file source reads in the signal data from a MATLAB-generated file. Two multiply constant blocks are used on each signal to fine-tune the power levels of the two radios. Finally another multiply constant block was used to align the phase of one radio to the other in order to guarantee circular polarization. These outputs go out to the USRP sink for transmission. Similar to the receive flowchart, waterfall and FFT GUI blocks exist to check the signal before it is sent out to the USRP block.

How GNU Radio handles the carrier frequency

GNU Radio processes samples in I/Q form; which means that is that signals are represented in complex form. When modulating a signal up to a carrier frequency, that signal will be frequency modulated - not amplitude modulated. This is relevant because amplitude modulation is more susceptible to noise and interference in this setting.

MATLAB

LFM code

The formula for a chirp is as follows:

$$x = e^{j(d\omega/dt * t^2/2 + \omega_o t + \phi)} \quad (2)$$

where ω_0 is the angular start frequency, t is time, Φ is a phase shift in radians and $d\omega/dt$ is the chirp rate. A common way to define the chirp rate is:

$$\frac{d\omega}{dt} = \frac{\omega - \omega_o}{t} \quad (3)$$

The bandwidth is changed by adjusting the chirp rate. To phase shift each signal by 90^o for the purposes of simulating the hybrid, Φ simply had to be defined as $\pi/2$. The benefit of using the exponential form of the chirp is that it yields both the real and imaginary parts of the waveform needed for the Ettus and GRC to read in I/Q data.

As described in the previous section, a Tukey taper was applied to the LFM to smooth the edges and reduce out of band noise**.** All of the scripts used can be found in Appendix A. Figure 24 shows the time domain signal of a tapered chirp with a bandwidth of 20 kHz, a chirp length of .05 seconds, and a sample rate of 400 kHz.

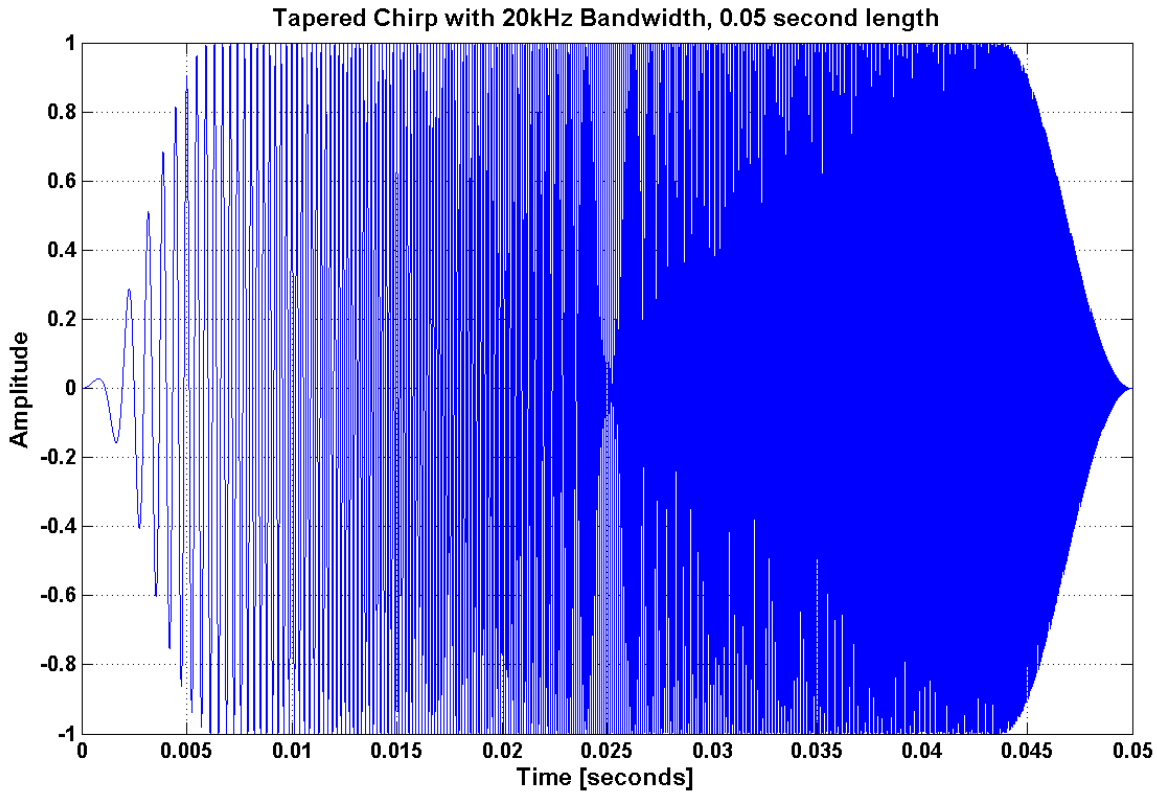

Figure 24. Time domain plot of a tapered, 20 kHz chirp.

Post Processing

Post-processing includes generating spectrograms and range-Doppler plots of the received signals. These plots allow the power at each frequency over time to be observed, as well as the range and Doppler of each received signal. The range and Doppler allow us to see if the X and O modes are visible, as their different velocities will result in different arrival times.

Methodology

This section will describe the times at which data was collected, as well as circumstances and problems that arose.

First Data Collection

Our first data collection was on Tuesday, October 15th 2013. Cecelia was at the receive site in Worcester and Nathan was transmitting in Bedford. It was a partly cloudy day. By the end of the day, we were able to successfully receive a signal in Worcester. We started early morning, but could not start receiving until afternoon because of various technical issues, most of which had to do with faulty power supplies at the transmit site. These issues were not properly identified and resolved until the second data collection. In addition, the GPS clock on the receive end took about three hours to lock to GPS. On transmit, the cross-dipole had to be repaired because a couple of the lines had been severed. This meant that the antenna had to be lowered, the wires replaced, and the antenna raised back up before transmission could occur. The VSWR also had to be measured again to make sure the replacement wires still allowed acceptable performance of the antenna. The received signal was a 20 kHz LFM transmitted at 5.005MHz at a power level of about 40W. A spectrogram in Figure 25 shows the received signal. It is not very clear because this was an early version of the LFM without the taper. However, the signal is still clearly visible. The colors in the figure indicate the power in dB.

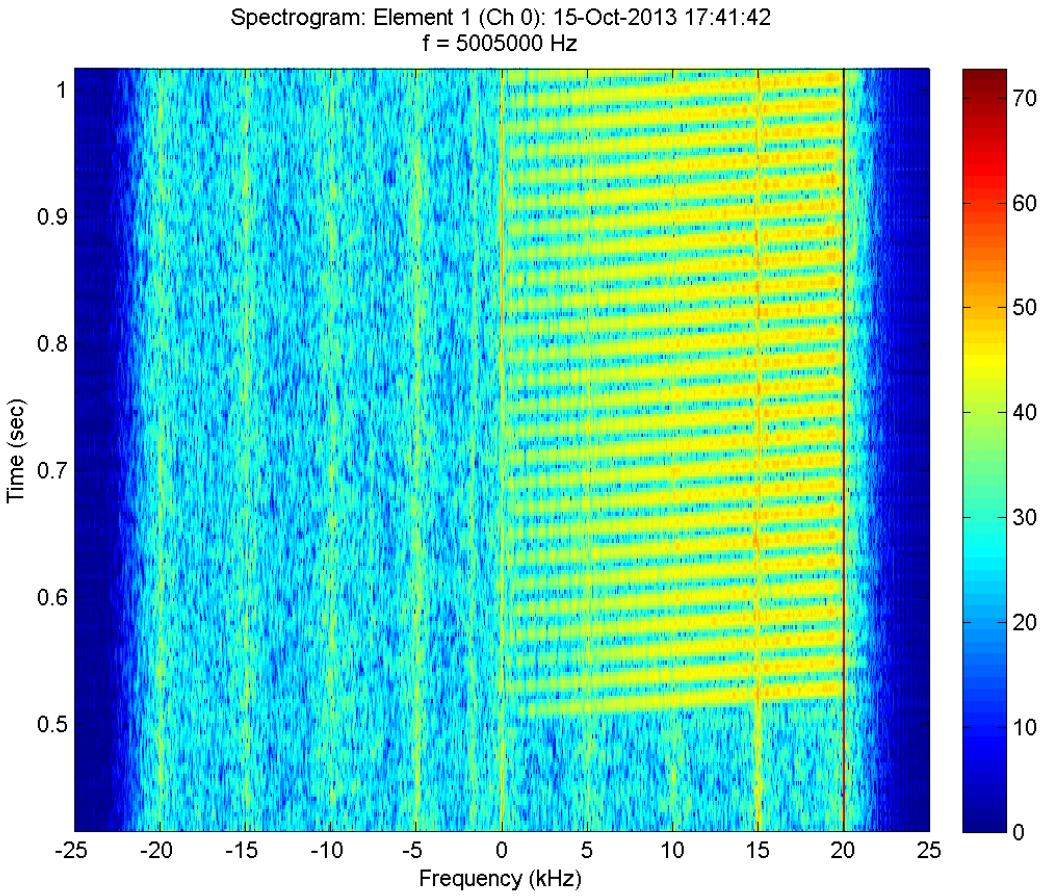

Figure 25. Received 20 kHz LFM in Worcester.

Second Data Collection

The second data collection occurred on Friday, October 18th 2013. Nathan was at the receive site and Cecelia was transmitting. The original plan was to do two full data collections, but we only ended up doing one because of problems with the power supply at the transmit site. A propane generator powered the trailer in which we kept our equipment, and this trailer has two Uninterrupted Power Supplies (UPS) that created regular AC power. However, the one we were using was only generating 108V. As a result, when our system attempted to draw too much current, there simply was not enough voltage and the DC power supply for the HPAs would short out. Once this problem was discovered, we were able to switch to the other UPS which yielded better results, but we were only left with enough daylight for one data collection. Table 1 shows the data we had planned to collect, and what we actually collected. Each individual signal was recorded for about two minutes. We did not test out the 90 kHz waveform because on the receive side, we saw a signal at 5.035MHz which we wanted to avoid interfering with. In the table, F1 is the simple LFM, F2 is the LFM offset by 10Hz, and +/-jF1 or jF2 is the signal shifted by +/-90^{o}.

Table 1. Data collection II

Time	Dipole 1	Dipole 2	Bandwidth	Transmit Power [dBm]
2:33pm	F1	-	3kHz	45.31
2:37				39.82
2:50	F1	-	20kHz	39.82
2:59				45.46
3:02				45.31
	F1	-	90kHz	
3:16	F1	jF1	3kHz	39.56
3:25				45.44
3:30	F1	jF1	20kHz	39.56
:32				45.44
	F1	jF1	90kHz	
4:20	F1-jF2	-jF1+F2	3kHz	38
4:22				44
4:26	F1-jF2	-jF1+F2	20kHz	38
4:28				44
	F1-jF2	-jF1+F2	90kHz	

3:44	F1	-jF1	3kHz	39.56
3:46				45.44
3:37	F1	-jF1	20kHz	39.56
3:40				45.44
	F1	-jF1	90kHz	
3:49	F1+jF2	jF1+F2	3kHz	38.1
4:04				43.94
4:14	F1+jF2	jF1+F2	20kHz	38.1
4:17				44
	F1+jF2	jF1+F2	90kHz	

Third Data Collection

The third collection occurred on Tuesday, October 22nd, 2013. Nathan was at the receive site and Cecelia was transmitting. For this data collection, the transmit frequency was 10 Hz higher than the receive frequency. This was because for the last data collection, there was noise at the 0 Hz Doppler frequency that obscured the possible presence of a ground wave. By reducing the receive frequency a little, our data would appear to be shifted and would thereby avoid this noise contribution. The waveforms were also adjusted differently. Instead of adding a 10Hz offset to F2, an FFT shift was performed in MATLAB on those signals. This swapped the left and right halves of the vector representing the signal, causing the transmission data to look as though it had been shifted by half its length. This resulted in the transmission of the data to begin in the middle of the LFM as opposed to the beginning. We also did not collect data on the 3 kHz waveform because the last data collection showed that the X and O modes could not be separated. We were, however, able to test the 90 kHz waveform. Only one power level was tested for the full hybrid because the maximum output power of the hybrid

signal was very low to start with, and could not be amplified more with the current set up. Table 2 shows what data was collected.

Table 2. Data collection III

Time	Dipole 1	Dipole 2	Bandwidth	Power [dBm] channel 1/channel2
11:26AM	F1	-	3kHz	40.0
11:21				45.6
11:31				48.5
11:38	F1	-	20kHz	39.18
11:43				45.24
11:47				48.07
11:53	F1	-	90kHz	38.84
11:57				44.88
12:06PM				48.13
12:21	F1	jF1	20kHz	39.44/39.53
12:25				45.52/45.37
12:29				48.95/48.88
12:38	F1	jF1	90kHz	39.22/39.42
12.42				44.85/44.92
12:45				48.25/48.32
12:54	F1	-jF1	20kHz	39.48/39.68
1:01				45.56/45.35

1:05				48.93/48.76
1:15	F1	-jF1	90kHz	39.08/39.24
1:19				44.95/44.92
1:22				48.20/48.13
1:45	-F1+jF2	jF1-F2	20kHz	41.25/41.1
2:08	-F1+jF2	jF1-F2	90kHz	40.43/40.62
1:57	F1+jF2	jF1+F2	90kHz	40.43/40.62

Results

This section will describe some of the interesting results from the data collections. Data will be presented as range-Doppler plots. It should be noted that for this data, the range displayed is arbitrary and has no meaning. This is because the start time of our collection was not exactly on a full second due to a limitation of GNU Radio software, so actual start time of transmission, and therefore the travel time for the signal, is unknown. The range difference between signals is valid however, and is significant because it allows us to determine off which ionospheric layer the signals are bouncing and to see if there are multiple bounces. This is calculated with reference to the ground wave if it is visible. An F-layer bounce is typically about 450km from the ground wave, and a second F-layer bounce will be another 450km. An E-layer bounce is about 200km from the ground wave. This type of plot also allows us to see both polarizations if they exist. If they do, they will appear side by side because the time difference is reflected in the Doppler calculation.

Unfortunately, it was discovered after all data collections were complete that a resistor was disconnected on the antenna located at WPI during at least the third data collection and possibly the second. This means only one of the dipoles at the receiving site was active. As a result, we could only observe one component (either horizontal or vertical) of all transmitted signals. However, we could still observe all of the signals and their multiple bounces as well as several modes. The idea of the hybrid is that we would transmit two signals of opposite polarizations and each signal would contain two different messages. Upon reception, the signals would be reconstructed to extract the two messages. With only half of the signal data, the signals could not be reconstructed. Nevertheless the data collections still yielded important results with respect to useful signal bandwidths, power levels, visibility of modes, and technical issues to be avoided.

Signal Bandwidths

Our results from the second data collection showed that the 3 kHz signal could not be separated into two different signals, so that bandwidth was not a part of the third data collection. The 20 kHz had been used in previous experiments by The MITRE Corporation, so it was expected that the particular bandwidth would work. The 90 kHz was new, however, and it was uncertain whether or not the ionosphere would support a signal with such a wide bandwidth. Fortunately the third data collection

showed that the 90 kHz bandwidth signal was in fact viable, which is useful because it would allow transmission of more data at once. Results can be seen in Appendix B.

Power levels

One of the goals of this experiment to see how low a power level could be used to transmit and still be clearly received. The lowest power level used was in the second data collection; the F1-jF2 circular polarized signal transmitted at 38dBm, or about 6W, and was still clearly received. This result can be seen in Figure 26, and means that transmitting at very low power for short distances is viable. Although the low power usage will vary with the signal path and length, it is possible for discreet communications over small distances.

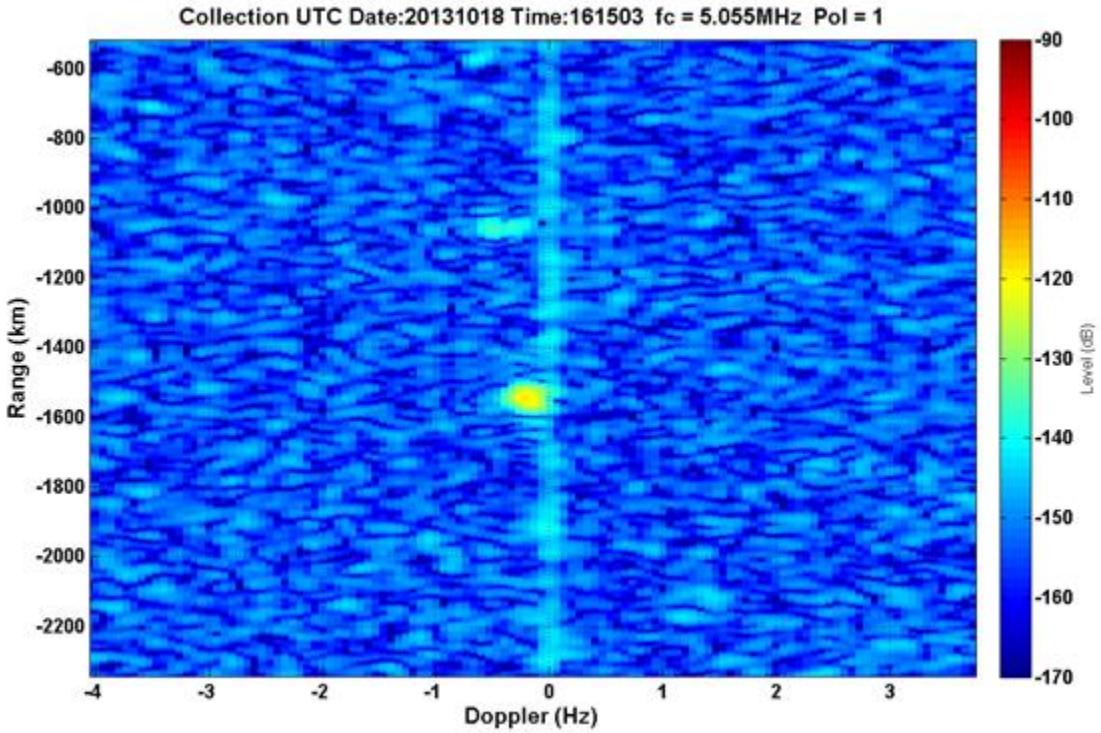

Figure 26. Lowest power measurement, F1-jF2 at 6W.

Signal Mode Visibility

Figure 27 shows the 20 kHz LFM sent at about 10W. The signal is clear at 2400 km and appears to only have one mode. The ground wave is not visible because of the previously mentioned noise at 0Hz. There is another signal at 2900 km that may have two modes. The difference between these two modes is about 450km, which means that it is most likely a second bounce from the F layer. It is expected that this type of signal would separate into two modes, although it may not be distinguishable in

the first bounce because of the relatively short path. A second bounce doubles the signal path length, resulting in more time for the modes to become farther apart.

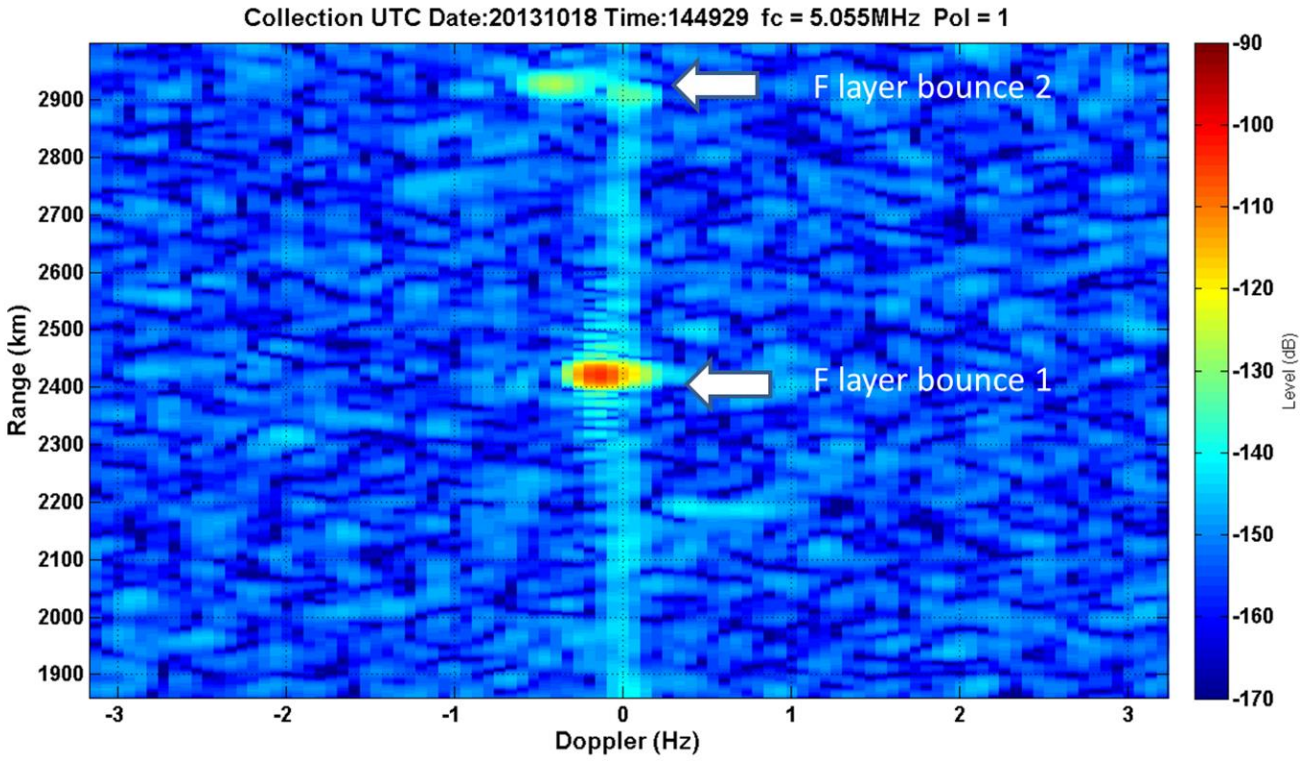

Figure 27. 20 kHz LFM at 10W with two F layer bounces.

While we expected to see two modes for linear chirps, we hoped to not see them both for the signals that were supposed to be circularly polarized. However, this did not end up being the case. Figure 28 shows the circularly polarized F1+jF1 signal from the third data collection at the highest power; there are clearly two modes in the first bounce, although one is much lower power than the other.

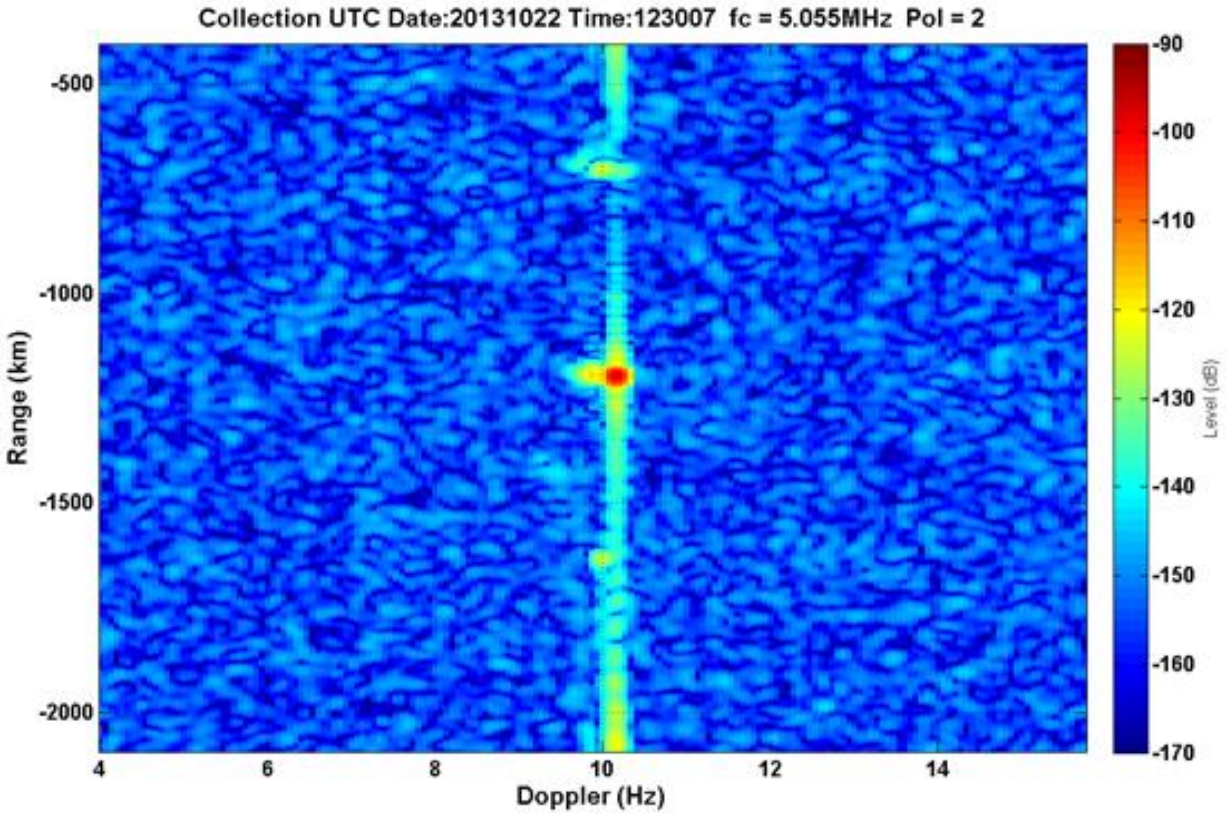

Figure 28. 20 kHz F1+jF1 signal at 78.5W with two F-layer bounces and a ground wave.

.

It is worth noting, however, that a power level of 78.5W is far more than we would need to transmit a signal over the given distance. Figure 29 shows the same signal transmitted at only 9W, and only one mode appears to be visible, along with a possible ground wave and second bounce. In the high power case, the second mode was much weaker than first. In the low power case, this likely still holds, but the second mode simply is not strong enough to be visible.

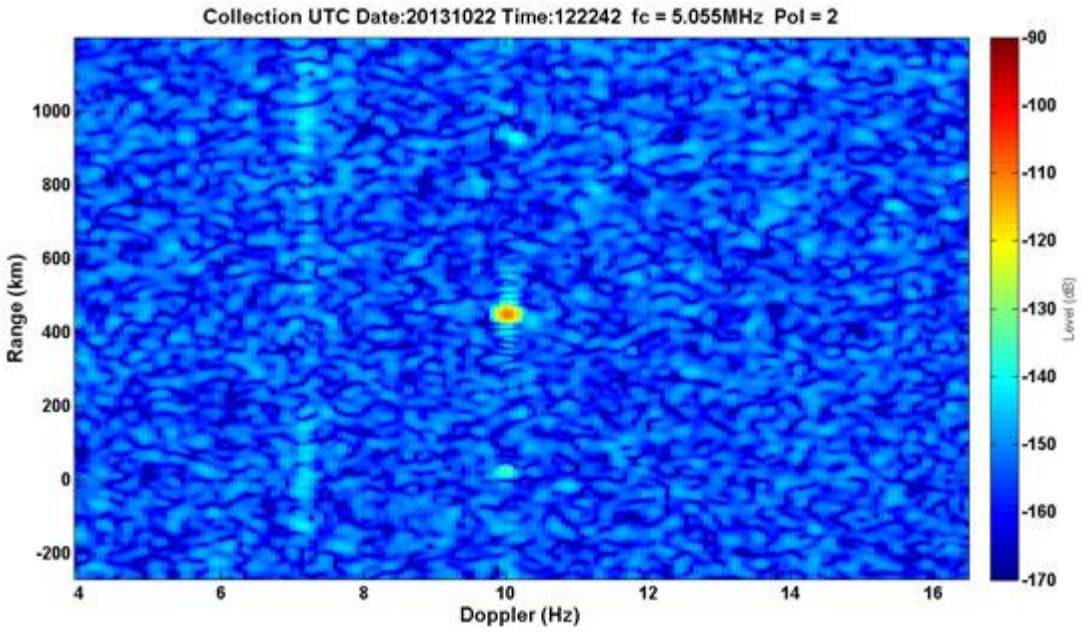

Figure 29. 20 kHz F1+jF1 signal at 9W with two F-layer bounces and a ground wave.

Results varied with the full hybrid. In the case of the second data collection, the F1+jF2 hybrid appeared to only have one mode at all power levels, where the F1-jF2 had two modes at all power levels. In the third data collection, only low power could be tested because the method by which the hybrid waveform was generated made it inherently lower. Only one mode appeared to be visible for the 20 kHz hybrid. The 90 kHz hybrid may have a second mode, but if it does, it is of much lower power. We would expect to see two modes with the full hybrid.

Measurement Viability

The Figure 30 illustrates that for both the second and third data collections, the signals were consistent in that they were traveling the same path and were experiencing similar conditions. The figures are Doppler plots over time for the entirety of the data collection; the peak signal power is taken from each data sample and plotted. The color bar in the figures indicates power in dB. Because the Doppler plots do not deviate greatly throughout a single day, it indicates the measurements are good.

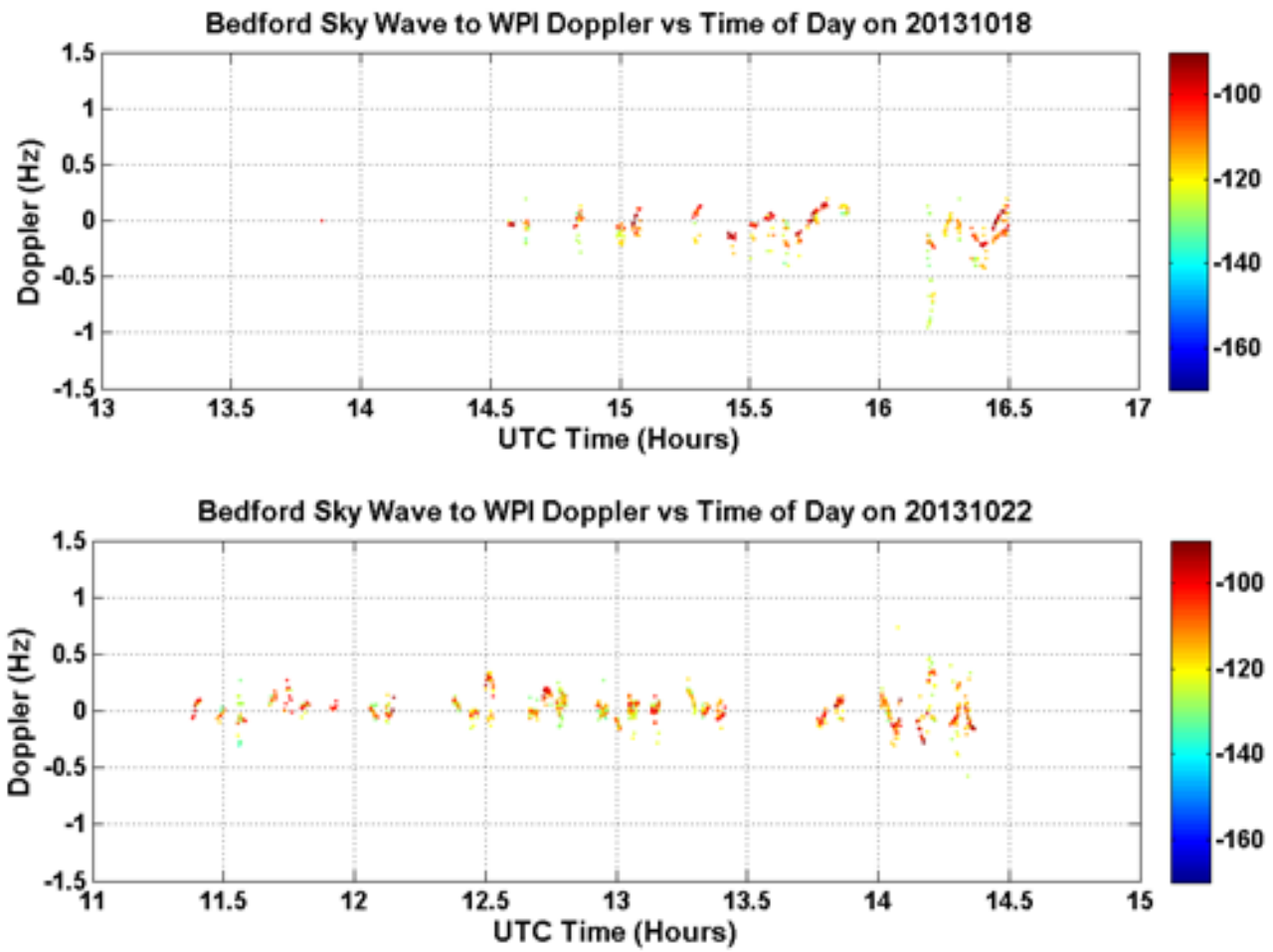

Figure 30. Doppler data versus time for data collections II and III.

The images in Figure 31 are also plots over time, but they show phase. Data points at the positive value are one polarization and points at a negative value are the other polarization. For the second collection on October 18th, the positive polarization seems to dominate, although it would have been expected to change polarizations around 15:45 according to Table 1a. The third data collection also seems to be dominated by one polarization. This is most likely due by the fact that only one dipole of the receiving antenna was collecting data at this time.

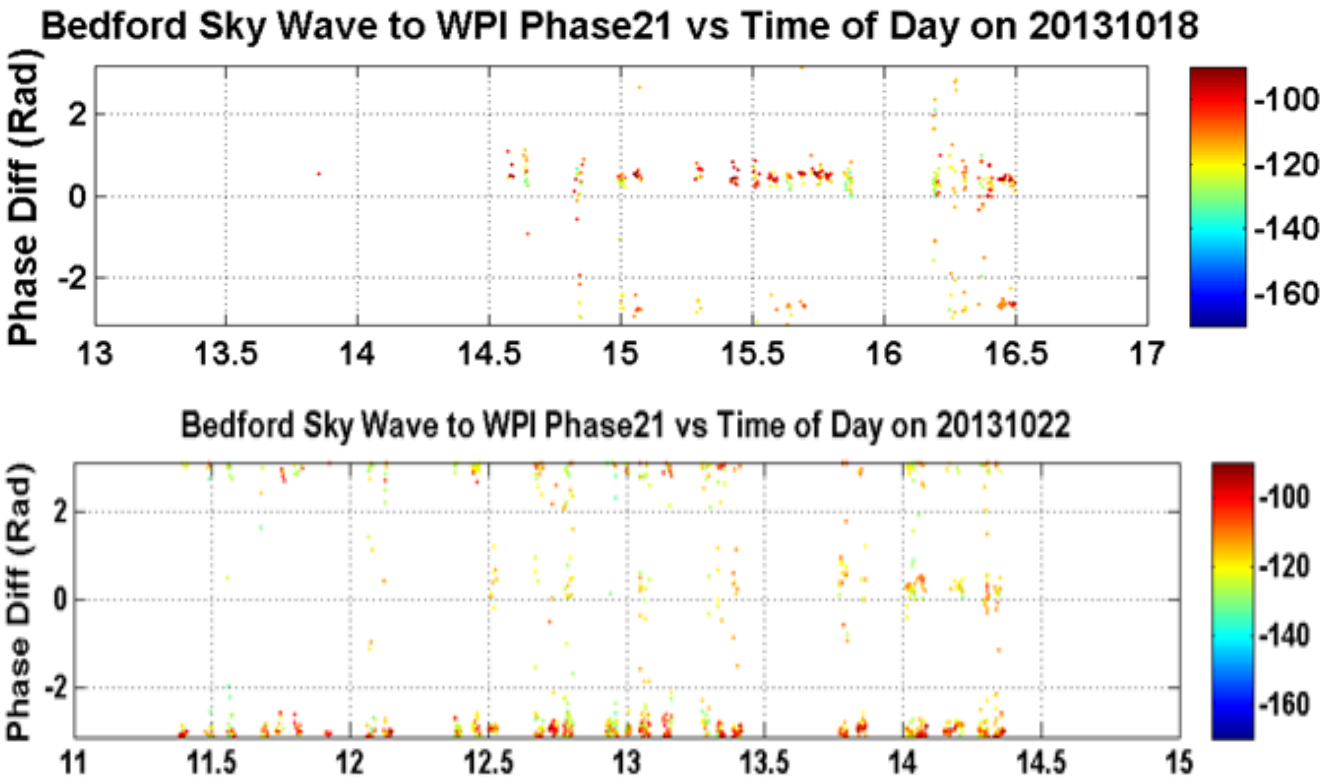

Figure 31. Phase versus time for data collections II and III.

Cost Analysis

Although cost analysis was not an integral part of this study, it is still important to consider when deciding whether or not to implement a new system. Table 3 shows the approximate cost of the materials used for this experiment. These costs are based on this experiment in particular. If this setup was to be constructed in a commercial setting, some of these costs would vary. For example, the Heros Preselectors were used in this case because they were available and did not have to be purchased. They are tunable filters, which is why they are expensive. If the system were set up to communicate at a particular frequency, a less expensive fixed filter could be used instead. The TC-300 amplifiers were also unreliable, so a better replacement would be more expensive.

Table 3. Approximate cost of parts

Part (number required)	Cost per unit	Total Cost
Cross-dipole antenna (2)	$750	$1,500
Ettus USRPs (4)	$7,000	$28,000
TC-300 HPA (2)	$100	$200
ZHL-32A (2)	$230	$460
ZFL-500LN (2)	$80	$160
Heros Preselector (2)	$900	$1,800
	Total	$31,920

The method tested in this project is intended to decrease the cost of HF transmission in several ways. First, because more than one signal can be sent from the same antenna, fewer antennas would be needed to achieve data rates equal to larger antenna arrays. To be more explicit, the polarization technique sends two signals from one antenna. An antenna array requires one antenna array per signal, so the former method cuts the number of antennas in half. The transmit and receive chains would essentially stay the same. Halving the hardware required saves valuable construction time and real estate for the antennas. Second, if transmission is done at low power this greatly reduced the cost of the amplification hardware needed. Quality high power amplifiers can easily cost several thousands of dollars. Overall this technique does not save a lot of money, but using fewer antennas is convenient because less maintenance needs to be done and less space needs to be found to place them.

Conclusion

HF communication is used for a variety of applications, from government use to amateur radio. In addition to being widely used, it also has the unique advantage of allowing communication over the horizon through skywave propagation. This process involves reflecting the signal off the ionosphere, which, due to its variability, can lead to serious communication problems such as fading and low data rates. In order to combat these low data rates, we conducted research into MIMO systems. The disadvantage to using an array of antennas, however, is due to the long wavelengths of HF signals. The antenna arrays needed for a MIMO system need to be spaced at very large intervals. A possible alternative to this would be to implement left and right handed circular polarized signals. This project uses the USRP, GNU Radio, and MATLAB, along with a variety of hardware to test the viability of using polarization in a MIMO system to reduce fading and provide reliable communications.

Our project saw the successful implementation of USRPs and GNU Radio, as well as the assembly of the hardware chains, to transmit and receive HF signals. Ultimately, due to technical issues, it could not be proven whether or not sending two oppositely polarized signals at the same time would allow them to be clearly received. However, other significant conclusions could be drawn from the collected data. It was confirmed that very low power (less than 10W) can be used to successfully transmit signals, which was the other major goal of the project. It was also shown that the ionosphere can support a waveform with a bandwidth of 90 kHz, which allows for more data to be transmitted.

This experiment also advanced The MITRE Corporation's previous experiments with HF antenna arrays, and served as a set up as they continue to investigate the viability of this technique. In addition to setting up and building test equipment, programing software, and researching, the project also found and solved many technical issues which arose. This will mean faster and more efficient testing for MITRE. These technical issues ranged from unreliable power supplies at the transmit site to poor performance of the high-power amplifiers. For the issues that could not be solved for this testing such as starting the signal transmission on a full second or the lack of ferrites at WPI (ferrites are iron cores that surround the receiving lines out of the balun of the antenna to keep the polarized signal from getting distorted), the problems were identified and research into solutions began. Progress is already being made in further waveform development and fine-tuning transmission from the USRPs by programming directly to the FPGA in the C programming language, rather than through GNU radio. The transmission hardware chain is also being modified to use 5W power amplifiers to test the limits of the low power signals, and initial

testing has shown that a signal at even that low power can still be successfully received and that the two circular polarizations can be successfully simultaneously transmitted and then separated on receive.

Recommendations

We recommend the following steps to The MITRE Corporation to advance this work and acquire further results:

- Replace unreliable hardware including:
  - Power supplies on transmit
  - TC-300 amplifiers
- Add ferrites to receive antenna
- Ensure antenna performance before testing
- Address issues with starting transmission and reception on a full second, may need to control Ettus USRPs with something other than GNU radio.

References

[1] L. F. McNamara, The Ionospheric Communications, Surveillance, and Direction Finding, Malabar: Krieger Publishing Company, 1991.

[2] G. Lane, Signal-to-Noise Predictions Using VOACAP, Cedar Rapids: Rockwell Collins, Inc., 2001.

[3] J. D. Kraus, Electromagnetics, McGraw-Hill, Inc., 1984.

[4] P. Ndao, Y. Erhel, D. Lemur, M. Oger and J. Le Masson, "First Experiments of a HF MIMO system with polarization diversity".

[5] P. M. Ndaol, Y. Erhel, D. Lemur and J. Le Masson, "A MIMO solution based on Polarization diversity for ionospheric radio links," 2010.

[6] "About HF Radio," Spectratek, [Online]. Available: http://www.spectratek.co.nz/about_hf_radio.htm. [Accessed 04 09 2013].

[7] T. Stimac, "Definition of frequency bands(VLF,ELF... etc.)," [Online]. Available: http://www.vlf.it/frequency/bands.html. [Accessed 04 09 2013].

[8] G. Moernaut and D. Orban, "The Basics of Antenna Arrays," [Online]. Available: http://www.orbanmicrowave.com/The_Basics_of_Antenna_Arrays.pdf. [Accessed 04 09 2013].

[9] M. H. De Canck, "Ionosphere Properties and Behaviors - Part 2," [Online]. Available: http://www.antennex.com/prop/prop0706/prop0706.pdf. [Accessed 04 09 2013].

[10] "Circular Polarization," [Online]. Available: http://en.wikipedia.org/wiki/Circular_polarization. [Accessed 04 09 2013].

[11] "Refraction," [Online]. Available: http://en.wikipedia.org/wiki/Refraction [Accessed 09 09 2013].

[12] D. McMahill, "Air Core Inductor Analysis/Synthesis Calculator," SourceForge, [Online].Available:http://wcalc.sourceforge.net/cgi-bin/air_coil.cgi?wc_unit_menu_3_0=GHz&N=7&synth_n=calc&dia=0.5&wc_unit_menu_1_0=inch&len=0.499503&wc_unit_menu_0_0=inch&use_fill=yes&fill=1.36385&AWG=16&rho=3e-08&wc_unit_menu_4_0=Ohm&wc_unit_menu_4_1=m&freq=100&wc_unit_me. [Accessed 10 2013].

[13] "VOACAP, propagation analysis and prediction program," 18 February 2012. [Online]. Available:http://www.foxcomputer.se/VOACAP%20propagation%20analysis%20and%20prediction%20program%20review.pdf. [Accessed 4 11 2013].

[14] P.M. Ndao, Y.M Erhel, D. Lemur, M. Oger and J.Le Masson, "First experiments of a HF MIMO system with polarization diversity" IRST 2012, Session 8: MIMO, 15 - 17 May 2012, York, UK.

[15] D.M Pozar, Microwave Engineering, Fourth Edition, Dancers: John Wiley& Sons, Inc, 2012.

[16] Mini-Circuits, "Low Noise Amplifier ZFL-500LN," [Online]. Available: http://www.minicircuits.com/pdfs/ZFL-500LN.pdf. [Accessed 2013].

[17] Ettus Research, "USRP N210 Product Details," National Instruments, 2013. [Online]. Available: https://www.ettus.com/product/details/UN210-KIT. [Accessed 2013].

[18] GNURadio, "GNURadio: The Free & Open Software Radio Ecosystem," Redmine, 2006-2011. [Online]. Available: http://gnuradio.org/redmine/projects/gnuradio/wiki. [Accessed 2013].

[19] BAL-300. Available: http://www.cwsbytemark.com/images/BAL-%20300%20Rev%20C-Web.pdf [Accessed 2013].

Appendix A

Matlab Code

Generate chirp

```
function z = createChirpFile_Weighted(startF, chirp_rate, samp_rate, chirp_length, filename);
        fs =samp_rate; % sampling frequency is sample rate
        ts = 1/fs;        % Time step is the inverse of sampling frequency
        t = 0:ts:chirp_length;
        t = t(1:samp_rate*chirp_length);
        w = exp(1i*2*pi*((chirp_rate*t.^2)/2 + startF*t)); %generate LFM
        Icomponent = real(w);                    %store real parts
        Qcomponent = imag(w);                    %store imaginary parts
        IQData = Icomponent + 1i*Qcomponent;   %Combine as I/Q data
        T=tukey_taper(length(IQData),0.25);%Generate Taper
        IQData2=IQData.*T;                       %Apply taper to data
        x = write_complex_binary(IQData2, filename); %save data
end
```

Generate chirp with 90° phase shift

```
function z = createChirpFile_Weighted_90_PhaseShift(startF, chirp_rate, samp_rate, chirp_length,
filename);
        fs =samp_rate;  % sampling frequency is sample rate
        offset=pi/2;     % positive 90 degree phase shift
        ts = 1/fs;        % Time step is the inverse of sampling frequency
        t = 0:ts:chirp_length-ts;
        w = exp(1i*2*pi*((chirp_rate*t.^2)/2 + startF*t)+1i*offset); %generate LFM
        Icomponent = real(w);                    %store real parts
        Qcomponent = imag(w);                          %store imaginary parts
        IQData = Icomponent + 1i*Qcomponent;               %Combine as I/Q data
        T=tukey_taper(length(IQData),0.25);          %Generate Taper
```

```
    IQData2=IQData.*T;                          %Apply taper to data
    x = write_complex_binary(IQData2, filename);    %save data
end
```

Generate chirp with -90° phase shift

```
function z = createChirpFile_Weighted_90_PhaseShift_Negative(startF, chirp_rate, samp_rate, chirp_length, filename);
    fs =samp_rate;   % sampling frequency is sample rate
    offset=-pi/2;    % negative 90 degree phase shift
    ts = 1/fs;       % Time step is the inverse of sampling frequency
    t = 0:ts:chirp_length-ts;
    w = exp(1i*2*pi*((chirp_rate*t.^2)/2 + startF*t)+1i*offset); %generate LFM
    Icomponent = real(w);                       %store real parts
    Qcomponent = imag(w);                       %store imaginary parts
    IQData = Icomponent + 1i*Qcomponent;            %Combine as I/Q data
    T=tukey_taper(length(IQData),0.25);             %Generate Taper
    IQData2=IQData.*T;                          %Apply taper to data
    x = write_complex_binary(IQData2, filename);    %save data
end
```

Tukey Taper

```
function w=tukey_taper(N,aa)

N1=round(aa*N/2);
N2=(N-N1+1);

w=ones(1,N);
ix1=1:N1;
ix2=N2:N;

w1=0.5*(1+cos(pi*(2*(ix1-1)/(aa*N)-1)));
```

```
w(ix1)=w1;
w(ix2)=fliplr(w1);
end
```

Simulate Hybrid

```
function z = Create_Hybrid_LFM_File(filename1,filename2,filename3);
        f1=read_complex_binary(filename1);          %read in both signal files,where
        f2=read_complex_binary(filename2);          %one has already been shifted by
                                                    %90 degrees

        F=f1+f2;                                    %sum the signals

        Normalizer=max(abs(F));                     %Normalize the signals to have an
                                                     amplitude of one

        normalizedF = F/Normalizer;

        x = write_complex_binary(normalizedF, filename3);    %Save data
end
```

Appendix B

Dipole Measurements

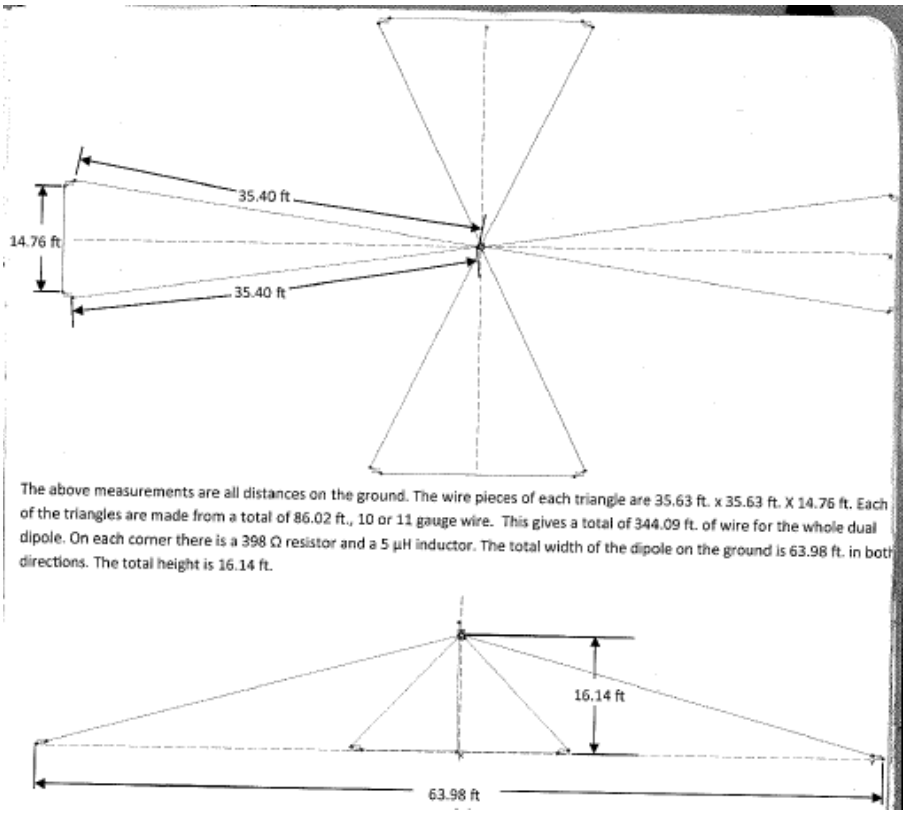

Figure 32. Small Dipole measurements

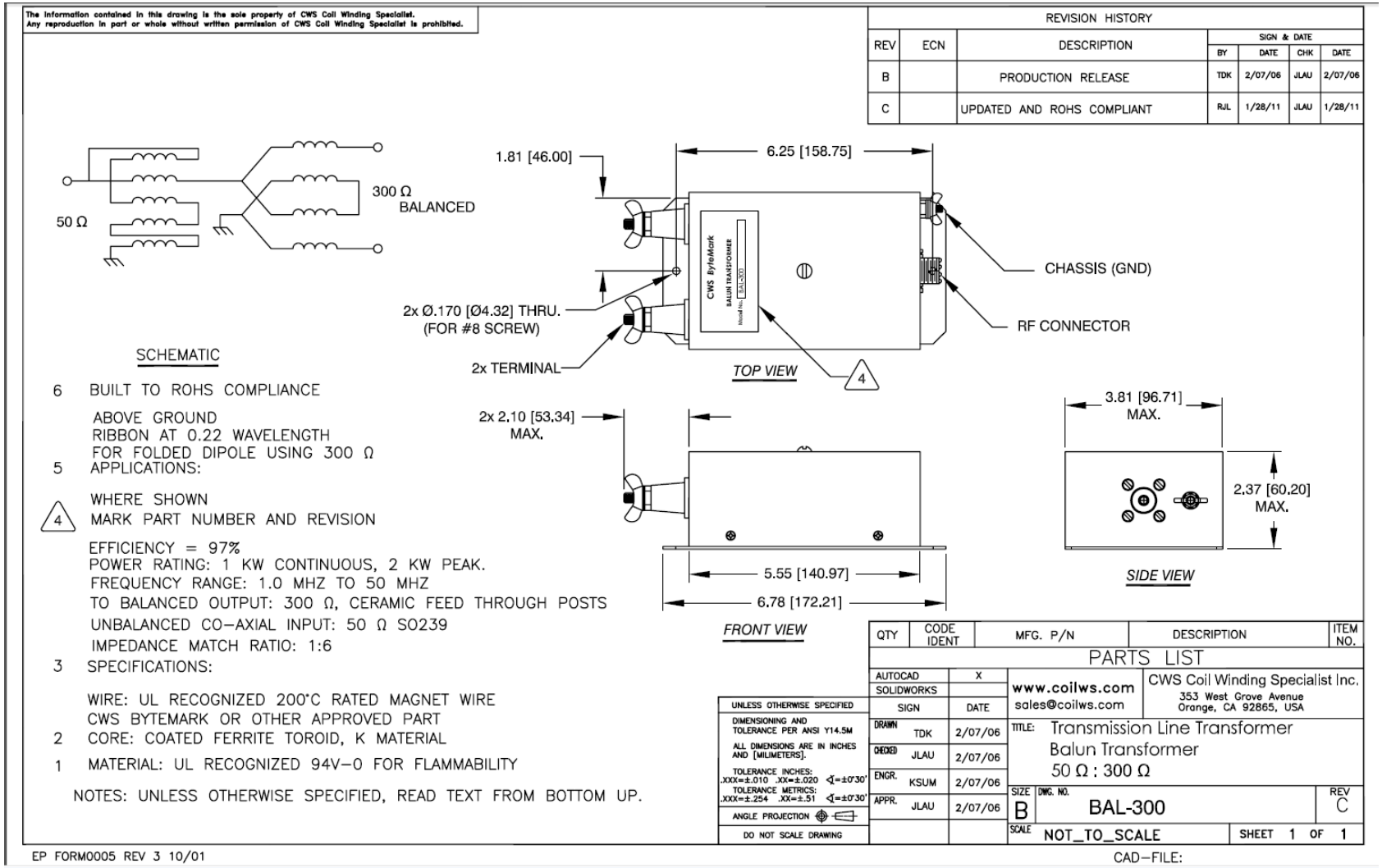

Figure 33. CWS ByteMark Bal-300 Balun Schematic[19]

Data Collection II

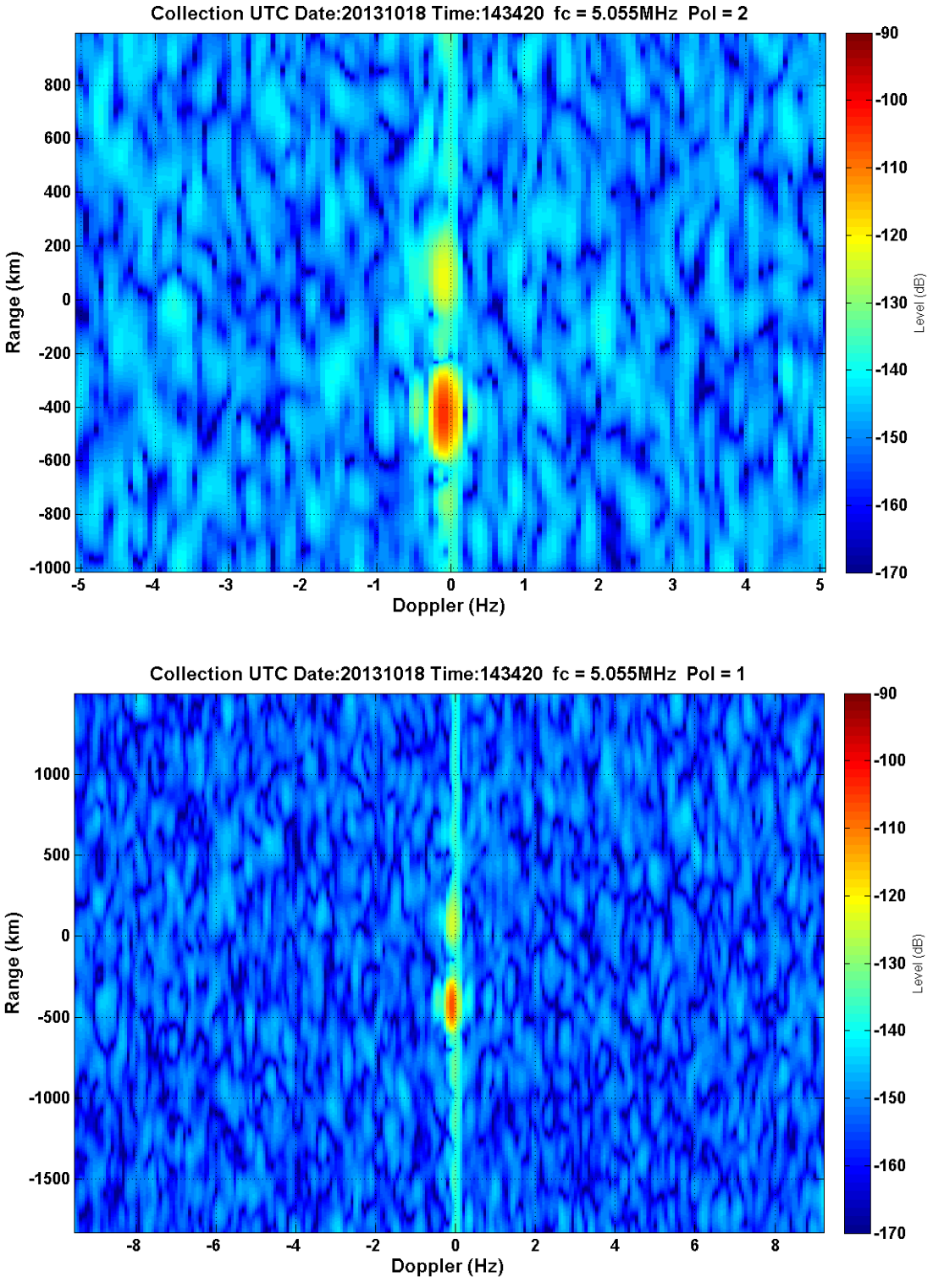

Figure 34.2:33/F1/3kHz/34W – F layer, one mode

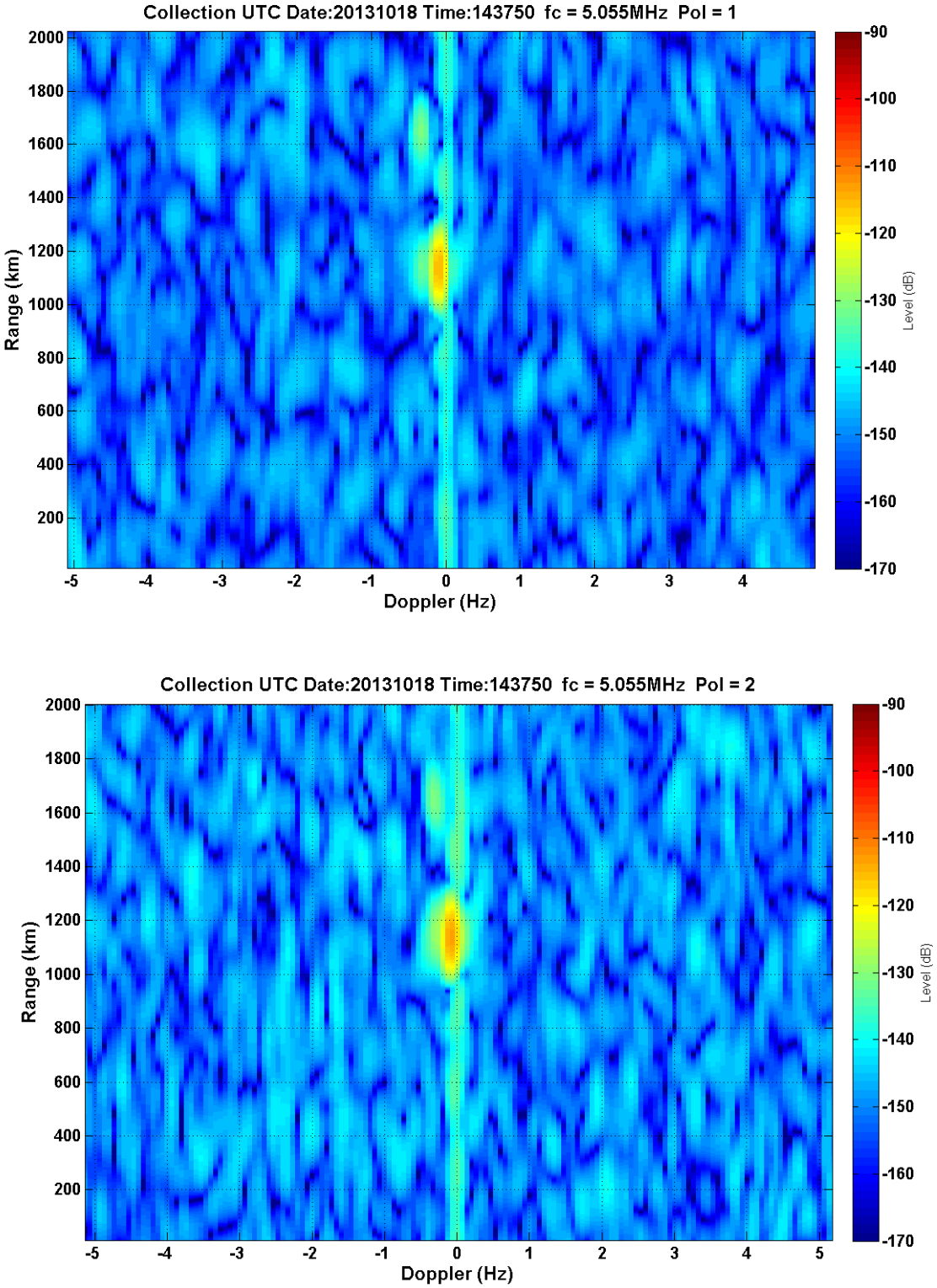

Figure 35.2:37/F1/3kHz/10W – F layer? One mode

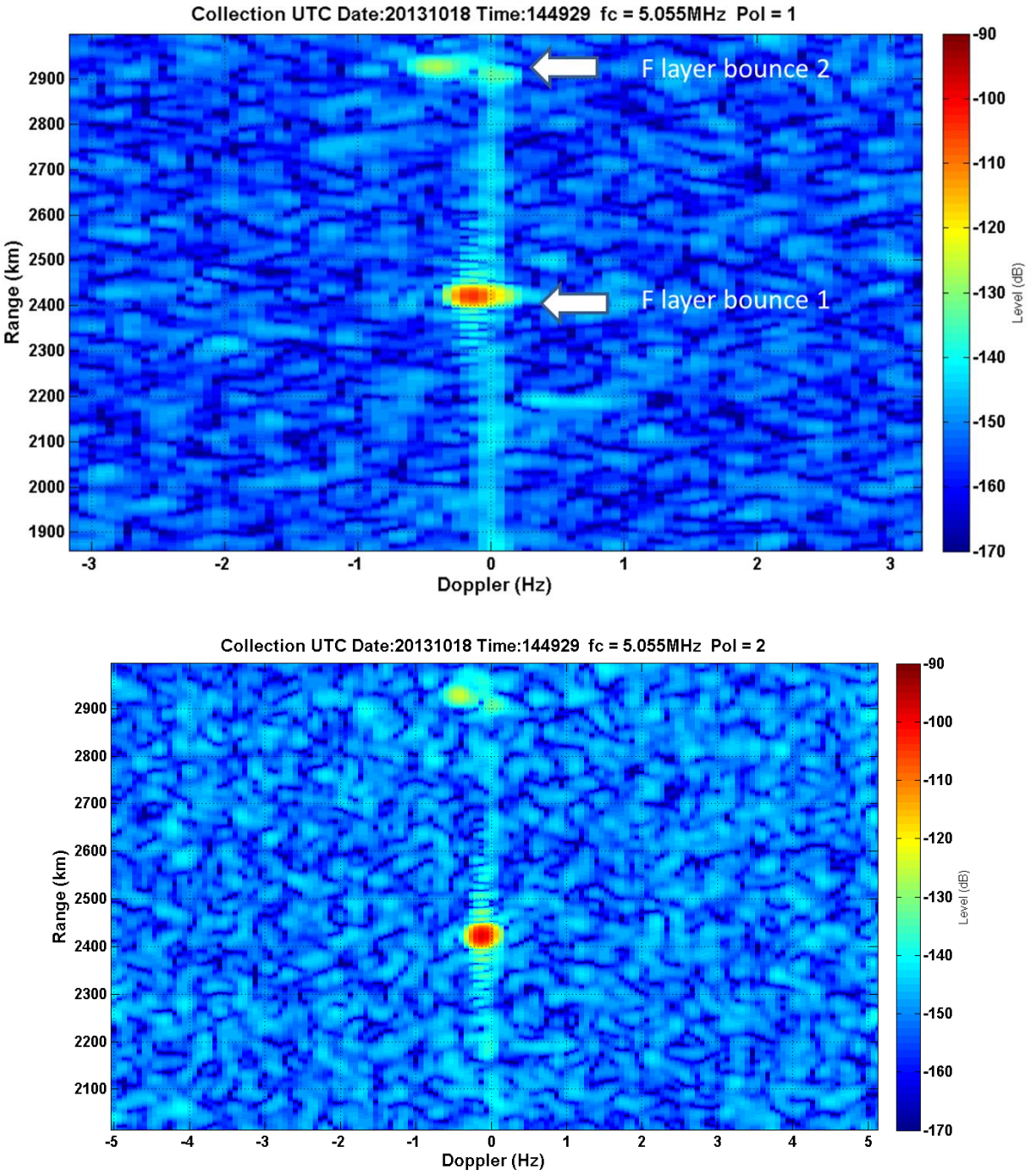

Figure 36.2:50/F1/20kHz/39.82dBm – F layer, one mode, two on second bounce

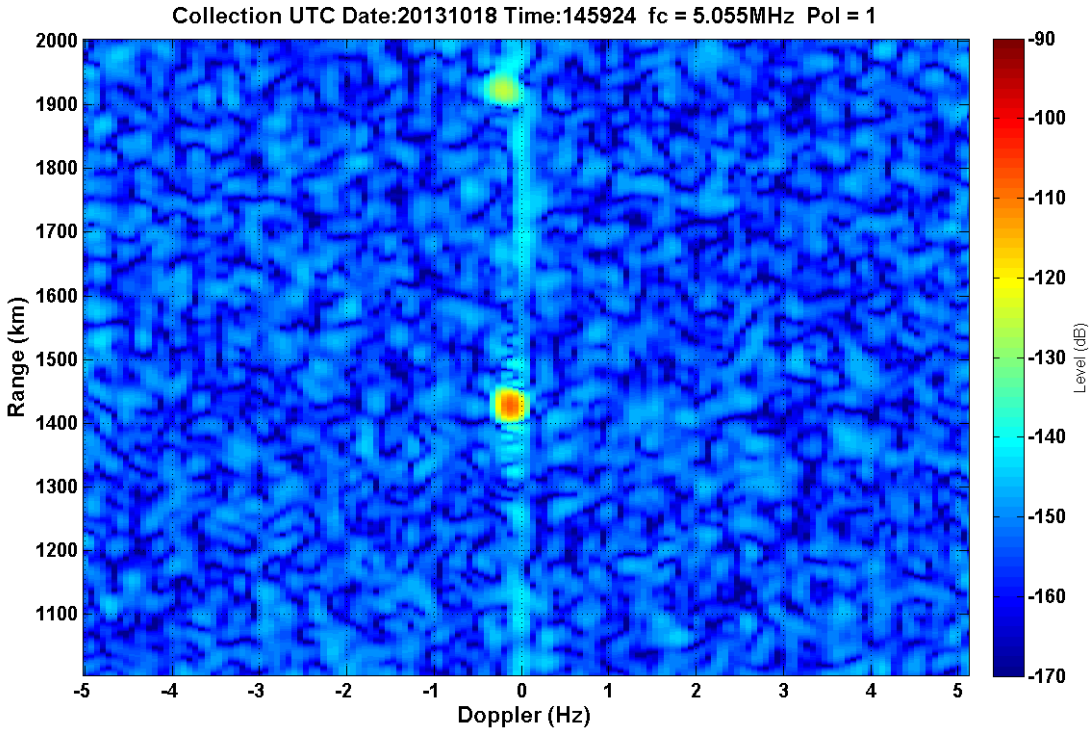

Figure 37.2:59/F1/20kHz/45.46dBm – F layer, one mode

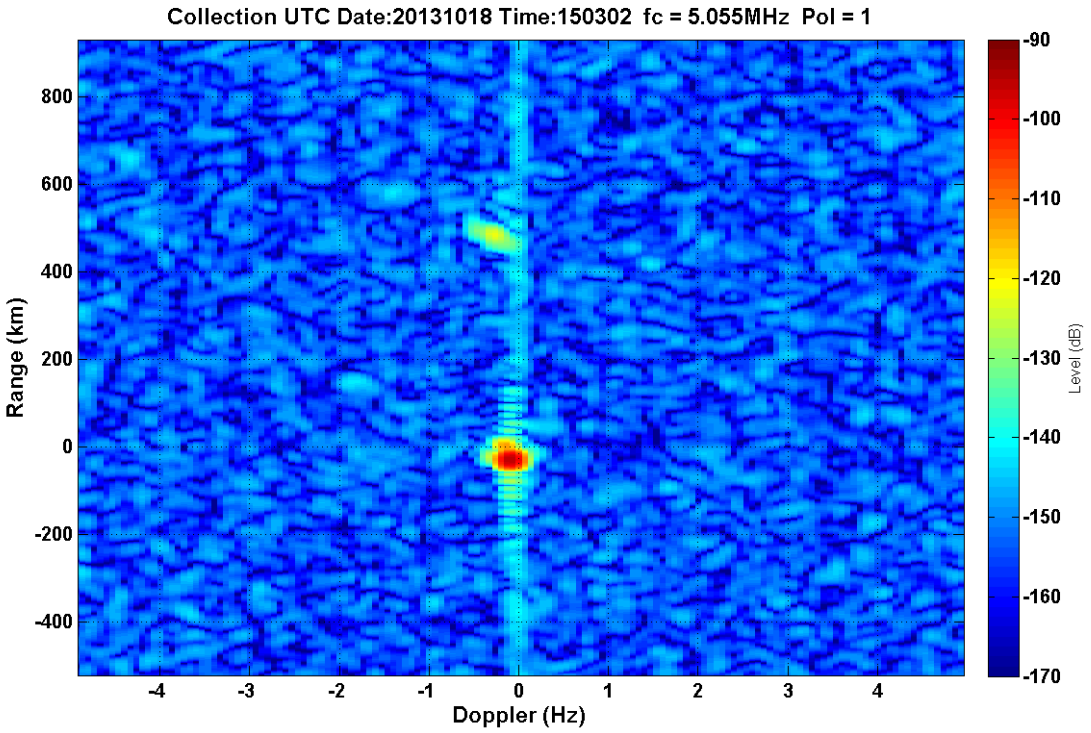

Figure 38.3:02/F1/20kHz/34WdBm – F layer, one mode

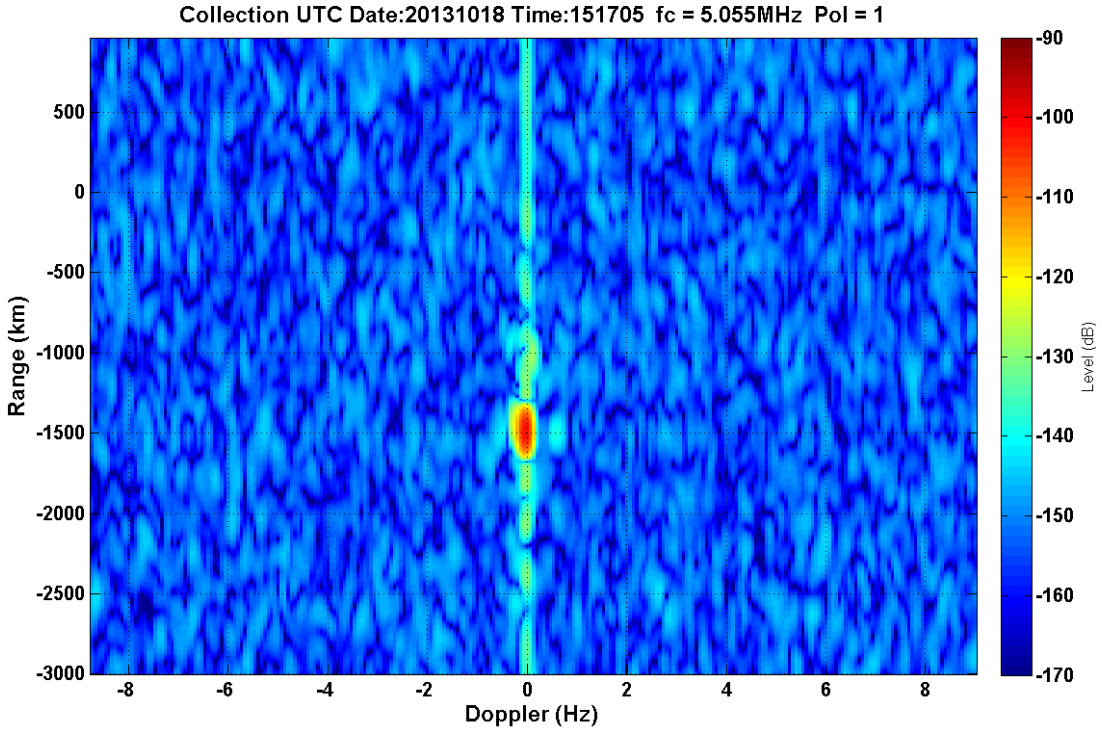

Figure 39.3:16/F1+jF1/3kHz/39.56dBm – one mode

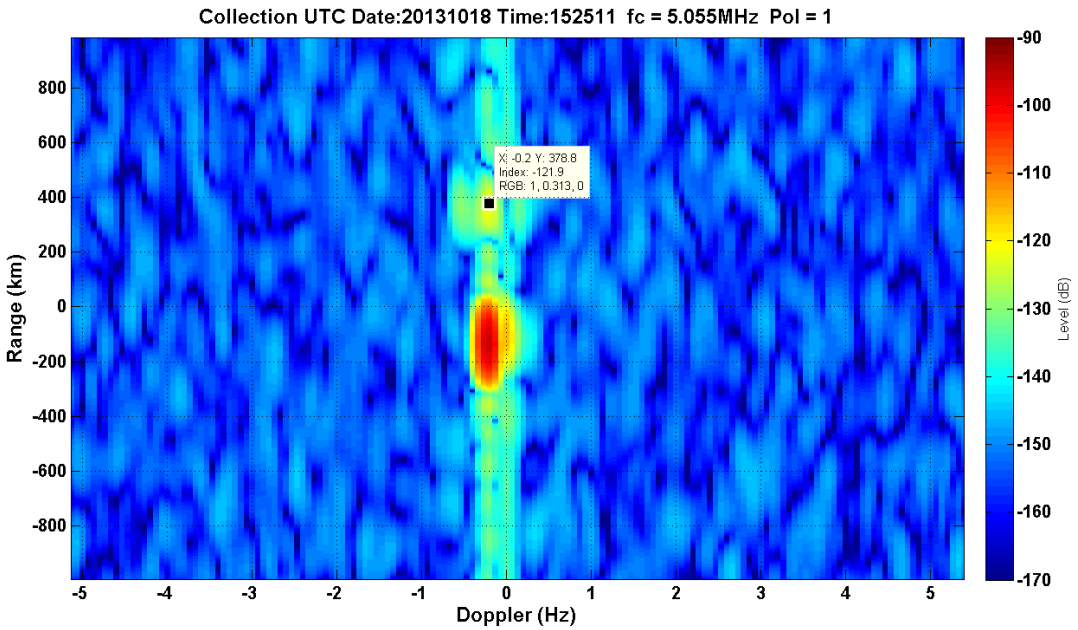

Figure 40.3:25/F1+jF1/3kHz/45.44dBm – F layer, one mode

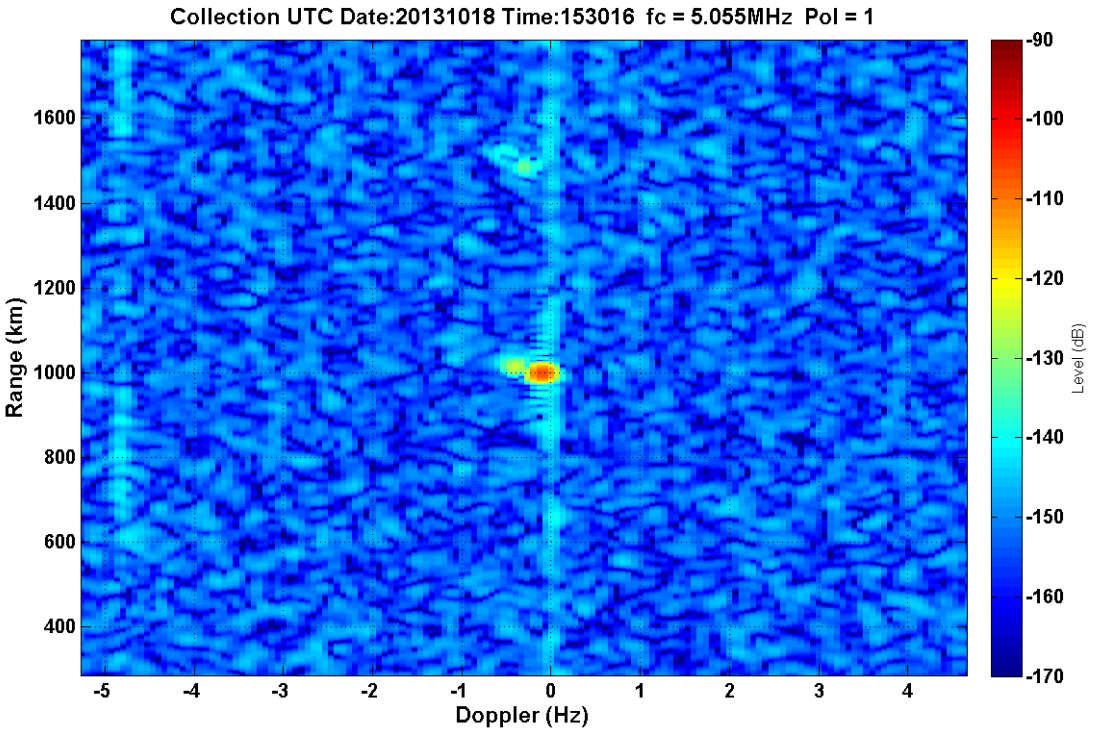

Figure 41.3:30/F1+jF1/20kHz/39.56dBm – F layer, two modes

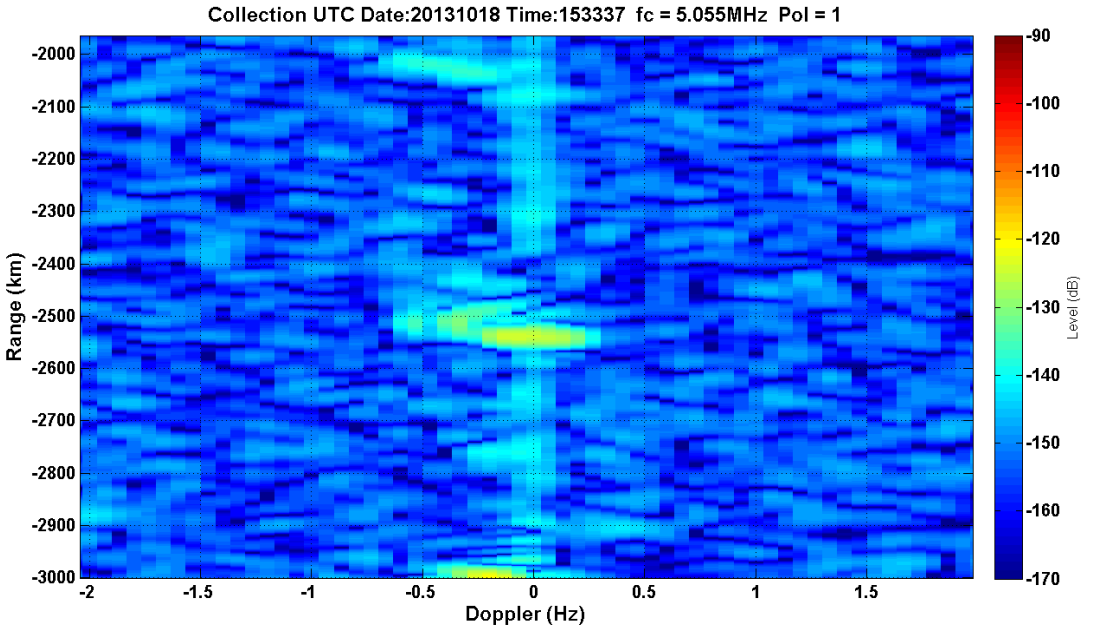

Figure 42.3:32/F1+jF1/20kHz/45.44dBm – F layer, two modes?

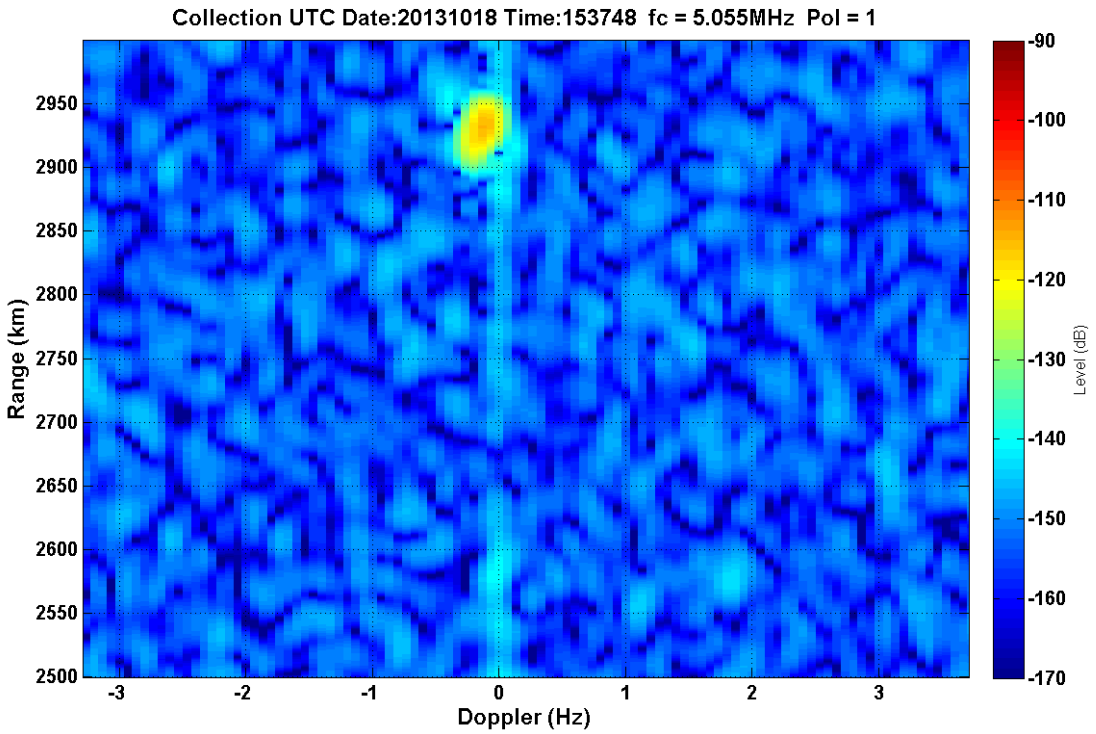

Figure 43.3:37/F1-jF1/20kHz/39.56dBm – one mode

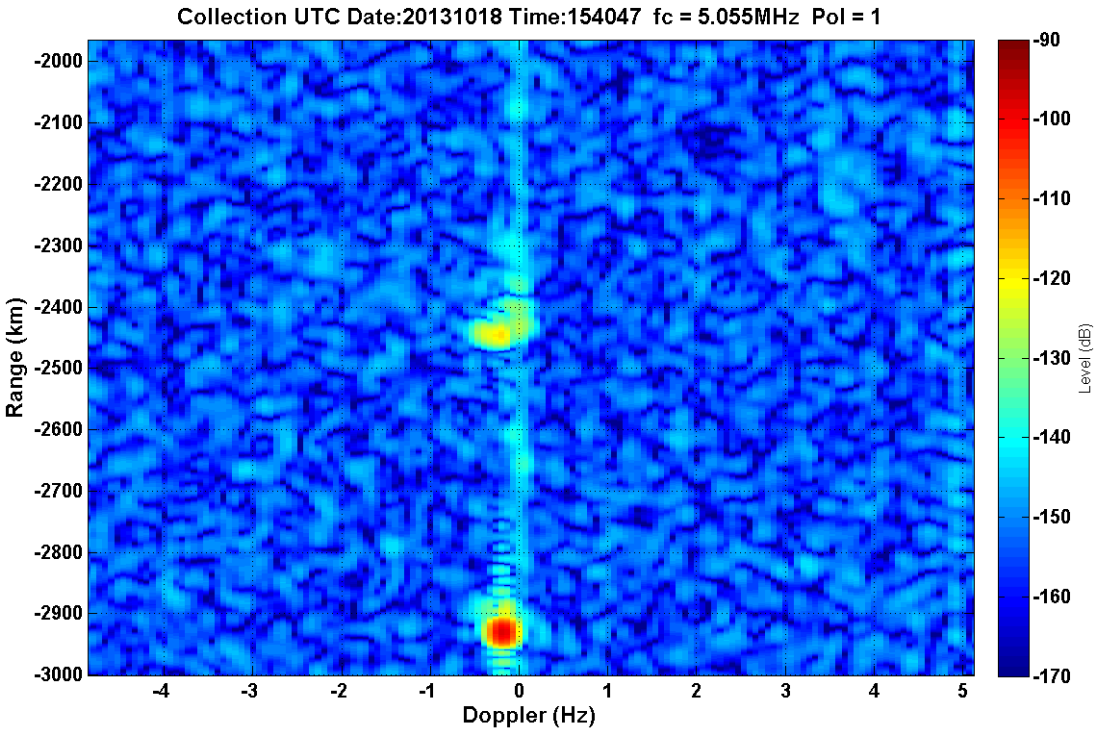

Figure 44.3:40/F1-jF1/20kHz/45.44dBm – F layer, one mode, two modes on second bounce

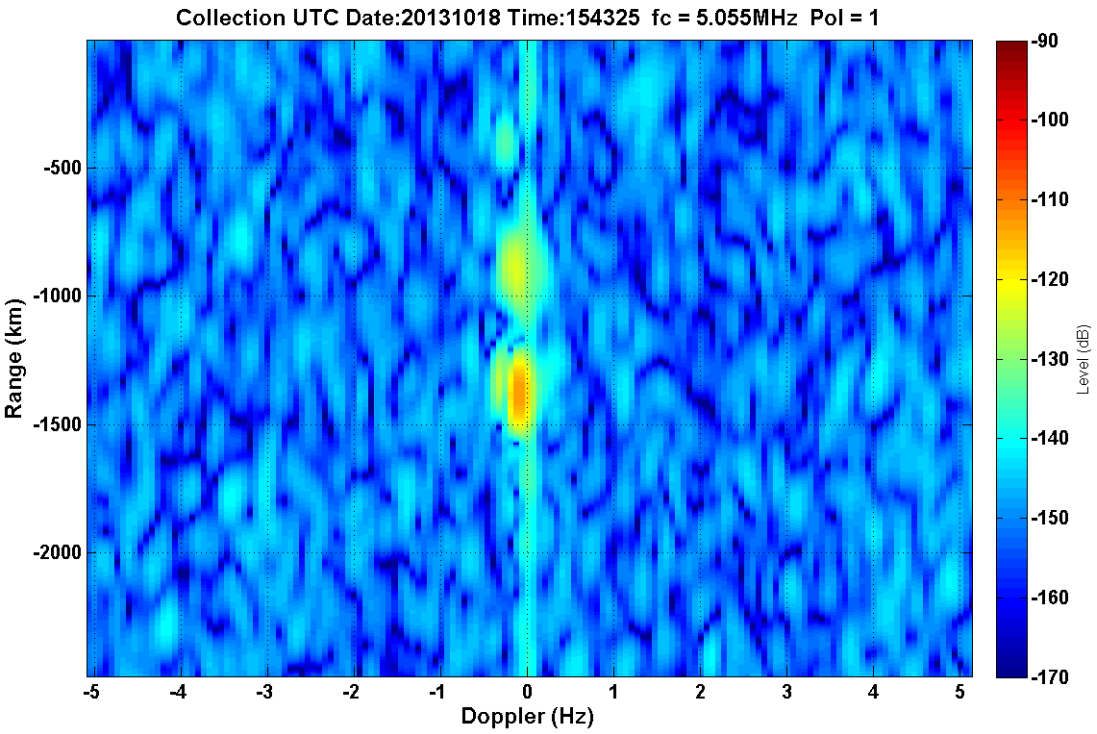

Figure 45.3:44/F1-jF1/3kHz/39.56dBm – F layer, two modes(?)

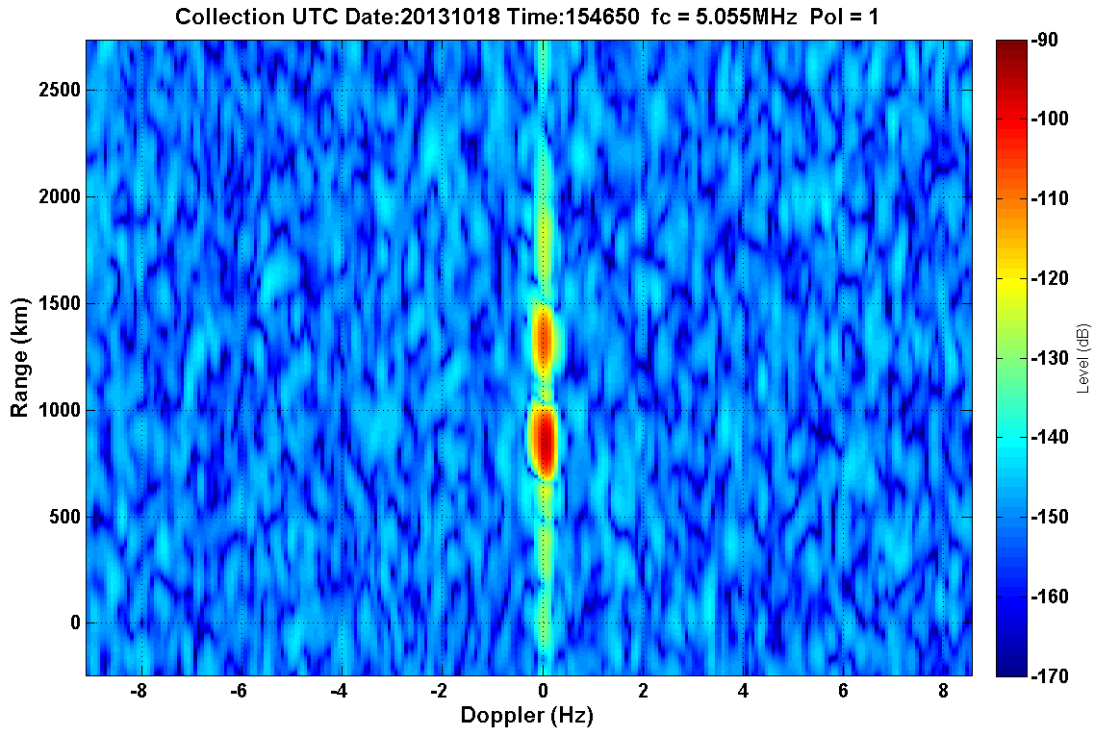

Figure 46.3:46/F1-jF1/3kHz/45.44dBm – F layer (3 bounces?), one mode

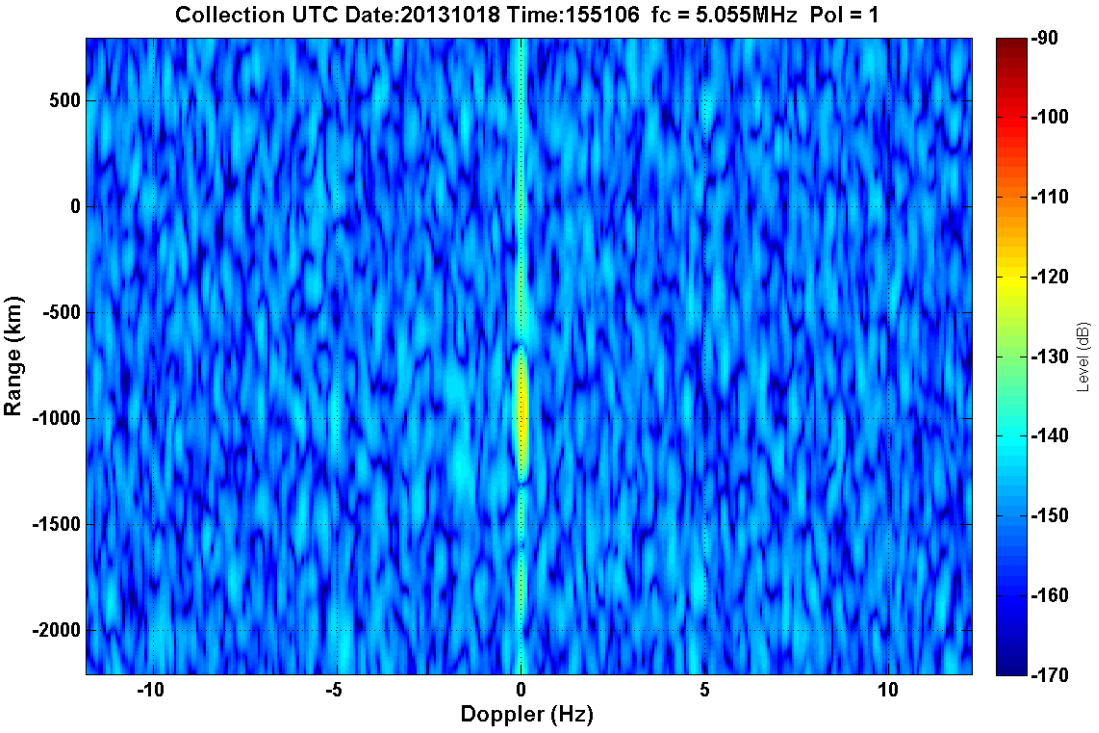

Figure 47.3:49/F1+jF2/3kHz/38.1dBm – one mode

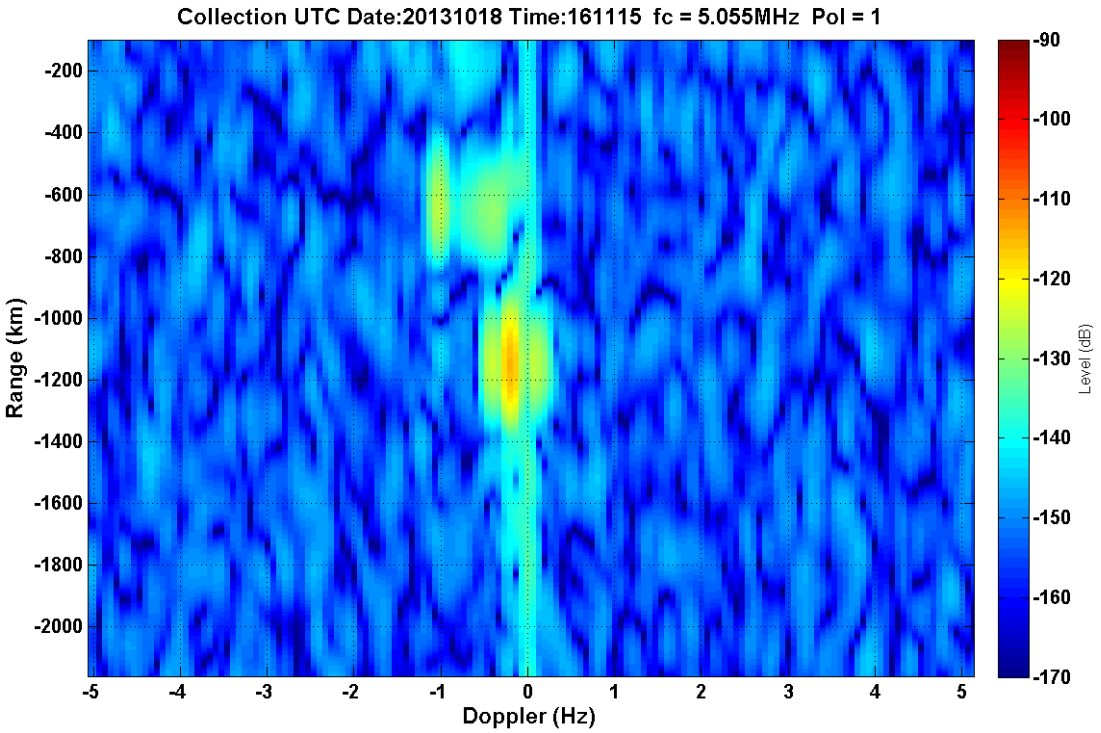

Figure 48.4:04/F1+jF2/3kHz/43.94dBm – F layer, two modes

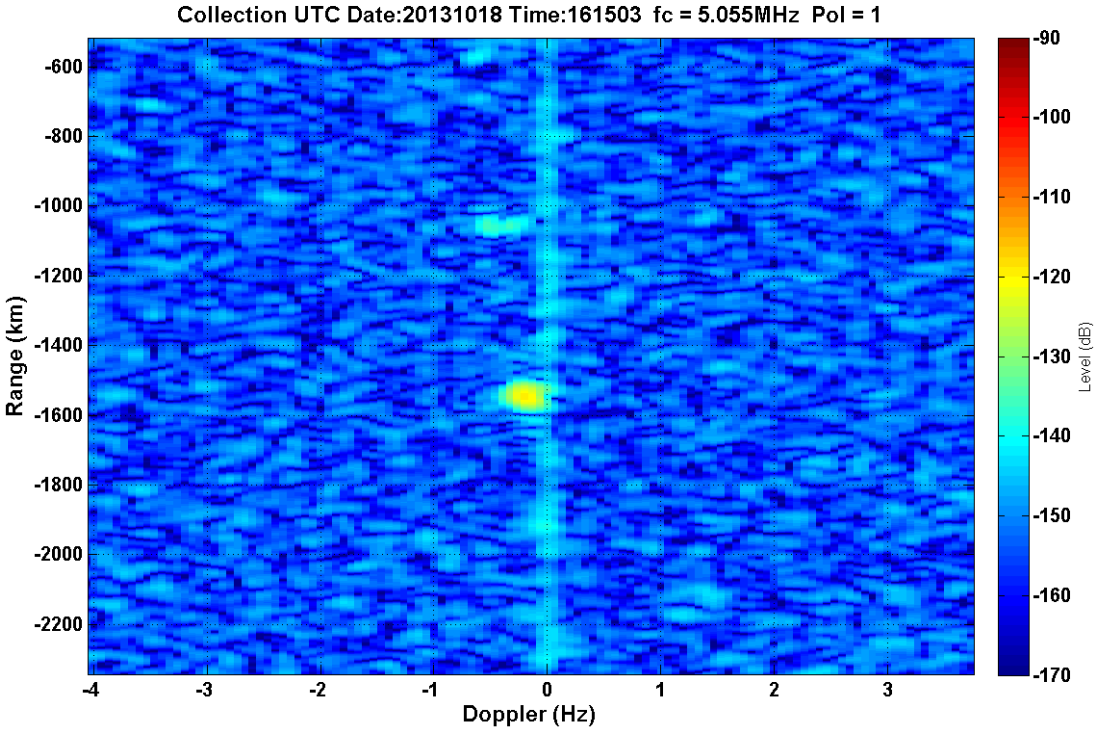

Figure 49.4:14/F1+jF2/20kHz/38.1dBm – F layer, two modes

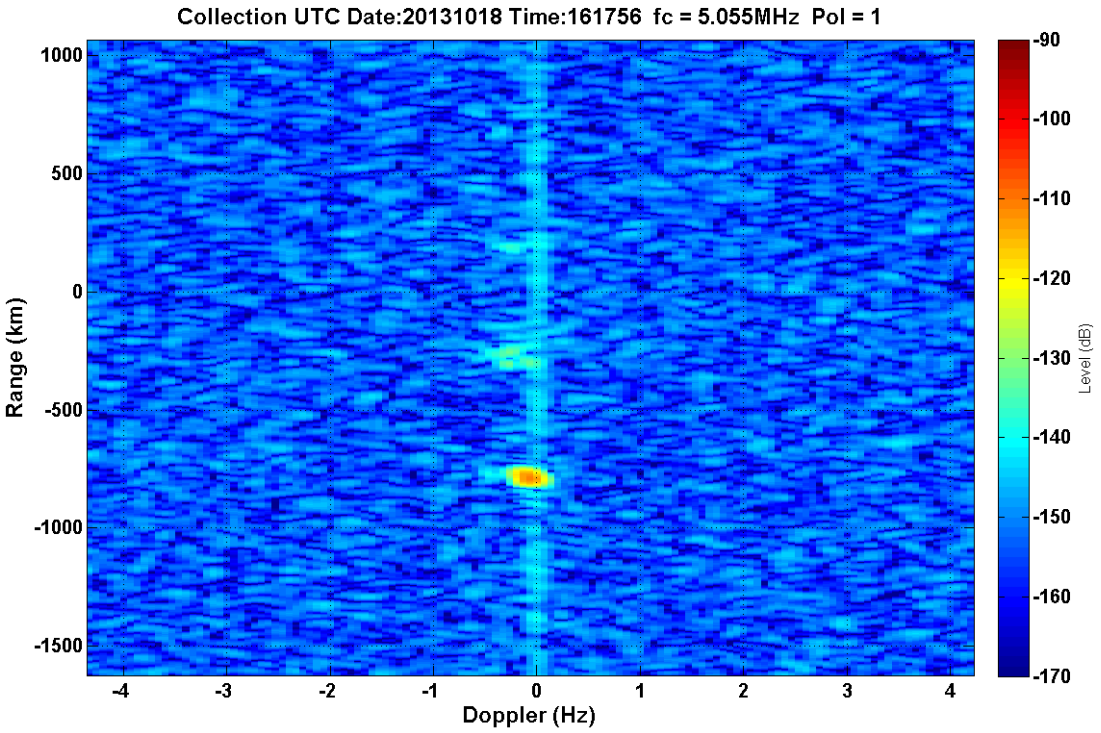

Figure 50.4:17/F1+jF2/20kHz/44dBm – F layer, two modes (?)

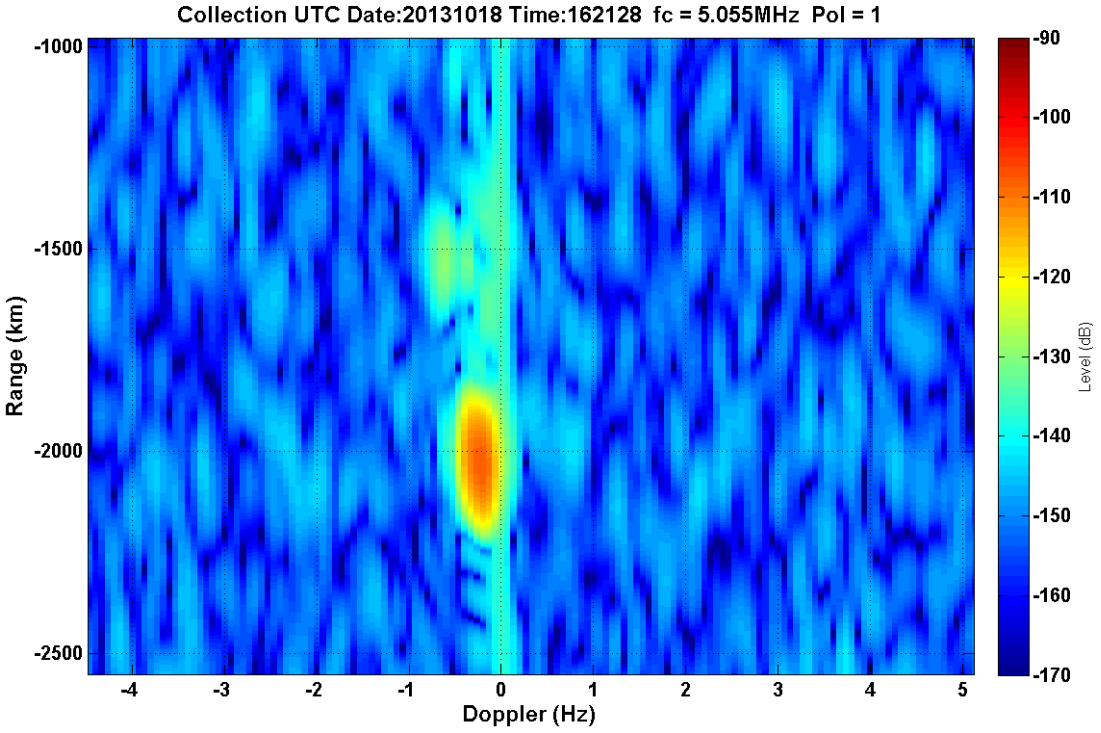

Figure 51.4:20/F1-jF2/3kHz/38dBm – F layer, one mode, two on second bounce

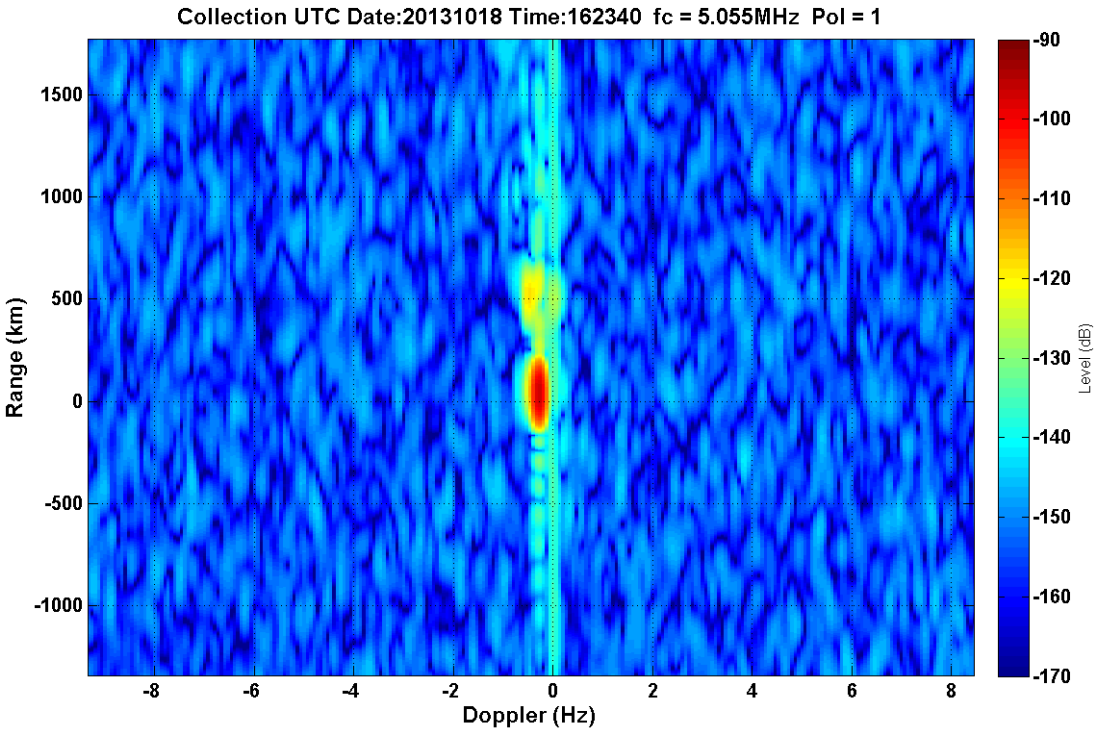

Figure 52.4:22/F1-jF2/3kHz/44dBm – F layer, one mode, two(?) on second bounce

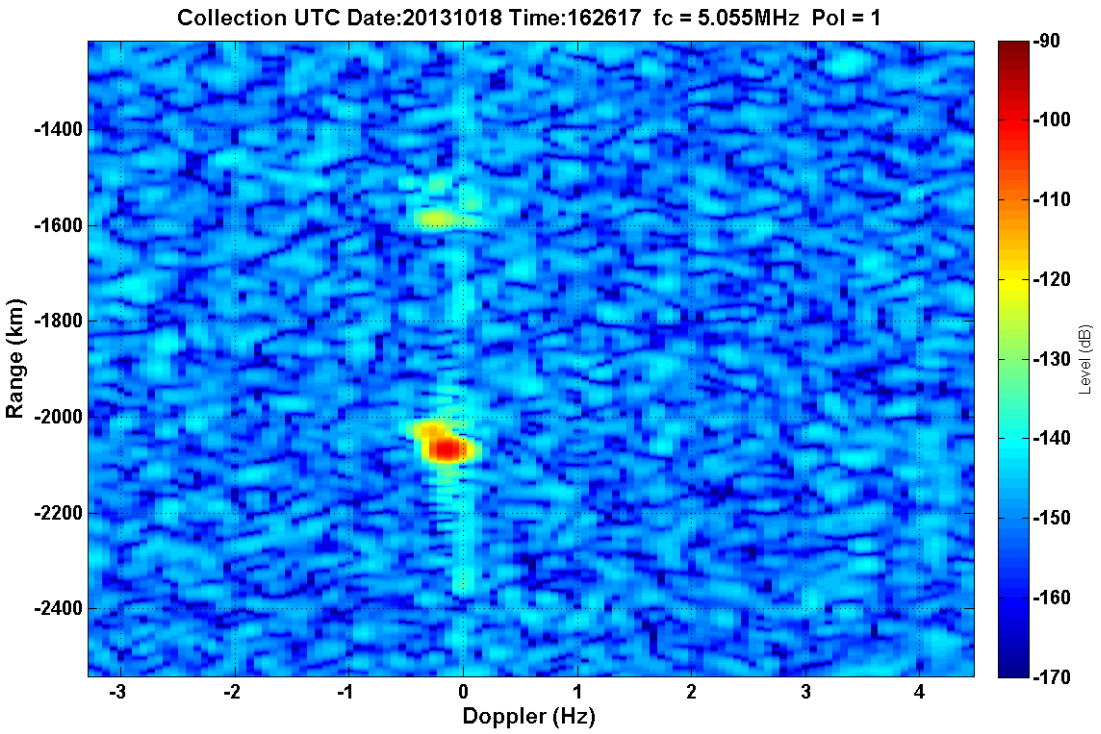

Figure 53.4:26/F1-jF2/20kHz/38dBm – F layer, two modes

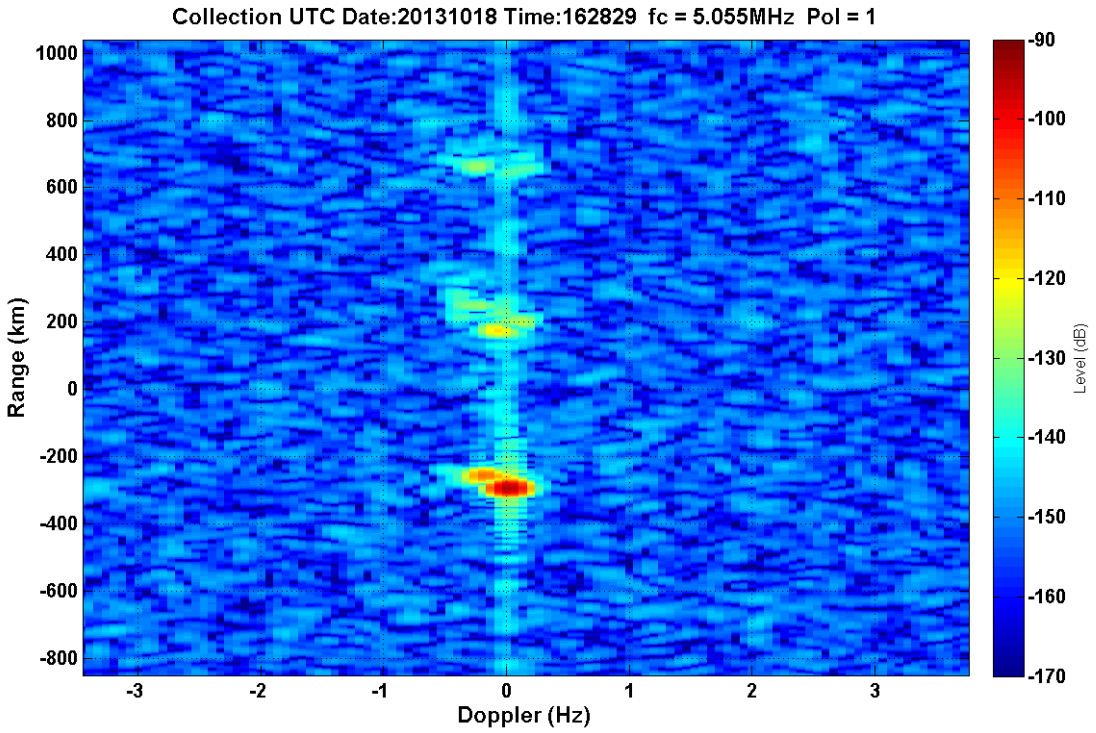

Figure 54.4:28/F1-jF2/20kHz/44dBm – F layer (three bounces), two modes

Data Collection III

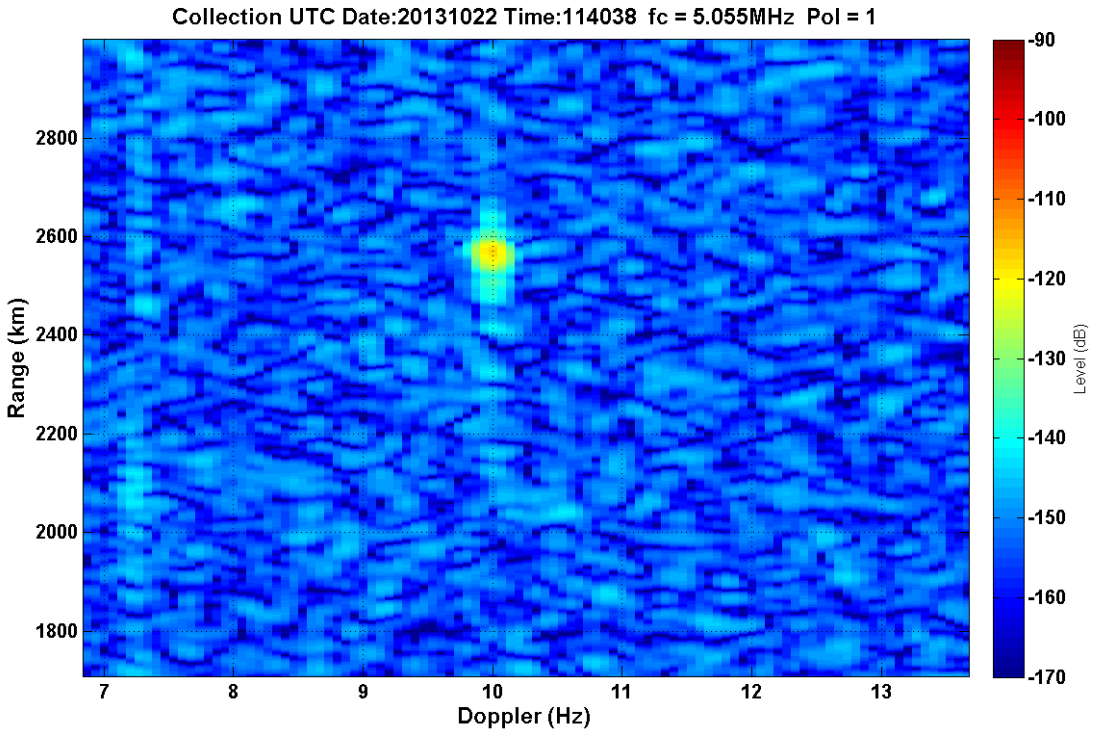

Figure 55.11:38/F1/20kHz/39.18dBm – one mode

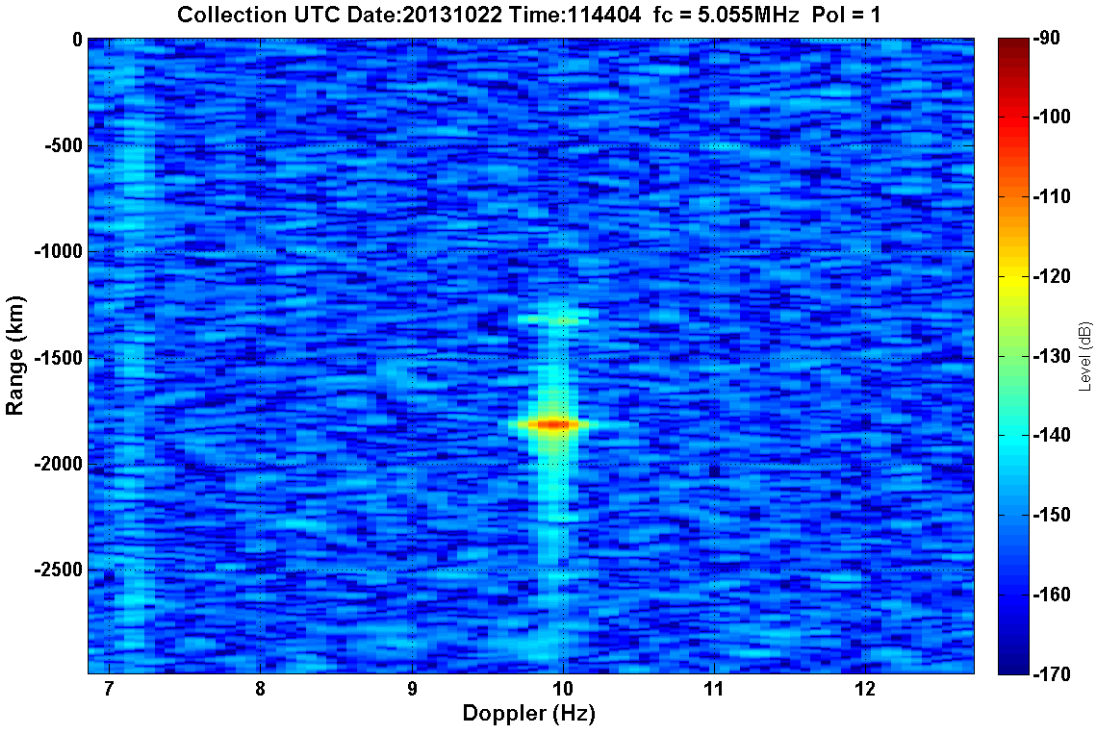

Figure 56.11:43/F1/20kHz/45.24dBm – F layer, one mode (two on second bounce?)

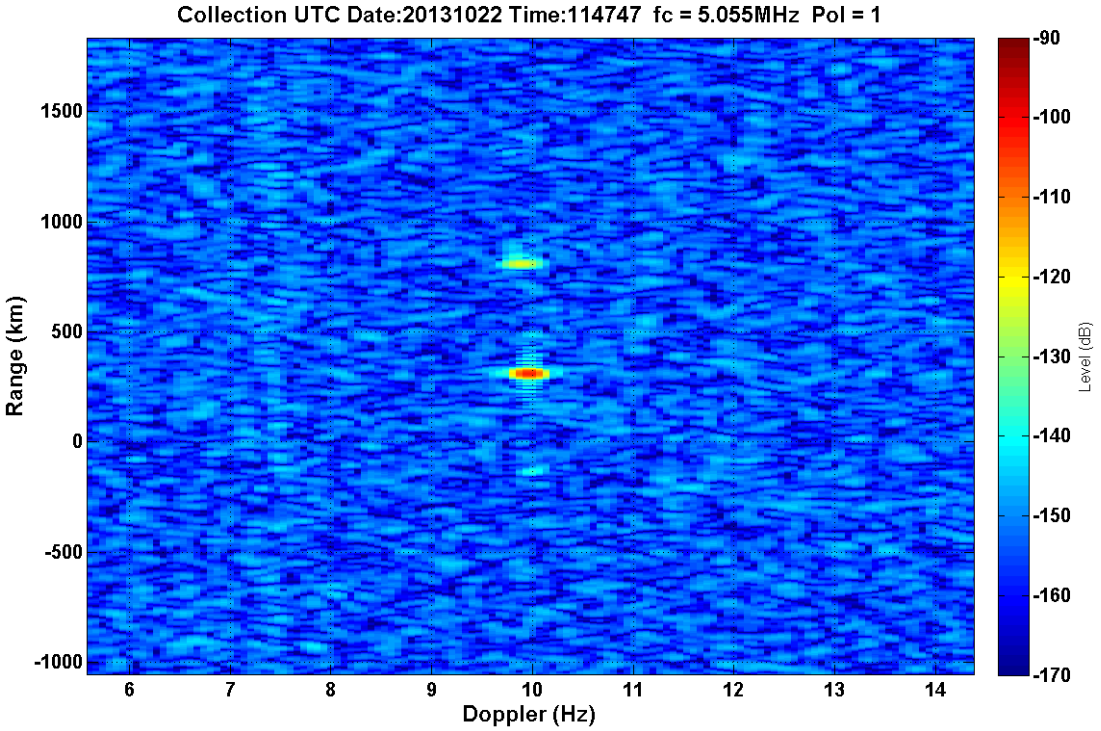

Figure 57.11:47/F1/20kHz/48.07dBm – F layer, one mode, ground wave

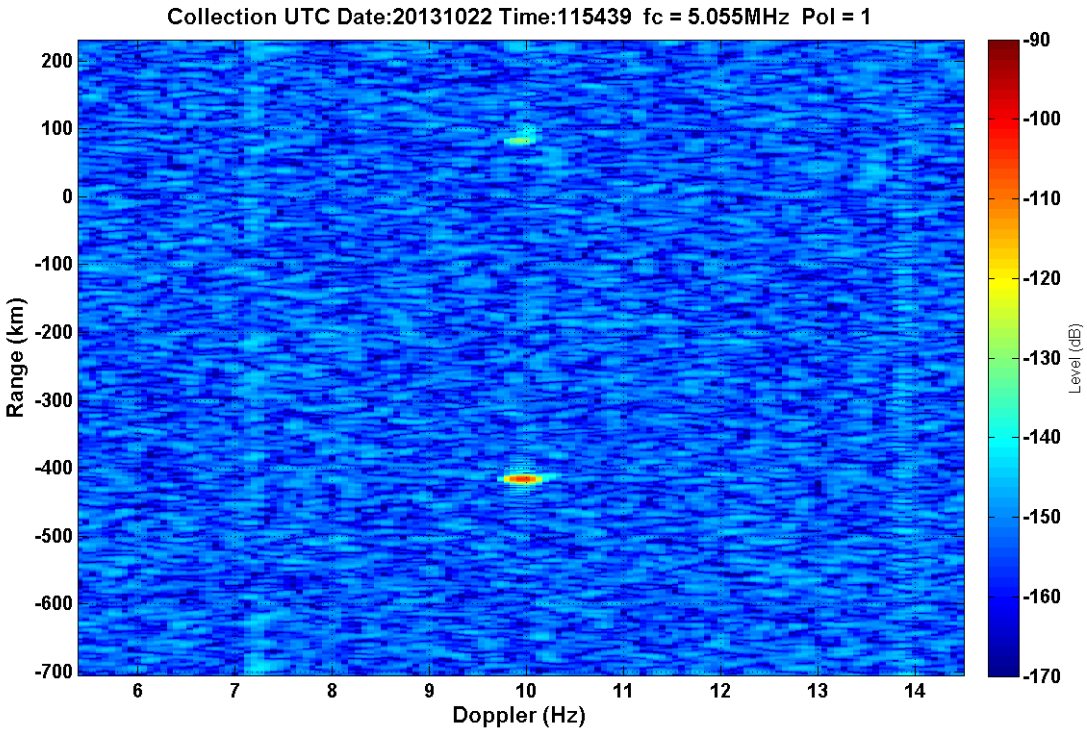

Figure 58.11:53/F1/90kHz/38.84dBm – F layer, one mode

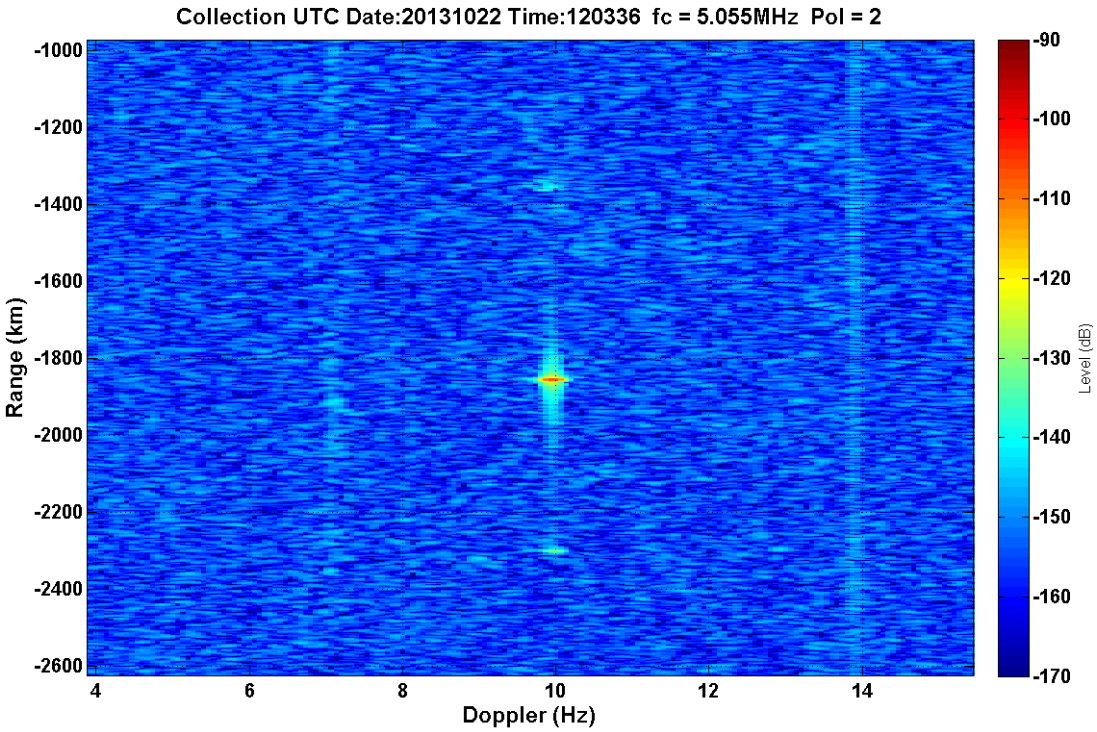

Figure 59.11:57/F1/90kHz/44.88dBm – F layer, one mode, ground wave

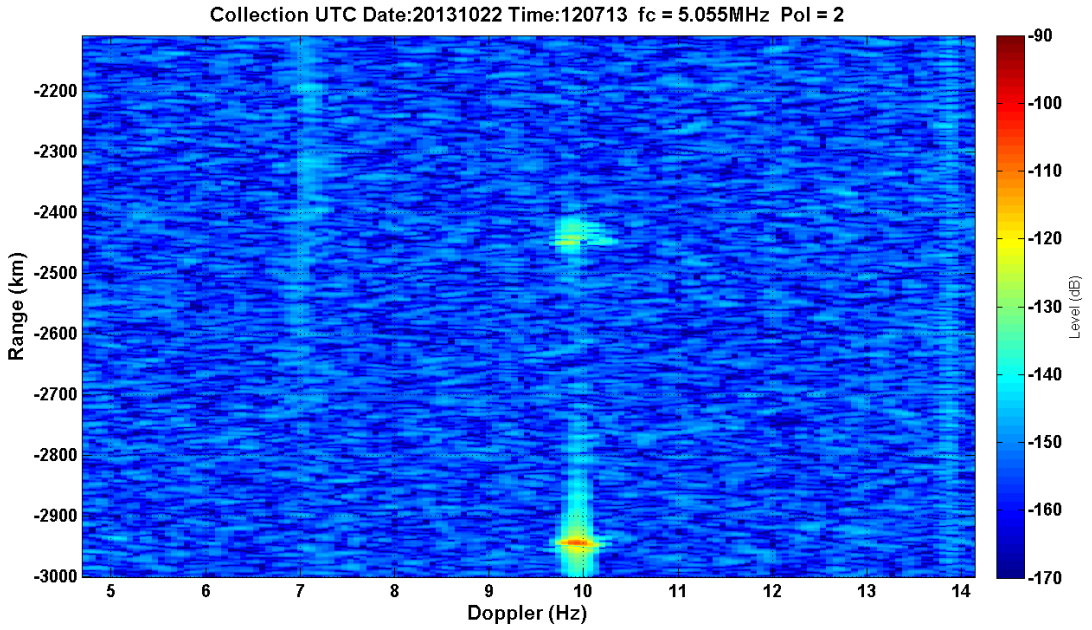

Figure 60.12:06/F1/90kHz/48.13dBm – F layer, one mode

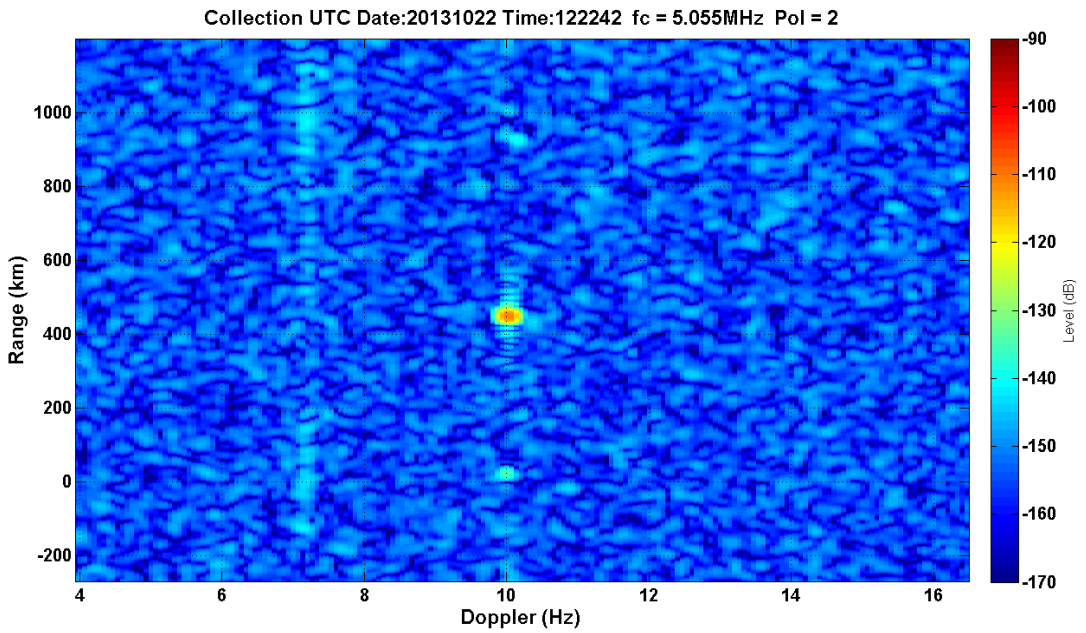

Figure 61.12:21/F1+jF1/20kHz/39.44dBm – F layer, one mode, ground wave

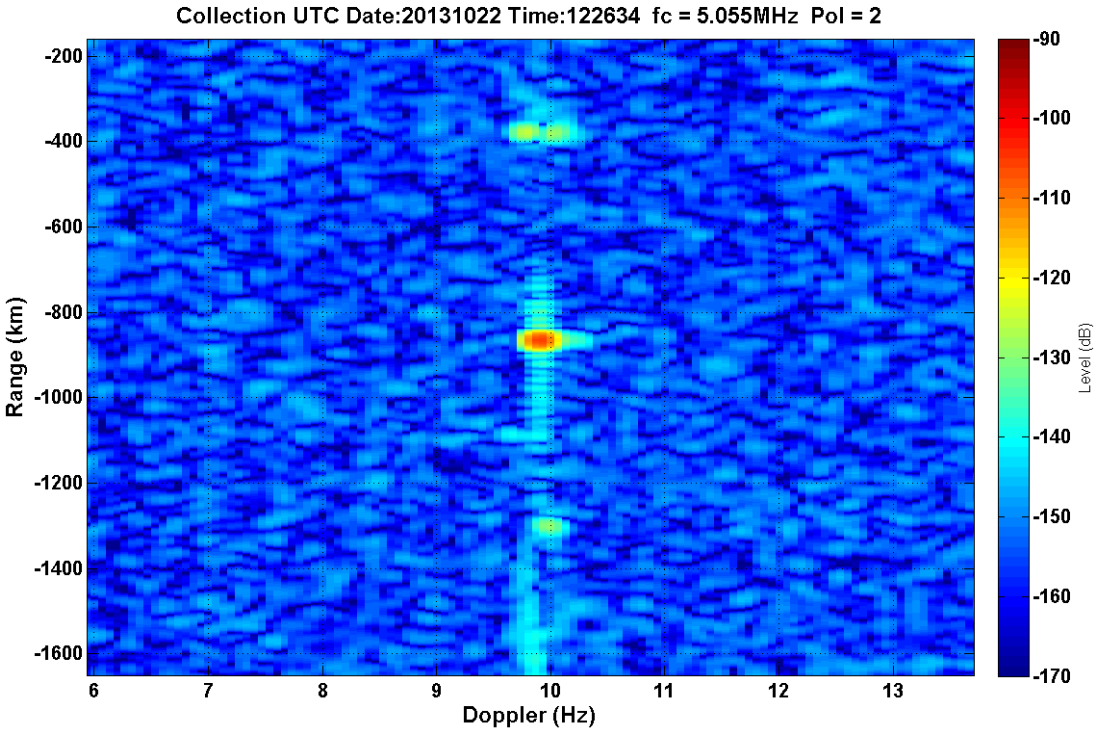

Figure 62.12:25/F1+jF1/20kHz/45.52dBm – F layer, one mode (two on second bounce), ground wave

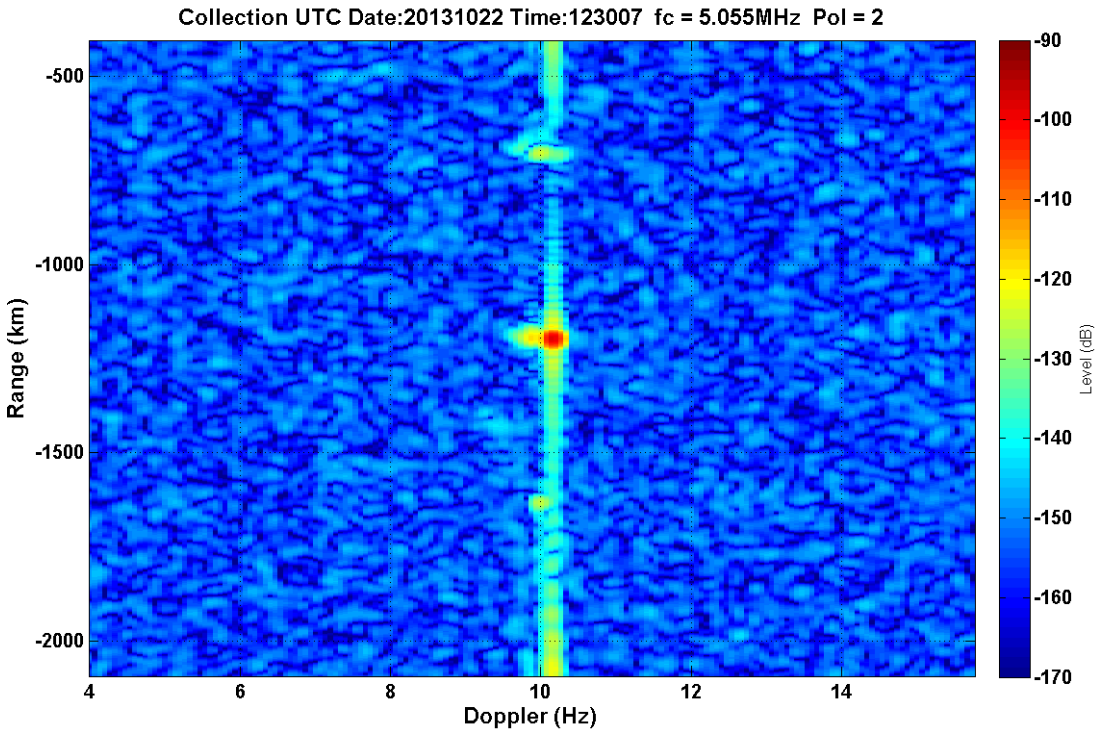

Figure 63.12:29/F1+jF1/20kHz/48.95dBm – F layer, two modes, ground wave

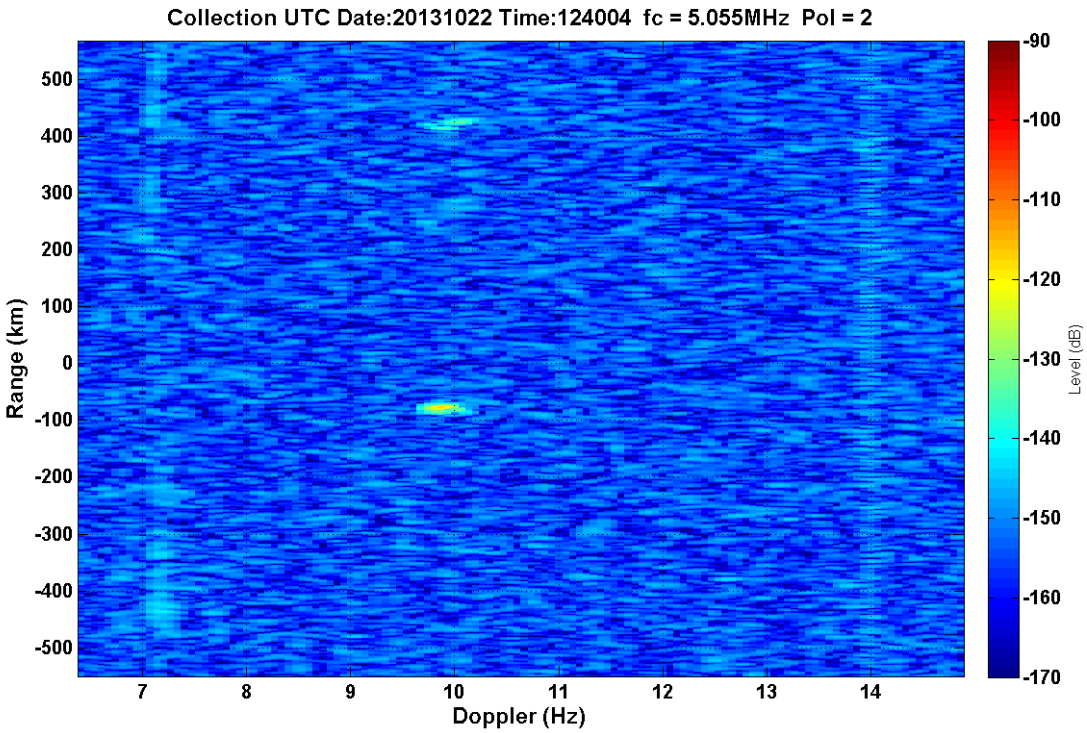

Figure 64.12:38/F1+jF1/90kHz/39.22dBm – F layer(?), two modes on second bounce

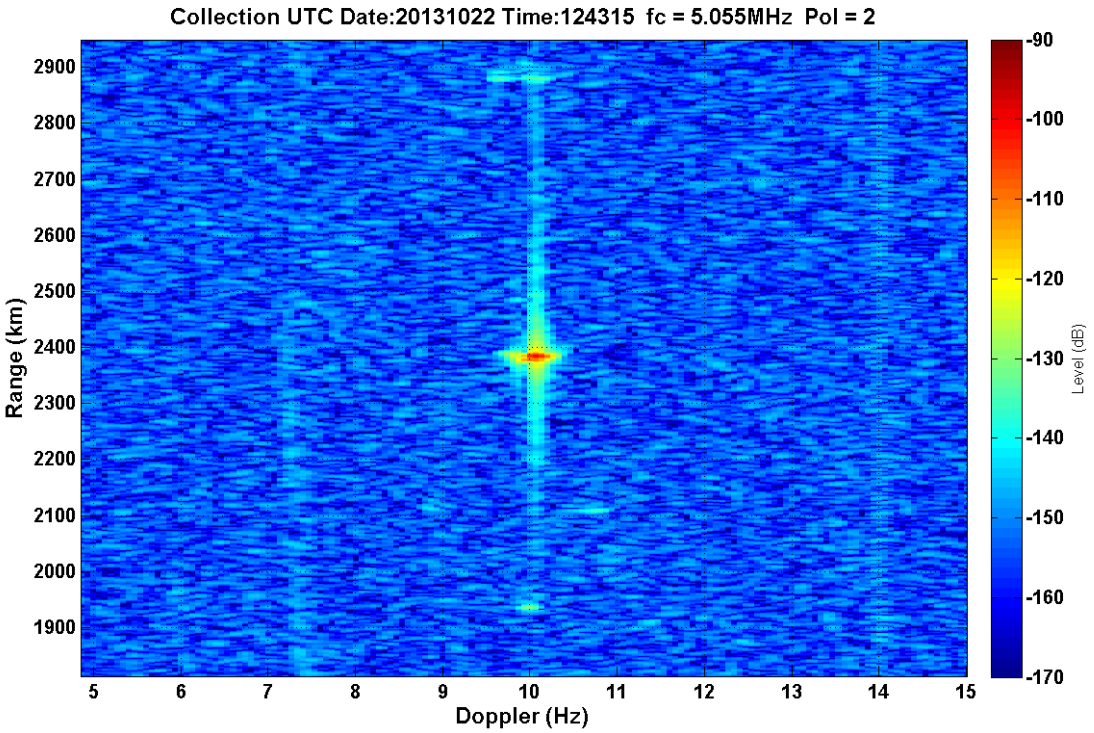

Figure 65.12:42/F1+jF1/90kHz/44.85dBm – F layer, two modes, ground wave

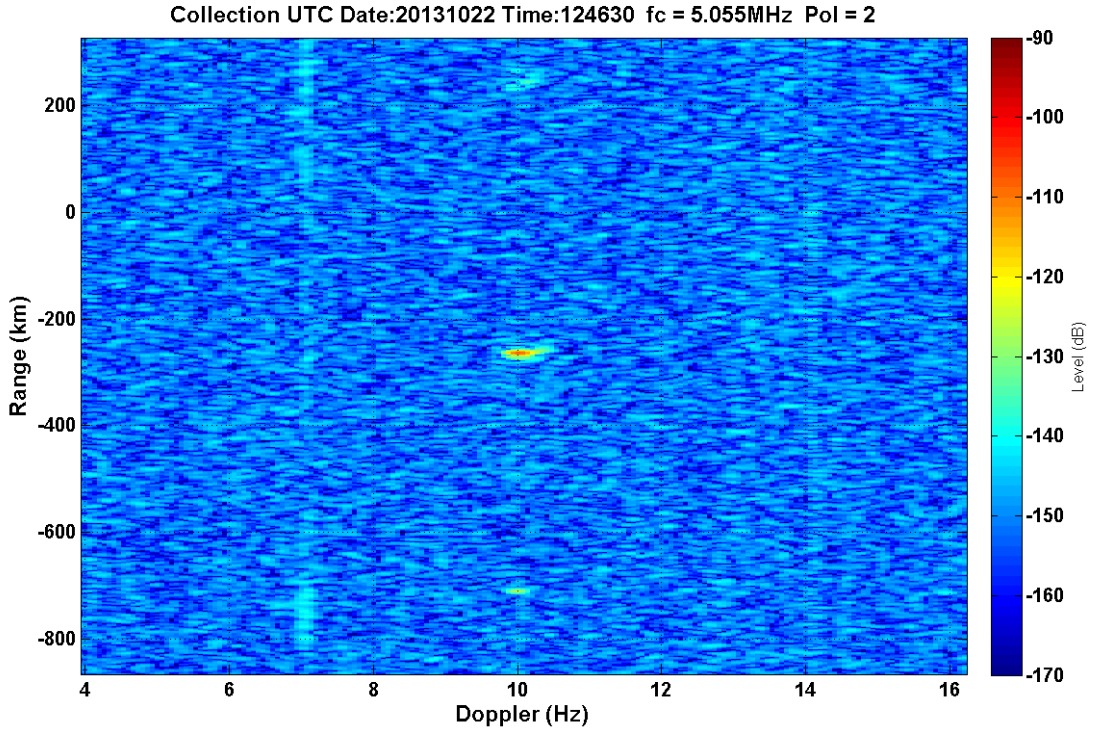

Figure 66.12:45/F1+jF1/90kHz/48.25dBm – F layer, two modes(?), ground wave

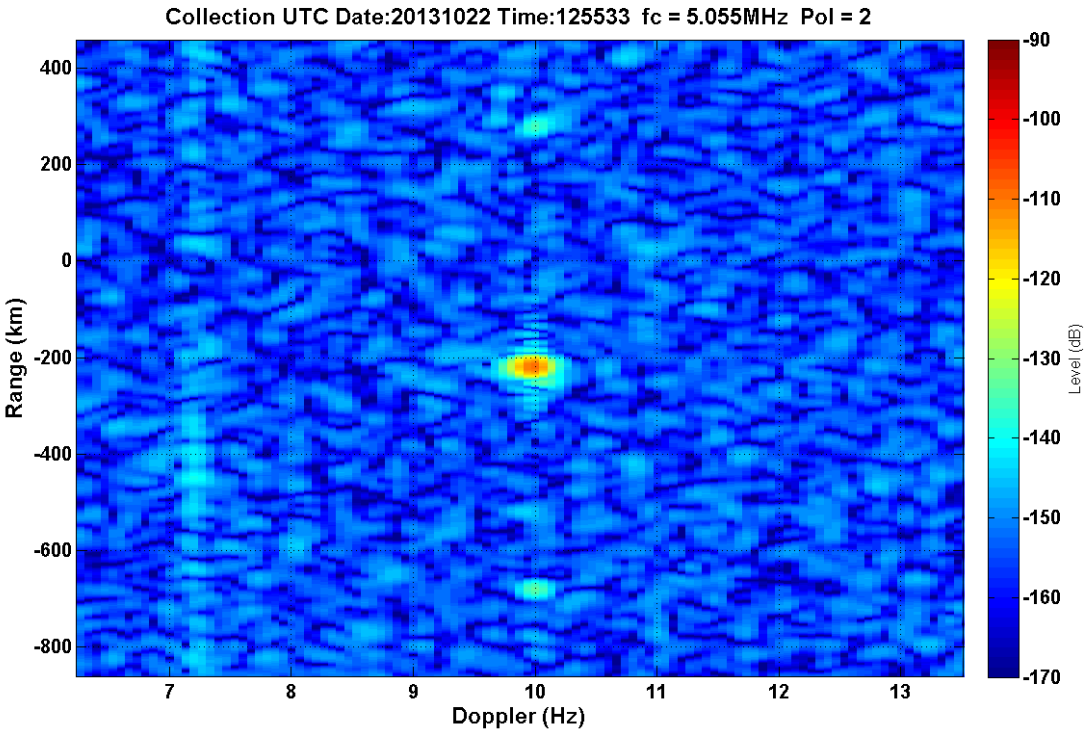

Figure 67.12:54/F1-jF1/20kHz/39.48dBm – F layer, one mode, ground wave

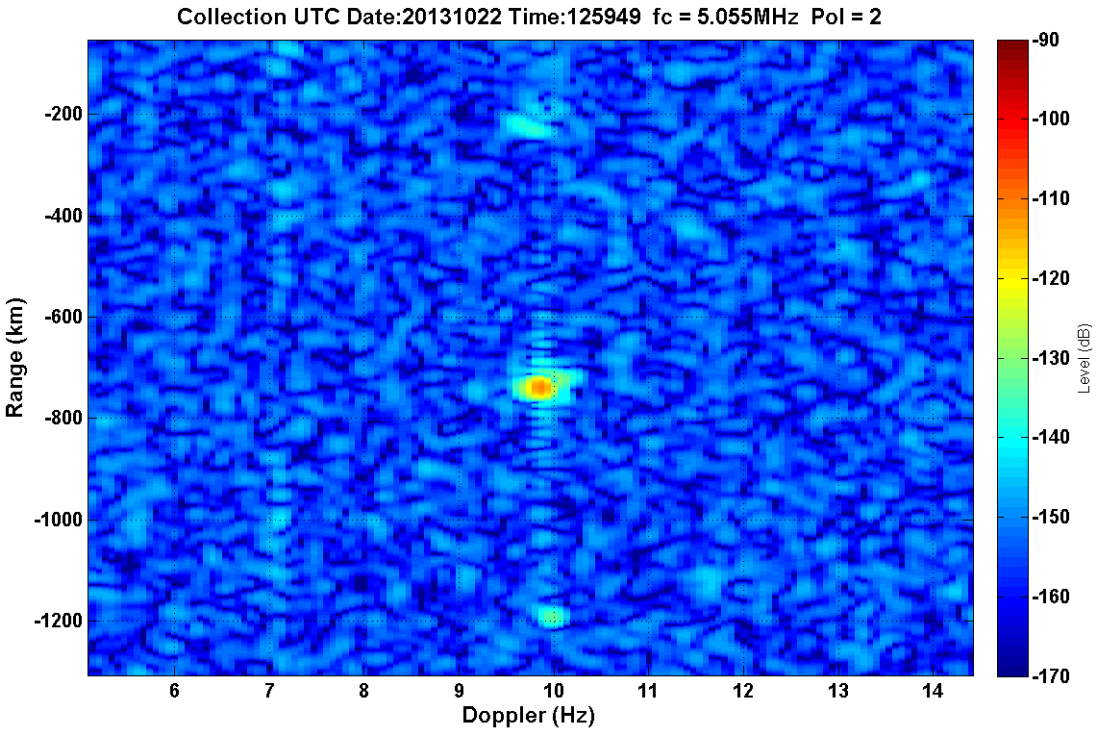

Figure 68.1:01/F1-jF1/20kHz/45.56dBm – F layer, one mode(?), ground wave

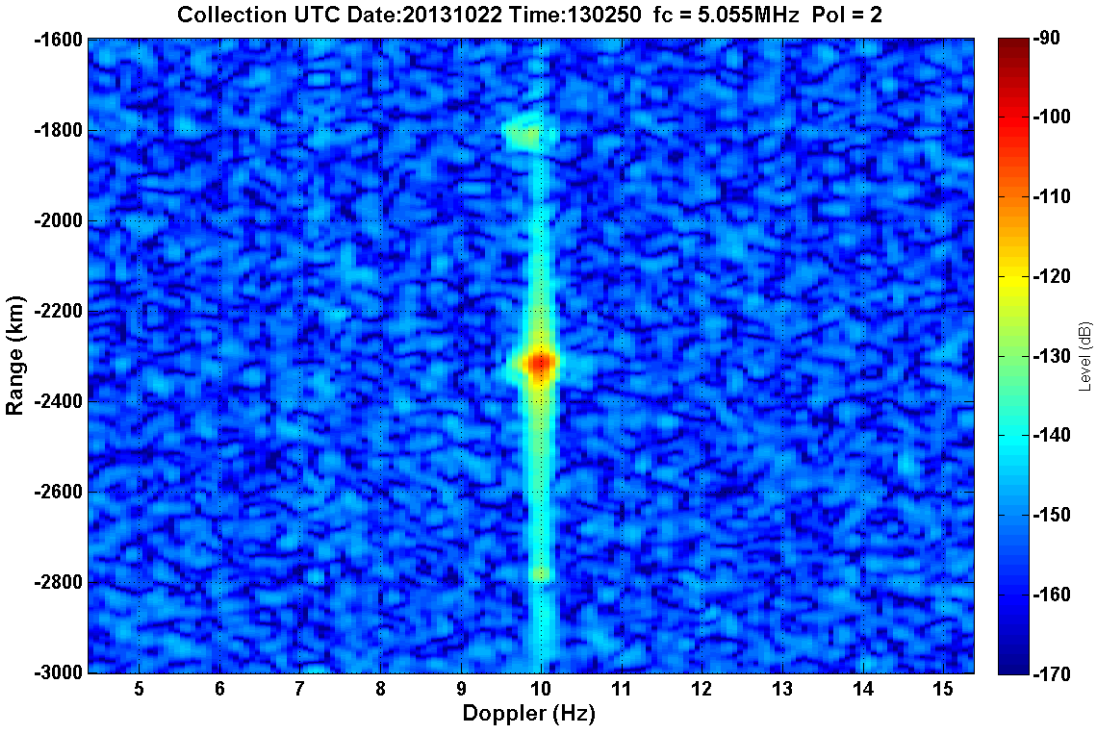

Figure 69.1:05/F1-jF1/20kHz/49.93dBm – F layer, one mode, ground wave

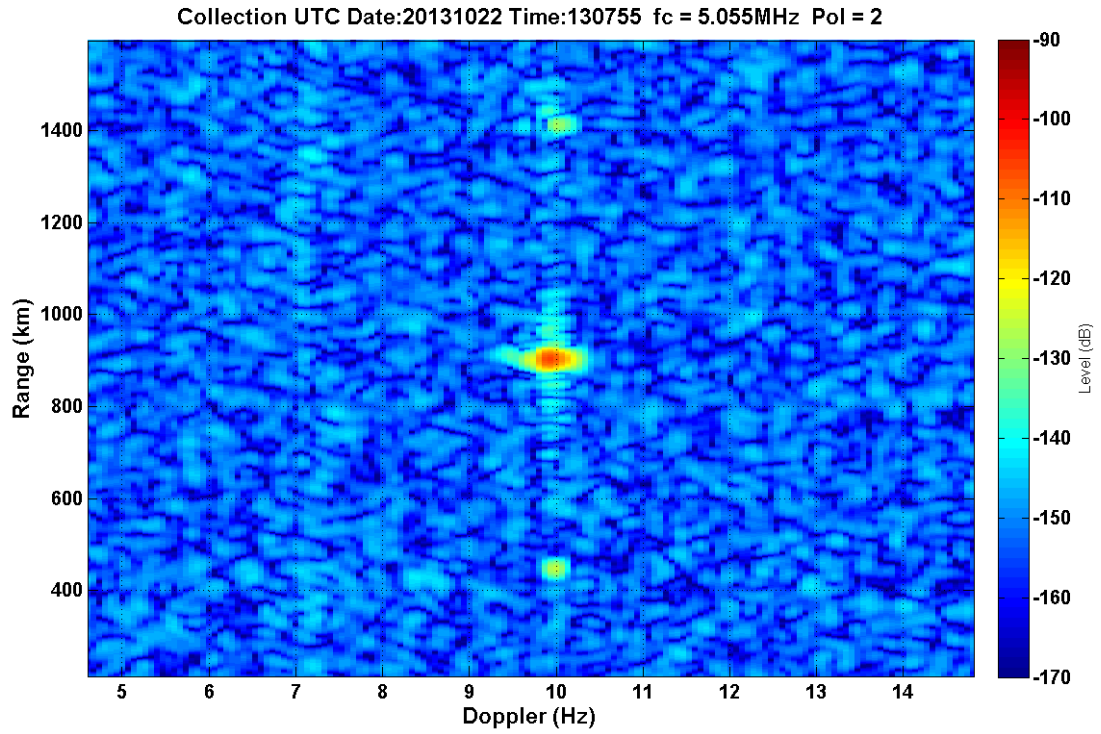

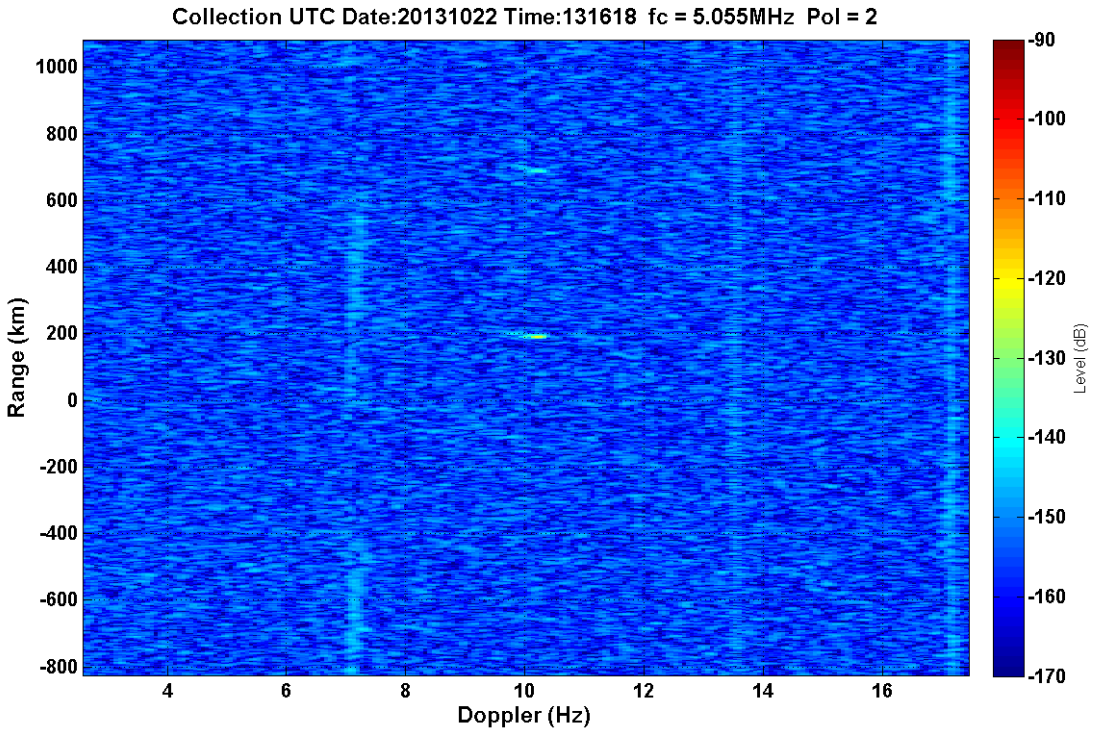

Figure 70.1:15/F1-jF1/90kHz/39.0822dBm – F layer, one mode(?)

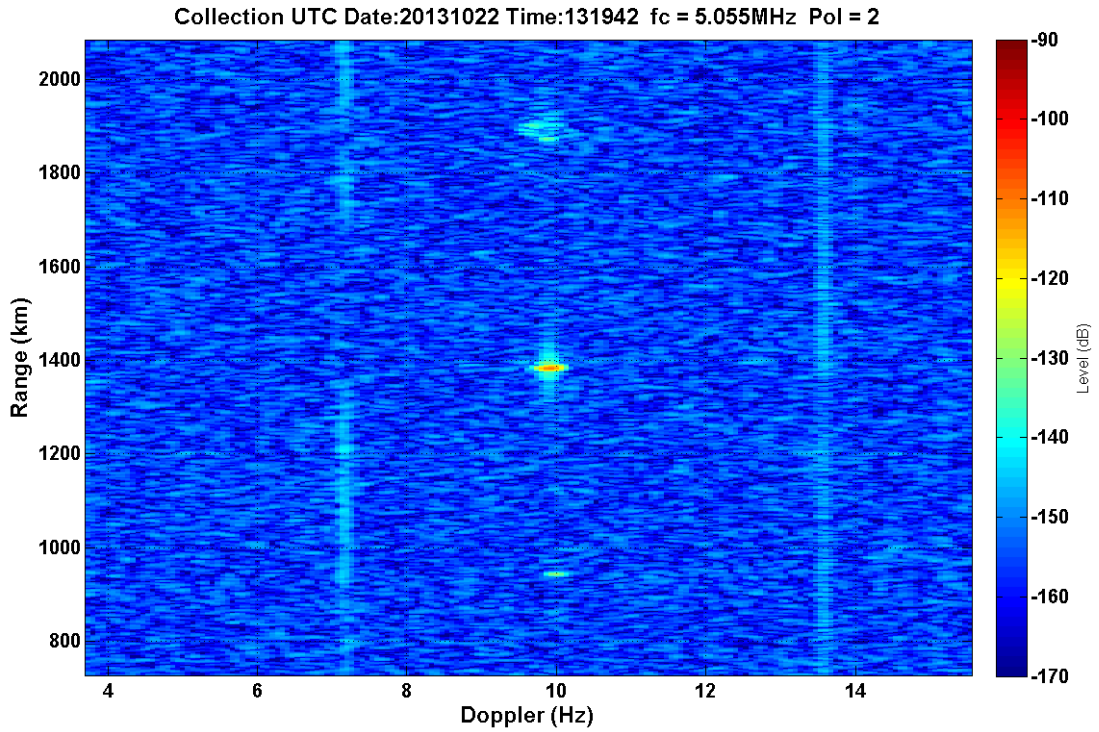

Figure 71.1:19/F1-jF1/90kHz/44.95dBm – F layer, one mode (two on second bounce), ground wave

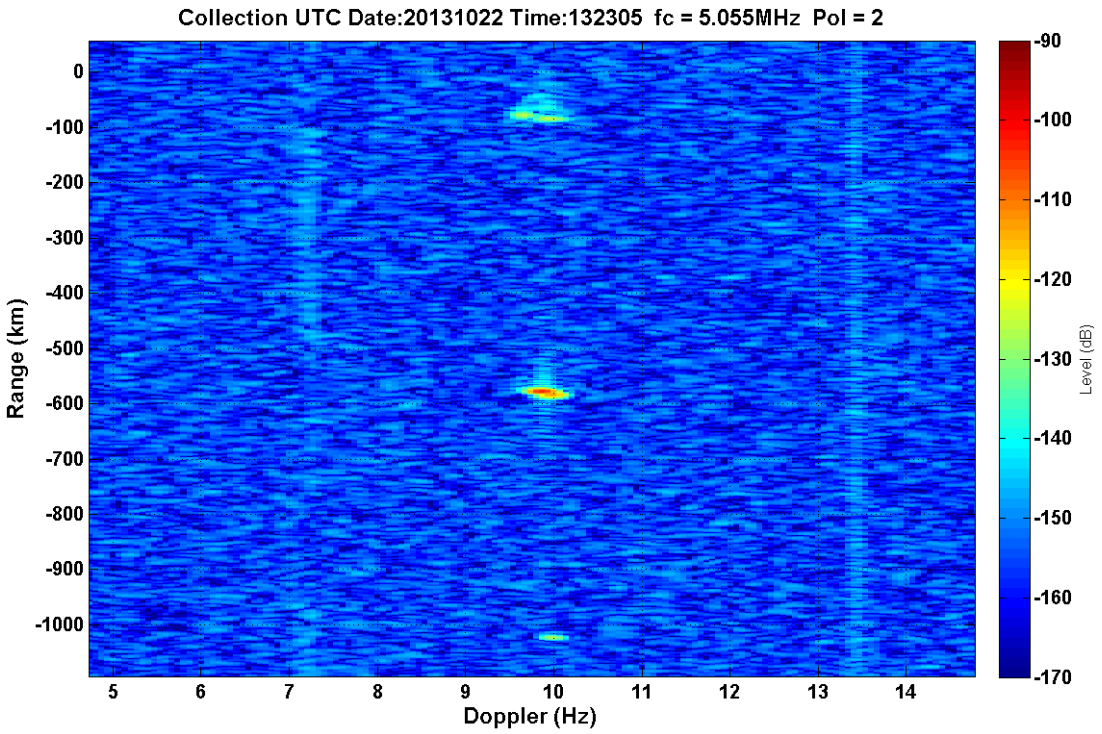

Figure 72.1:22/F1-jF1/90kHz/48.20dBm – F layer, two modes, ground wave

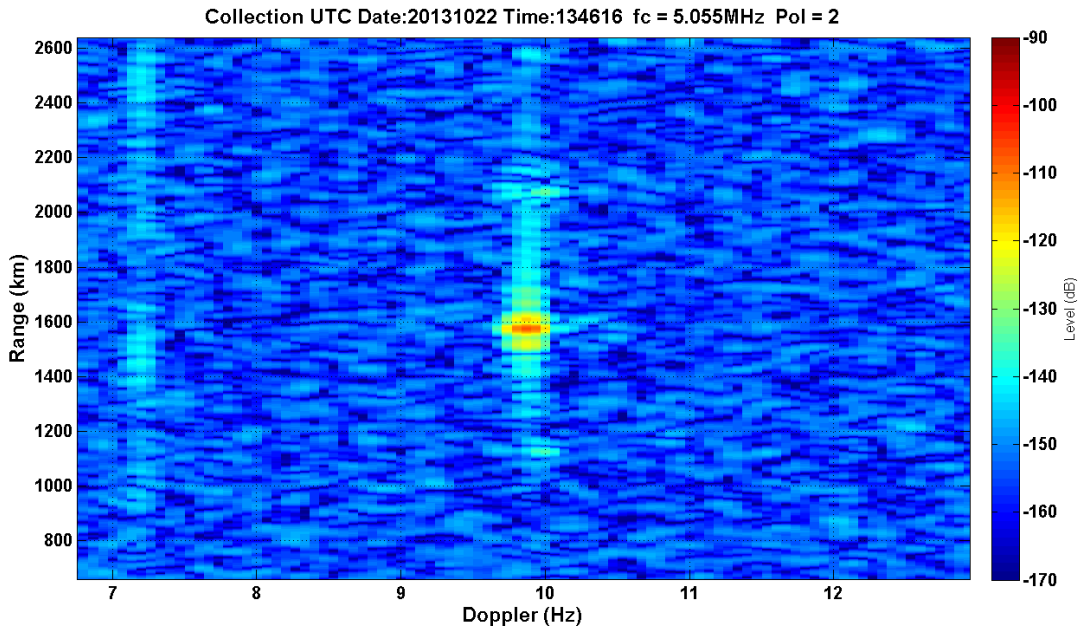

Figure 73.1:45/-F1+jF2&jF1-F2/20kHz/41.25dBm – F layer, two modes(?), ground wave(?)

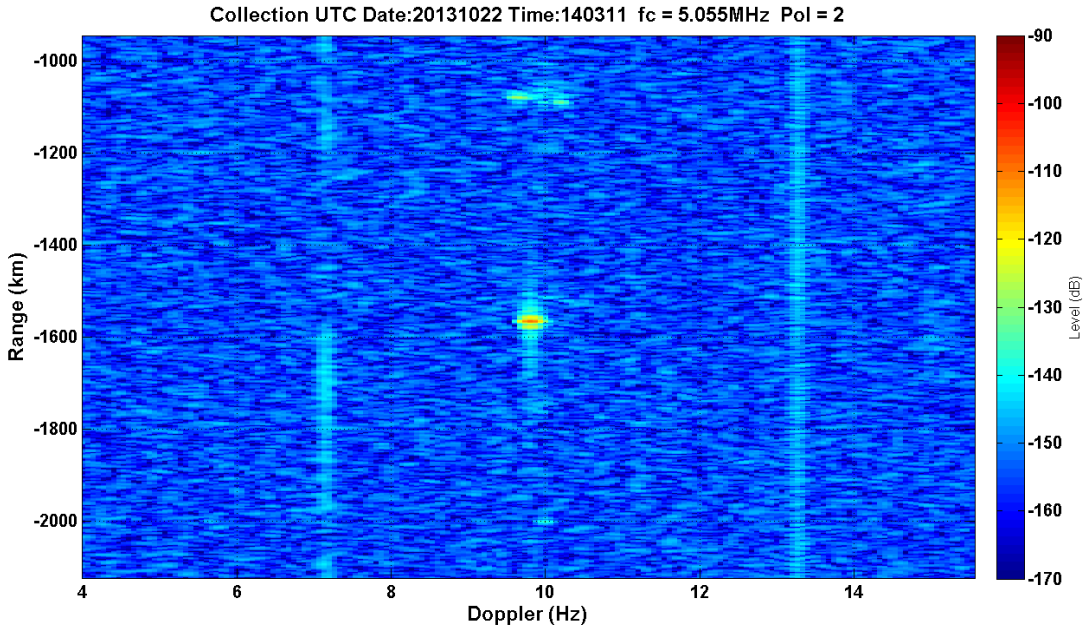

Figure 74.1:57/F1+jF2&F1+jF2/90kHz/40.43dBm – F layer, two modes(?), ground wave(?)

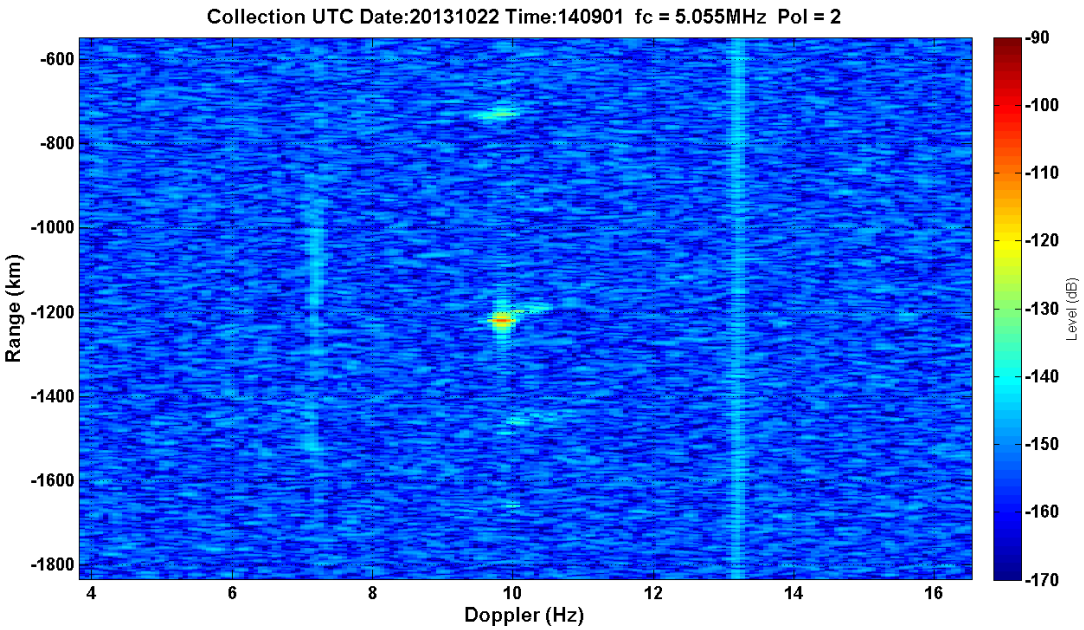

Figure 75.2:08/-F1+jF2&F1-jF2/90kHz/40.43dBm – F layer, two modes(?), ground wave(?)